Development of Small-scale Systems for Power Generation and Hydrogen Production by Biomass Thermochemical Conversion

Yohanes Andre Situmorang

A Dissertation Submitted in Partial Fulfillment of the Requirements for the Degree of Doctor of Philosophy in Engineering

GRADUATE SCHOOL OF SCIENCE AND TECHNOLOGY

HIROSAKI UNIVERSITY

2021

ABSTRACT

World's energy demand is increasing year by year. The depletion of fossil fuels leads the world to take a glance at renewable sources as the alternative for energy production, which biomass is considered as the most potential one. Thermochemical conversion is viewed as the best way to convert biomass into various convenient energy. However, unlike the fossil fuels, biomass growing and collection limits its large-scale application with low cost. As such, conversion of biomass into energy in a small-scale with the local biomass resource system is more preferable and attractive for its complete and efficient utilization. Meanwhile, during the thermochemical conversion process, various byproduct and impurities such as tar will be generated. It is important to avoid the unwanted byproducts generation and improve the utilization efficiency during the biomass energy system designed and operation. This dissertation, on the one hand, considers the compatibility and synergistic effect existence in various biomass mixture during the thermal conversion process, the co-pyrolysis of various biomass with different properties and co-gasification of their char were experimentally investigated to give a guidance of biomass selection in the two-stage gasification system. On the other hand, advanced small-scale biomass energy systems especially for the power generation and hydrogen production were designed and analyzed. This dissertation includes 7 chapters.

Firstly, compatibility and synergistic effect existence on co-pyrolysis of biomass was investigated to support biomass selection requirement in two-stage gasification system, in which biomass pyrolysis and biochar gasification were conducted separately to reduce tar formation. It was found that less reactive co-pyrolysis biochar could be generated from the biomass with high content of silica species such as rice straw and rice husk since the silica species can react with the AAEM species in woody biomass to form alkali silicate compounds, which always greatly inhibit the gasification rate. In contrast, the gasification of the co-char involving combinations of different woody biomass showed synergistic effect to improve the gasification efficiency since the AAEM contents in woody biomass was stably maintained in the co-char after the co-pyrolysis process. This study provided a guidance for the biomass selection in the application of two-stage gasification system.

Secondly, the performance of a novel separated-type biomass gasification system as further development of conventional two-stage gasification system composed of an auger-type pyrolyzer, a steam tar reformer, an air-steam char fluidized bed gasifier, and a spent char riser-type combustor with circulating heat carrier particles for small-scale power generation was investigated. Herein, the system performances based on two typical biomass pyrolysis processes, i.e., slow and fast pyrolysis process, were analyzed in details. It is found that the cold gas efficiency of the system had a range of 71.7-73.8% from slow to fast pyrolysis. This study offered a new viewpoint on addition of steam tar reforming process in the conventional two-stage gasification system could not only solve the tar formation problem in gasifier, but also increase the overall system performance.

Thirdly, a new concept of chemical looping process combined with a steam tar reforming process for the hydrogen production from biomass feedstock was proposed and simulated. The system consisted of a biomass pyrolysis unit, a steam tar reforming unit, and a biochar chemical looping unit for hydrogen production (CLH) with a heat circulation design to achieve an auto-thermal operation condition. As such, the overall system can generate a total of 6.9 kg/h of H_2 and net power of 58.3 kW simultaneously from 100 kg/h feeding rate of woody biomass. The hydrogen production efficiency of this novel system was obviously higher than other reported biomass hydrogen production systems. Herein, the combination of two types of hydrogen production units boosted the system efficiency. It is expected to provide a new way for the effective hydrogen production from biomass.

Finally, a small-scale combined heat and power (CHP) system combining a biomass direct chemical looping combustion (BDCLC) and organic Rankine cycle waste heat recovery (ORC-WHR) was proposed and simulated. The BDCLC unit produced 170.2 kWe power whereas the ORC-WHR unit generated additional 21.0 kWe. As such, the system produced 191.2 kWe total power from 1000 kWth biomass input. Moreover, this system applied two evaporators in the ORC-WHR unit to recover the heat from two reactors in the chemical looping combustion process for the additional power generation. Therefore, it has the potential for the small-scale power generation using the biomass resource.

ACKNOWLEDGEMENTS

First and foremost, I would like to express my deepest and sincere gratitude for my research supervisor, Prof. Dr. Guoqing Guan, for giving me the opportunity to do research in his fascinating group. His motivation, advices, comments, teaching, and support gave me great supports both academically and personally during my life in Japan. It is a great honor and privilege to work and study under his guidance.

Deepest appreciation is also given to Assoc. Prof. Dr. Akihiro Yoshida for all valuable comments on my research works and all the help he gave me during daily lab activities. In addition, I would like to give thanks to Prof. Dr. Abuliti Abudula and Assistant Prof. Tao Yu from Graduate School of Science and Technology, Hirosaki University for all advices and comments during our discussion in group meeting seminar. Also, many thanks to all students and researchers in our lab for all their supports, help, and friendship.

I deeply acknowledge Ministry of Education, Culture, Sport, Science, and Technology (MEXT) of Japan (Monbukagakusho) for providing the scholarship during my Ph.D. study in Hirosaki University, Japan.

Sincere gratitude I give for Dr. Irwan Kurnia and his family and Shiraishi's family for all the help and friendship they give during my life in Japan.

Special thanks I present to my wife Rahajeng Pakpahan for all her supports, patience, love, and sacrifice for me. My deepest appreciation is also given for all my family in Indonesia.

Finally, praises and thanks to the God for His guidance and blessings in all my life.

Yohanes Andre Situmorang

March, 2020

Aomori, Japan

TABLE OF CONTENTS

LIST OF TABLES

LIST OF FIGURES

CHAPTER 1 : INTRODUCTION

1.1 Biomass for power generation and hydrogen production

Energy sector is indispensable in our daily life and the energy consumption rises year by year. Among various energy forms, electricity is the largest energy sector consumed in the world. As shown in **Figure 1.1,** about 37.23 QBtu of energy in the US was consumed for electricity utilization in 2017, while most of countries especially those developed and those rapid developing countries are in the similar situation [1, 2]. Consistently, power generation demand is predicted to grow about three times more quickly when compared to other forms of energy [3].

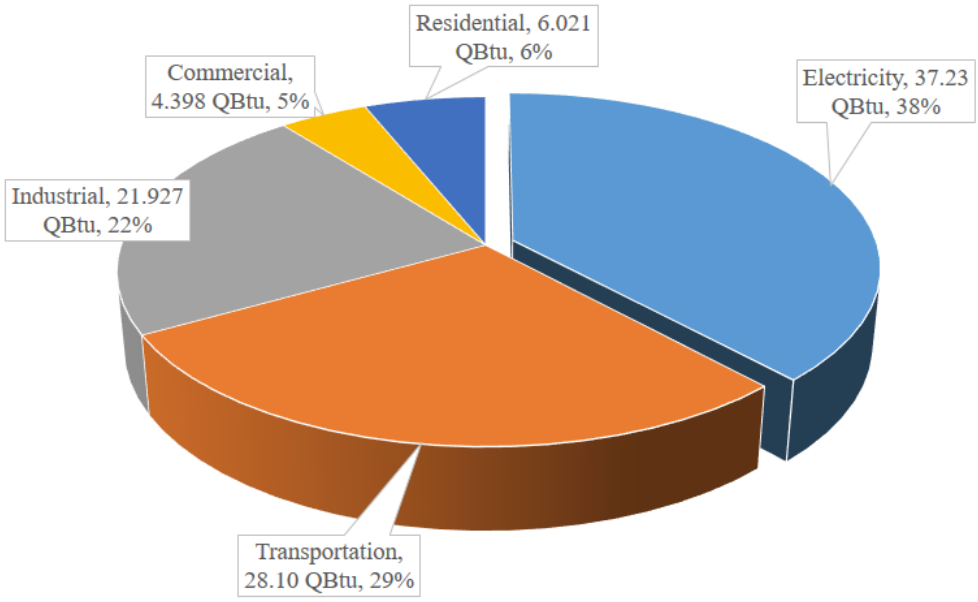

Figure 1.1 U.S. energy consumption per sector in 2017 [1]

Currently, power generation still depends on two main sources: fossil fuels such as coal, natural gas, and oil; and nuclear energy. However, the declining of fossil fuel production, the increasing of environmental awareness, and the risk on nuclear energy utilization make the world trying to find new alternative energy with more sustainable, environmentally friendly,

and less risks. As such, renewable energy sources such as biomass, solar, wind and geothermal energy are now pulling attention to replace fossil fuels and nuclear as the alternative energy sources for power generation in the future.

In the energy sector, hydrogen (H_2) is considered as a promising clean energy source and efficient energy storage medium with growing global demand [4]. Besides, H_2 is a basic feedstock that has about 60 million ton per year total consumption in industries, in which 44% contributes to oil refining industry, 38% is used in ammonia production, and the remaining is for other chemical processes [5]. To date, commercial H_2 is mainly produced by steam reforming of natural gas, which contributes to 48% of the global demand [6]. However, with the same consideration to fossil fuel utilization for energy generation, there is growing interest in finding alternative renewable sources for H_2 production [7] and as such, biomass emerges as an attractive and promising one for H_2 production.

Biomass is biodegradable non-fossilized organic materials derived from plants, algae and animals that composed of lignin, cellulose and hemicellulose, and small amounts of proteins, lipids, simple sugars and starches [8, 9]. However, with lower heating value than coal, biomass collecting and transporting are the main obstacles when handling biomass as energy source. Even so, biomass is sustainable energy source that is considered as the largest potential one to replace fossil fuels to supply fuel in the future and to reduce global warming issue. It is ranked as the 4^{th} largest energy source after coal, natural gas and crude oil [10]. As the most available one, biomass contributes about 50% of energy production among the renewable energy sources [11] and shares about 14% of world's final energy consumption in 2014 [12, 13].

In particular, biomass resources can be classified into many different types, including wood from forestry, agricultural crops and residues, dedicated energy crops, industrial wastes and residues, animal residues, municipal solid waste (MSW), and sewage [10, 14-16]. Among these resources, agricultural crops and residues and industrial and domestic wastes occupy 27% and 30% of the total respectively [10]. Although the woody biomass from the forestry only occupies around 23% of the total biomass resource, due to its relatively high heat value,

it is the most promising resource and its importance and demand will increase significantly in the future [15]. As such, overall woody biomass could provide about 90% of the primary energy sources from all biomass sources annually and the worldwide primary energy supply from the forest biomass is estimated at about 56 EJ [17].

Different biomasses always have different compositions, and even the different parts of a biomass could have different compositions and characteristics. Actually, heterogeneity of biomass is one of disadvantages during biomass application since the optimum operating conditions and final product properties are always difficult to be determined [18]. The basic analyses of biomass properties mainly include proximate and ultimate analysis, and heating value measurement. By the proximate analysis, moisture, volatile matter, fixed carbon, and ash contents in the biomass can be determined. The volatile matter consists of gases and organic vapors including paraffinic and aromatic hydrocarbons and sulfuric and nitride compounds, which are generated from the thermal decomposition of biomass. The fixed carbon is the nonvolatile hydrocarbon fraction in the biomass. Meanwhile, by the ultimate analysis, the compositions of carbon, oxygen, hydrogen, nitrogen, and sulfur in the biomass can be known. The carbon content includes fixed carbon in char and volatile carbon in volatile matters. Chemical components in biomass can be also classified as lignin, hemicellulose, cellulose and other inorganic matters [19, 20]. After biomass is burnt out, the remained ash always contains alkali and alkali earth metal (AAEM) species such as Na, K, Mg, Ca, which are reported to have catalytic activity during biomass thermal decomposition process. The catalytic activity of these AAEM components attracts blending of coal and biomass to increase coal reactivity [21].

Generally, there are two ways to convert biomass into conveniently applicable energy, i.e., the thermochemical process and the bio-chemical/biological process. The thermochemical process includes direct combustion, torrefaction, pyrolysis, gasification, and hydrothermal liquefaction to convert mostly solid and dry biomass into gas and/or liquid fuels by involving heat. While, the biological process includes three main routes, i.e., fermentation, aerobic and anaerobic digestion, and enzymatic hydrolysis to convert wet biomass into gas and/or liquid

fuels and chemicals by involving microorganism [16, 22]. Especially, the thermochemical process is considered as the most effective way for the converting of wood biomass into gas and/or liquid fuels.

1.2 Thermochemical conversion

1.2.1 Pyrolysis

Pyrolysis is a thermochemical process occurred at a temperature range of 300-600 °C in the absence of oxygen, by which the condensable volatile matters of tar and water, and non-condensable gas including CO, CO_2, CH_4, H_2, and other gases, and carbon-rich material called char are generated from biomass. In general, the pyrolysis can be classified into three types according to the heating rate and residence time of the process, i.e., slow, intermediate, and fast pyrolysis [23]. While the slow pyrolysis is conducted at a relatively low heating rate (10-100 °C/min) with a long residence time (about 5-30 min or even 25-35 h) to produce higher amount of char, the fast pyrolysis is always performed at a very high heating rate (about 500-1000 °C/s) with a very short residence time (0.5-2 s) to generate higher quantity of tar [24, 25].

The biomass pyrolysis process can be used for power generation by combustion of the tar (or pyrolytic oil) in diesel engine, gas turbine, or co-firing process. However, it is only applied in the lab-scale research and some pilot plants since there are some obstacles in using 100% pyrolytic oil as the fuel. Cetane number of biomass tar is only about 13-14 compared to common diesel oil with 48-50 so that a longer ignition time is needed in diesel engine. Moreover, solid impurities have also negative effect on the tar utilization for diesel engine. Nevertheless, mixture 96% of pyrolytic oil with 4% diesel oil for 12-hours operation on a 300 kW power generation diesel engine has been successfully achieved by PYTEC. Compared with the application of it in diesel engine, biomass tar is more suitable as a fuel for gas turbine with less problems occurred during the testing. Co-firing of biomass tar with coal or natural gas has also been investigated and demonstrated on the commercial scale [26]. Future improvement in producing homogenous liquid with water content less than 30% and

no solid impurities from the biomass pyrolysis process should be done for the wide application of it in the diesel engines. In addition, long-term performance and reliability test is also required for the gas turbine application.

Although pyrolysis is commonly designed for producing biofuels, it is also a well-known route for hydrogen production through fast or flash pyrolysis via the eq. (1) if high temperature and sufficient volatile phase residence time are allowed [27]:

$$\text{Biomass} + \text{heat} \rightarrow H_2 + CO + CH_4 + \text{other products} \quad (1)$$

Generally, hydrogen production by pyrolysis is controlled by temperature, heating rate, residence time and type of catalyst used. High pyrolysis temperature can increase hydrogen yield percentage in the total gas produced. It is reported that pyrolysis of biomass at 1023 K can increase gas production to around 45-50% and high heating rate and long volatile phase residence time are also favored for the high hydrogen production. In addition, the liquid products of pyrolysis can be further processed for the hydrogen production through steam reforming reaction [27, 28].

1.2.2 Gasification

Gasification is a thermochemical process that converts organic or carbonaceous materials into valuable gases, usually called as synthesis gas (syngas), which mainly contains CO, H_2, CO_2, and CH_4, in the presence of gasifying agent (e.g., controlled amount of air or oxygen, steam, CO_2, or a mixture of these) at a temperature higher than 700 ^oC [23]. In general, a gasification process involves many reactions occurred simultaneously. **Table 1.1** lists the main reactions in the gasification process [18, 29]. Since gasification itself is a complex process, its efficiency is influenced by many factors, which include biomass composition, gasifying agents, biomass particle size, operating condition of gasification (temperature and pressure), and type of gasifier.

Table 1.1 Main reactions in biomass gasification

No.	Reaction	Name of reaction
1	$C + CO_2 \longleftrightarrow 2CO$	**Carbon reaction (**Boudouard**)**
2	$C + H_2O \longleftrightarrow CO + H_2$	**Carbon reaction** (Primary steam reforming)
3	$C + H_2O \longleftrightarrow CO_2 + H_2$	**Carbon reaction** (Secondary steam reforming)
4	$C + 2H_2 \longleftrightarrow CH_4$	**Hydrogasification**
5	$C + 0.5O_2 \longrightarrow CO$	**Oxidation reactions**
6	$C + O_2 \longrightarrow CO_2$	
7	$CO + 0.5O_2 \longrightarrow CO_2$	
8	$CH_4 + 2O_2 \longleftrightarrow CO_2 + H_2O$	
9	$H_2 + 0.5O_2 \longrightarrow H_2O$	
10	$CO + H_2O \longleftrightarrow CO_2 + H_2$	**Shift reaction**
11	$2CO + 2H_2 \longrightarrow CH_4 + CO_2$	**Methanization reactions**
12	$CO + 3H_2 \longleftrightarrow CH_4 + H_2O$	
15	$CO_2 + 4H_2 \longrightarrow CH_4 + 2H_2O$	
13	$CH_4 + H_2O \longleftrightarrow CO + 3H_2$	**Steam reactions**
14	$CH_4 + 0.5O_2 \longrightarrow CO + 2H_2$	

To date, air or oxygen, steam, carbon dioxide, or their mixtures are generally applied for the gasification. Which gasifying agent used for gasification process depends on the desired gas

composition and energy consumption [29]. Air is the most common used gasifying agent as it is cheap and readily available. However, since its high nitrogen content always lowers the heating value of syngas produced, pure oxygen or oxygen-rich air is proposed as the gasifying agent to produce the syngas with higher heating value, but it will increase the operating cost due to high energy required to separate oxygen and nitrogen in air. By using air as the gasifying agent, partial oxidation occurs in the gasifier depends on air to fuel ratio or equivalence ratio (ER) between air and biomass used. Normally, ER ratio is set to be lower than 1 to avoid the complete combustion. Also, ER ratio is considered as the most important factor to determine final heating value of syngas obtained. To control the production of tar and char, reasonable range of ER in the gasification process is about 0.2-0.4.

Steam is considered as the most promising gasifying agent to produce hydrogen from biomass via the gasification technology. Steam biomass gasification can produce 53-55 vol.% of H_2 in the final gas product whereas air gasification can only produce 8-10 vol.% of H_2. Lower tar production as well as lower cost than the partial oxidation by using pure oxygen generated from air are the main advantages of steam gasification. However, more energy is required due to the endothermic reactions for primary and secondary steam reactions and water gas shift reaction. To overcome energy shortage in steam gasification, the air and steam mixture as the gasifying agent for the gasification of biomass is mostly applied to achieve better thermodynamic efficiency even though it can only produce 25-30 vol.% of H_2. For biomass with high moisture content, supercritical water gasification can be considered for high hydrogen production. The process is conducted at above critical temperature (647 K) and critical pressure (22 MPa) of water, in which biomass is rapidly decomposed into small molecules or gases in a few minutes at a high efficiency. However, this technology requires high cost and makes the hydrogen price is higher than the current hydrogen price from steam methane reforming [30-32].

Temperature is the most important key factor in the gasification process since it directly controls the overall process and the final gasification result. In general, gas composition and yield, gas heating value, tar and char produced, carbon conversion, and cold gas efficiency

are all affected by temperature. Higher gasification temperature results in higher CO and H_2 contents and less tar content in the gas product with higher heating value. Also, the cold gas efficiency and carbon conversion increase with the increase in temperature [33]. Normally, gasification is held at a temperature over than 700 °C, and for the steam gasification, the temperature should be over 750 °C since the spontaneous steam reforming reaction can only occur at such conditions.

Gasification normally runs at a constant pressure. Nowadays, atmospheric gasification and pressurized gasification are generally investigated and applied. The atmospheric gasification is more common for the small-scale gasifier since its investment cost is low. In contrast, the pressurized gasification is more efficient and gives a higher gasification efficiency with lower amount of tar. Moreover, the syngas from the pressurized gasification is already at the pressurized condition, which is better for the subsequent utilization [34]. However, the investment cost is higher. In addition, from the view of point of chemical equilibrium, it should be noted that the gasification prefers to be done at low pressure and high temperature [35].

Gasifier is the reactor vessel where gasification reactions take place. To date, two types of biomass gasifiers, i.e., fixed bed gasifier and fluidized bed gasifier are widely applied. **Figure 1.2** shows schematic diagrams of those gasifiers. Fixed bed or moving bed gasifier is the oldest yet simplest gasification system. It is also the most economic one and suitable for the small-scale gasification process. Two types of fixed bed gasifiers, i.e., updraft and downdraft gasifiers, are generally used. In the updraft gasifier, biomass is introduced from the top side of vertical vessel reactor with the gasifying agent from the bottom side. As such, it is also known as a counter-current gasifier because biomass and gasifying agents contact with each other in the counter-current direction. This type is an effective way for gasification with a highly thermal efficiency since the sensible heat of hot gas is used for the heating/drying step within the system before leaving from the top side of gasifier at a low temperature (between 200-400 °C). Therefore, this type of gasifier has high tolerance of moisture content and can handle biomass with moisture content up to 60% on wet basis [36, 37]. However, even though

it has highly thermal efficiency and low pressure drop, the updraft gasifier is less likely to be used since more tar is generally generated in it because the tar from the pyrolysis zone flows upward to the cooler region and cannot reach the high temperature zone so that it has no chance to be converted into gases [38, 39].

The downdraft gasifier is the opposite of updraft process in the way of the gasifying agents introduced into the reactor. The gasifying agent is fed in at the top or at sides of gasifier, and at the same time, the biomass is also introduced from the same top side of reactor. As such, the direction of contact becomes co-current. That is to say, the contact of biomass and gasifying agent takes place along with the gasification steps, resulting better quality of the produced gas which leaves the reactor from bottom side. In this case, the tar production is low since the devolatilization products can reach the high temperature oxidation zone despite the residence time in that zone is not long enough to convert all the tar completely [37]. However, the heat transfer between hot and cold zones inside the reactor is very poor, causing the tolerance of moisture content is lower. Thusly, only biomass with a moisture content lower than 30% is acceptable to be processed. Moreover, the biomass residence time in the reactor is shorter because the biomass moves downward faster due to the drag force is aligned in the same direction as the gravity. As such, the efficiency of carbon conversion is lower than that in the updraft gasifier. This type gasifier is suitable for the small-scale power plant application with the typical capacity in the range of 10 kW-1 MW [31, 40].

The fluidized bed gasifier has enhanced mixing capability and heat transfer rate than the fixed bed gasifier by adopting fluidization mechanism. In the fluidized bed gasifier, the reaction temperature has more homogeneous distribution. The decomposition of biomass in the fluidized bed gasifier occurs rapidly with great mixing condition between biomass and gasifying agent, which results in higher reaction rate as well as high efficiency and conversion. This temperature uniformity can be easily achieved by utilization of bed materials to assist the fluidization of biomass [41], which allows biomass gasification in the fluidized bed under nearly isothermal condition. In general, the biomass fluidized bed gasification process generally operates at the temperature in the range of 800-1000 °C [34].

Bubbling fluidized bed gasifier (BFBG) and circulating fluidized bed gasifier (CFBG) are two main types of fluidized bed gasifiers. BFBG operates at a fluidization velocity normally below than 5 m/s or in range of 1-3 m/s to create particle and bubble emulsions in the bed. In contrast, CFBG operates at three to five times higher fluidization velocity than BFBG, and the fluidization phase performs in a turbulent state. It drives better mixing of biomass with the bed materials and gasifying agent in a short residence time, which can improve the heat transfer and enhance the reaction rate. As a result, CFBG has better gasification efficiency and higher carbon conversion with very low tar yield. However, CFBG design is much more complex and higher investment and operating cost are necessary [42].

Synthesis gas or syngas is the main product from a gasification process. Synthesis gas term is used because the product gases mainly contain CO and H_2, which are the basic chemicals to produce many complex chemicals for various applications such as hydrogen production, synthetic liquid fuels through Fischer-Tropsch process, synthetic natural gas (S-NG), synthetic chemicals like ammonia, methanol and its derivatives, and dimethyl ether. Syngas is also a popular alternative energy source for power generation [34]. Conventional syngas direct combustion via steam turbine and combination of gas and steam turbine are the most popular ways for large-scale power generation by gasification [43]. Combustion of syngas using internal combustion engine (ICE) is an alternative method for power generation, which is the most vital technology for power generation with variable power outputs. ICE technology is not so sensitive to gas impurities compared to gas turbine so that it has cost competitiveness with low cost, high reliability, and high operating efficiency [44, 45].

Syngas can be converted further to hydrogen by water gas shift (WGS) reaction shown as follow:

$$CO + H_2O \rightarrow CO_2 + H_2 \qquad (2)$$

Such kind of process is well known in industry, especially in ammonia production where syngas from natural gas steam reforming is converted into hydrogen through WGS reaction. Application on WGS process to produce hydrogen from syngas is now also emerging. The WGS reaction is moderately exothermic and equilibrium limited. Therefore, to obtain higher

hydrogen yield, the reaction is better to be conducted at low temperature. However, kinetically, low temperature operation is not favorable. In general, two-step reactions at different temperatures are carried out. The high temperature shift (HTS) conducted at 350-500 ^{o}C to firstly converted syngas at better kinetic with low equilibrium conversion and low temperature shift (LTS) is later conducted at 150-250 ^{o}C to improve conversion [46-48].

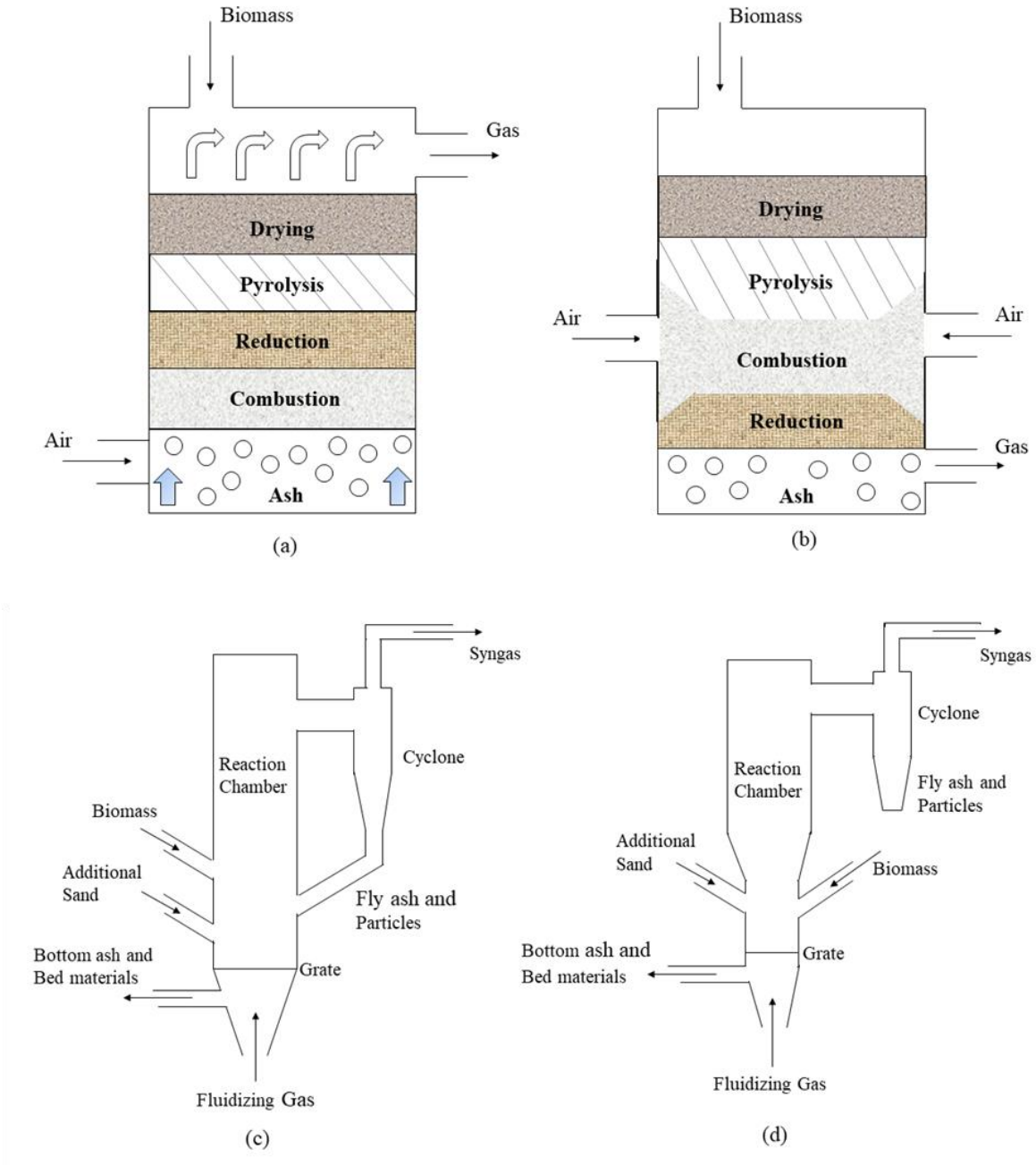

Figure 1.2 Schematic diagrams of (a) updraft, (b) downdraft, (c) bubbling fluidized bed, and (d) circulating fluidized bed gasifiers [36]

1.2.3 Direct combustion

Combustion is the simplest and the most conventional thermochemical process in which excess oxygen is used to burn biomass for the generation of heat. Direct combustion is the most widely utilized process for biomass conversion which contributes to over 97% of biomass utilization as energy production around the world [8]. Power generation capacity based on direct combustion process that has already installed globally is estimated at 40 GWe [12]. Recently, co-firing 5-10% of biomass with coal in the combined heat and power (CHP) process or co-generation of electricity is commonly known in the world. However, thermal efficiency of direct combustion is always low when compared with the gasification process. Moreover, the direct combustion is not an ideal process for hydrogen production from biomass.

1.2.4 Chemical looping process

Chemical looping process is a recently proposed thermochemical conversion concept to convert biomass into energy with the minimal energy penalty and cleaner waste products. The main principle of chemical looping process is the application of redox cycle of metal oxide as the oxygen carrier to convert biomass into energy with the minimal energy penalty and cleaner waste products. Based on the final products, various terminologies about the chemical looping were created, e.g., chemical looping combustion (CLC), chemical looping reforming (CLR), chemical looping gasification (CLG), and chemical looping hydrogen generation (CLH). While the CLC is usually used as a power generation through the combined heat and power (CHP) process, the CLH is more focusing on hydrogen production. Both CLR and CLG use the metal oxide as the catalyst as well as the heat carrier to produce syngas (CO and H_2) [49, 50].

The CLC process used two separated reactors. In the first reactor, the metal oxide is reduced by the fuel to produce CO_2 and H_2O, and in the second reactor, the reduced metal oxide is oxidized back to its initial state by oxygen in the air. This process has a great advantage over the conventional direct combustion process, that is, the flue gas of CO_2 and H_2O released separately from N_2 in air. Thus, the CLC process can be easily combined with CO_2 capture

process to recover almost 100% of CO_2 from the flue gas without consuming any extra energy for separation from H_2O. The CLH process adopts the similar concept with the CLC with one additional reactor between first and second reactors to convert steam to hydrogen by partially oxidized the metal oxide used in the cycle as shown in **Figure 1.3**. The main advantage of the CLH is that it can generate pure H_2 with only a simple separation process [50, 51].

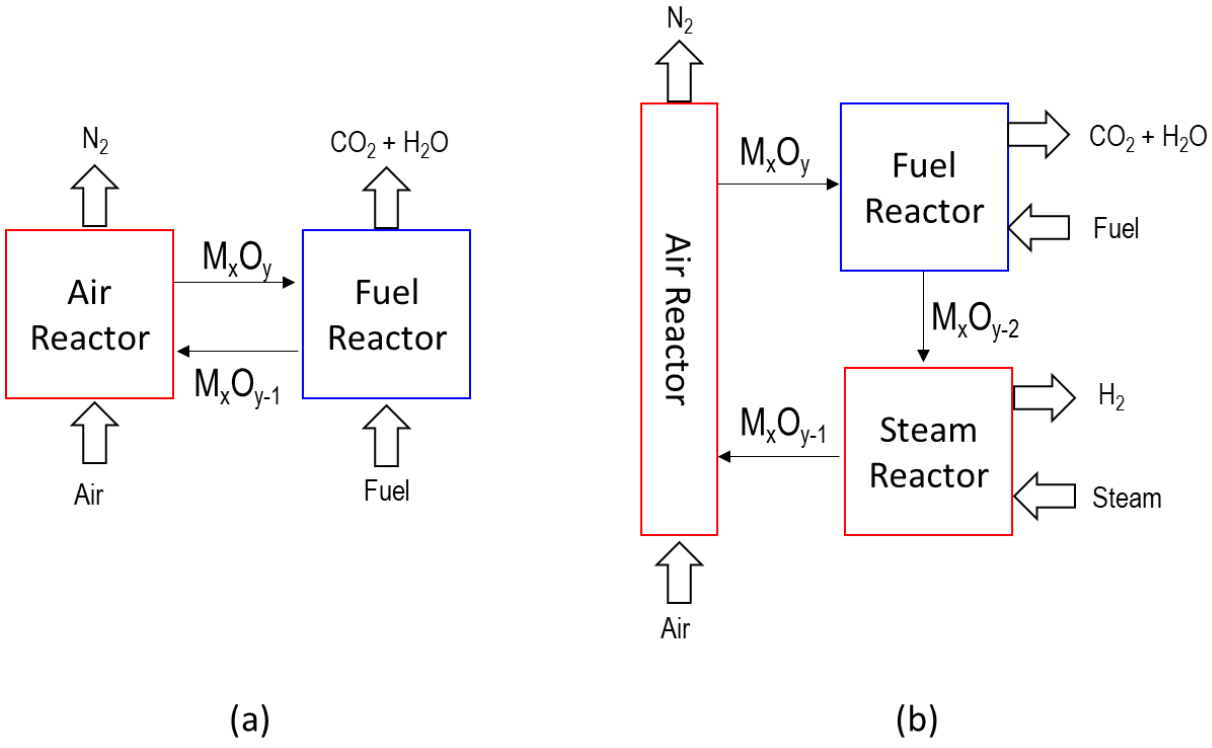

Figure 1.3 Schematic diagram of (a) CLC and (b) CLH processes

The primary fuels used as fuels for the chemical looping process can be gaseous materials, i.e. natural gas or methane, and syngas from the gasification process or solid materials, i.e. coal, biomass, and also biochar. While the gaseous fuels is more preferable for the chemical looping process because solid materials is less reactive and solid-solid reaction with the metal oxide hardly occurs in any appreciable rate than gas-solid reaction, there are increasing interests in using coal, biomass, and biochar directly for the chemical looping process since those are more abundant than natural gas. The direct solid chemical looping process

simplifies the process and increases the efficiency compared to generate syngas through gasification process at first [52].

1.3 Hybrid process of thermochemical conversion

1.3.1 Development of two-stage gasification system

In general, gasification process includes 4 primary steps: heating and drying, decomposition or pyrolysis, oxidation or partial combustion and/or reduction or gasification. Direct gasification of biomass always faces tar problems which produced during gasification in pyrolysis step at mild temperature (300-500 ^{o}C). Tar is undesirable side product that can comes out along with syngas and if it condenses at low temperature, it can cause pipe clogging and other problems within the systems. Two ways are commonly used to overcome the tar problem, i.e., *in-situ* treatment inside the gasifier and hot gas cleaning after the gasification process [29, 53]. Besides, tar formation during the gasification tends to hinder gasification of char in the next step of char gasification process. Thus, to improve the whole gasification efficiency, it is better to separate the pyrolysis and gasification process in early stage to remove tar firstly and simultaneously enhance the char gasification [54]. This concept is usually called as two-stage gasification system. **Figure 1.4** illustrates this two-stage gasification system.

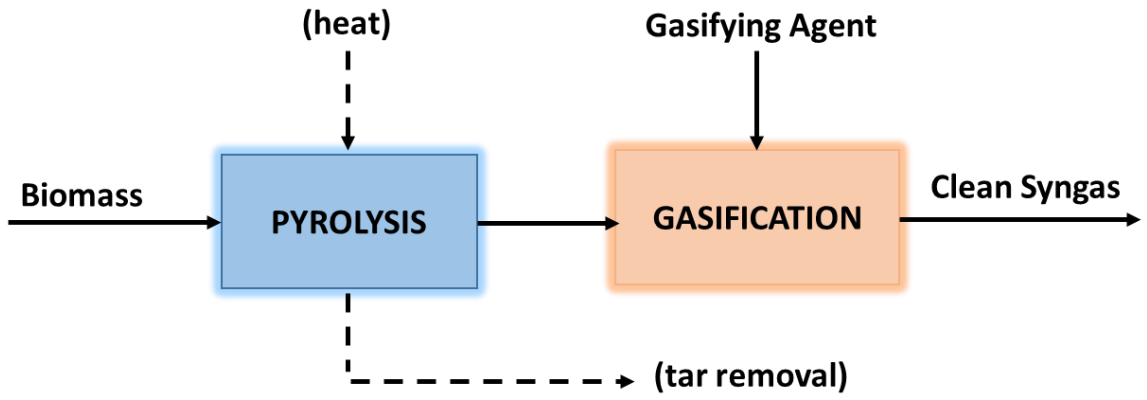

Figure 1.4 Schematic diagram of the two-stage gasification concept

An early successful two-stage gasification processes was Viking Gasifier developed by Biomass Gasification Group at Technical University of Denmark (DTU) in 2002 [55]. The system consists of a screw type pyrolyzer and a downdraft fixed bed gasifier while hot exhaust gas from the connected gas engine is used to provide heat for the pyrolyzer. The tar is reduced by partial oxidation at a very high temperature (over 1000 ^{o}C) between the pyrolysis and char gasification processes. It is reported that the tar content decreased to less than 15 mg/Nm^3 in the syngas [56]. Earlier than Viking Gasifier, Asian Institute of Technology (AIT) in Thailand proposed a two-stage throatless reactor which tried to separate the pyrolysis zone and gasification/reduction zone inside one downdraft gasifier so that the tar content was decreased to 92 mg/Nm^3 [57]. The concept of Viking Gasifier was later adapted for a coal processing unit at Institute of Process Engineering (IPE), Chinese Academy of Science (CAS). The system consists of an autothermal fluidized bed pyrolyzer and a downdraft fixed bed gasifier where the tar is further reformed by using hot char as the catalyst, by which the tar content was lowered to 84 mg/Nm^3 [58]. Recently, a comprehensive system consists of a downer pyrolyzer, a bubbling fluidized bed char gasifier and a riser combustor for combustion of unreacted char was proposed. The heat carrier of inert solids medium such as silica sand circulated in the system [54].

1.3.2 Combination with steam tar reforming

The tar from biomass pyrolysis can be converted into syngas by steam reforming reaction as follows:

$$C_xH_yO_z + (x\text{-}z)H_2O \rightarrow xCO + [y/2+x\text{-}z]H_2 \quad (3)$$

and with excess steam, the CO produced can be further converted into hydrogen by water gas shift (WGS) reaction as shown by Eq. 2 [29]. Thus, steam tar reforming is considered as the most effective and promising route to convert tar to H_2 or syngas [59]. Theoretically, about 6 kg of H_2 can be obtained by steam reforming of bio-oil produced from pyrolysis of 100 kg woody biomass. It is reported that the commercial Ni-based catalysts has good activity for the steam tar reforming and the deactivated catalysts can be also easily regenerated for reusing [60]. Besides Ni, other transition metals such as Co, Fe, Cu, and Zn also can be used

as the catalysts for the steam tar reforming. However, Ni has the higher activity compared with others, with the ranks of activity described as Ni > Co > Fe > Cu. Alkali and alkali earth metals, natural minerals such as dolomite, olivine, and shells, zeolite, and activated carbon are also reported to have high catalytic activity for steam reforming reaction [29, 61].

Wang *et al.* [62] used a two-stage gasification system by applying direct biomass gasification in the 1st stage and non-catalytic tar reformer in the 2nd stage, which was successfully reduced tar the tar content to be lower than 100 mg/Nm^3. Kaewpanha *et al.* [63] implemented steam biomass gasification and steam tar reforming simultaneously in one fixed bed reactor using Cu supported calcined scallop shell as the catalysts while Widayatno *et al.* [64] used the same procedure with biomass char as the catalyst. Considering the traditional two-stage gasification system, in which pyrolysis and gasification processes are separated, the tar generated from the pyrolysis process can be further converted into syngas with the increase in the total efficiency for the system. As such, a three-stage system consisting of biomass pyrolysis, biochar gasification, and steam tar reforming was also proposed as a potential process for the effective gasification of biomass.

1.3.3 Combined heat and power (CHP)

The combined heat and power (CHP) or cogeneration system is a common term to describe a process of power generation with the recovery of waste heat in the system to generate extra power and heat simultaneously. Nowadays, about 9% of world's power generation systems containing the CHP system [65]. In general, direct combustion is the most applied technology for biomass CHP. Biomass CHP plant in St Paul, Minnesota, USA can produce 33 MWe and 65 MWth simultaneously by using 250,000 tonnes of wood chips annually. Gasification with CHP can effectively produce syngas as the fuel for gas engine to generate power and recovered heat from both the gasifier and the gas engine for steam generation [66]. Integrated Gasification Combine Cycle (IGCC) is now a popular system for power generation combining gasification with gas turbine for syngas combustion and steam turbine for waste heat recovery to increase plant efficiency [67].

Recently, chemical looping combustion (CLC) is an emerging technology for CHP. The CLC is as an oxy-fuel combustion method with no contact between air and fuel that easily combined with CO_2 capture process since it is easy to recover almost 100% of CO_2 from the flue gas by a simple separation method [51, 68]. Utilization of syngas from gasification is considered as the most popular way to convert biomass into energy using chemical looping process since the gas feedstock is more favorable. Zhu *et al.* [69] suggested a hybrid power generation process consisting of biomass steam/O_2 gasification, chemical looping air separation (CLAS), syngas CLC with gas and steam turbines, by which the total energy and net power efficiencies of 66.2% and 16.3% were achieved, respectively. A pilot plant combining a fluidized bed biomass steam gasification and a dual circulating fluidized bed CLC process has been successfully run for 10 h operation by Penthor *et al.* [70]. The power generation using such a chemical looping process is also easily combined with the hydrogen production. For example, Calin-Cristian Cormos [71] proposed and assessed a co-production system of hydrogen and power generations using the biomass direct chemical looping (BDCL) concept, which exhibited a power net efficiency of 42%. A pilot plant of BDCL-CLC system with 0.5 kWth has been successfully tested for 40 h using three different kinds of biomass (pine sawdust, olive stone and almond shell) by Mendiara *et al.* [72]. **Table 1.2** shows possible technologies applied in the biomass CHP system [68, 73].

Table 1.2 Major technologies for biomass-based CHP systems

Primary technology	Secondary technology
Direct combustion	Steam turbine, ORC, Stirling engine
Chemical looping combustion (CLC)	Steam turbine, ORC, Stirling engine
Gasification	Internal gas engine, gas turbine, steam turbine, ORC
Chemical looping reforming (CLR), Chemical looping gasification (CLG)	Water gas shift (WGS), Internal gas engine, gas turbine, steam turbine, ORC

Chemical looping hydrogen (CLH)	Internal gas engine, gas turbine, SOFC, PEMFC
Bio-oils (from pyrolysis)	Internal gas engine
Biogas (from anaerobic biological process)	Internal gas engine, WGS, CLR, SOFC
Biodiesel	Internal gas engine

A conventional configuration of CHP consists of a combustor combining with a power generator and a heat exchanger to recover the heat brought by the exhaust from the combustor [74, 75]. While, the recovered heat can be further converted into additional power, in general, water/steam is usually used as a media for waste heat recovery by thermodynamic Carnot or Rankine cycle and convert it into power by steam turbine. The combination of direct combustion and steam turbine is the most widely applied technology for the large-scale and medium-scale biomass CHPs. However, the steam needs to be in a superheated form in order to prevent the condensation inside the turbine, which needs the temperature of turbine inlet higher than 450 ^{o}C at a high pressure over than 60 bar. However, since biomass has low heating value, the gas produced from the combustion of biomass only can obtain the heat with a temperature around 300 ^{o}C The steam also requires larger equipment and several expansion stages to achieve higher efficiency, making the cost for classic steam boiler is not competitive and the traditional steam cycles not effective for the small-scale biomass CHP [76].

In order to solve this issue, organic fluid is proposed to replace water as the heat absorber media in the Rankine cycle. Thus, the organic Rankine cycle (ORC) process has more advantages and higher efficiency for the waste heat recovery at low temperature. Moreover, organic fluid has a lower boiling point and does not need to be in the superheated state as the steam in order to prevent the condensation in the turbine. As such, it needs only a single expansion stage to achieve high efficiency. Thus, it has simpler design and is more suitable for a small-scale power generation system. Biomass-fired CHP with the ORC waste heat

recovery system is now commercially available with a typical electrical efficiency of ca. 20% [73, 77].

1.4 Motivation and objectives

One of major problems in biomass utilization for energy production is biomass feedstock collection since it can increase the operating cost or disturb the process of energy generation and impact the energy price. Many large-scale systems tend to experience this problem. Thus, the small-scale biomass to energy system is more preferable since it can utilize locally-produced biomass effectively and simultaneously resolve the biomass collection problem. The emergence of novel hybrid system such as the two-stage gasification system drives the focus of biomass gasification research to find the suitability of such a system in the small-scale operation. Especially, the novel small-scale biomass conversion system should be suitable for various types of biomass since the present ones are more suitable for the high-quality biomass resources like woody biomass. Furthermore, there is an open opportunity for development of novel hybrid systems combining various conventional biomass conversion processes for effective conversion of various biomass resources. Therefore, the main objectives of this study are focusing on the following points:

a. To investigate suitability of different biomass feedstocks for two-stage gasification system;
b. To develop novel hybrid system for the small-scale biomass to energy applications, especially in power generation and hydrogen production;
c. To evaluate the process efficiencies of the proposed novel small-scale biomass conversion systems for power generation and hydrogen production.

1.5 Organization and outline of this dissertation

This dissertation, firstly considers about the compatibility and synergistic effect existencein various biomass mixture during the thermal conversion process by experimentally

investigating the co-pyrolysis of various biomass with different properties and co-gasification of their char to give a guidance of biomass selection in the two-stage gasification system.Later, advanced small-scale biomass energy systems especially for the power generation and hydrogen production were designed and analyzed. The following 7 chapters includes:

Chapter 1 briefly introduces the current state of biomass into energy technologies and their current applications. The recent research and development progress and the issues are summarized and discussed. Finally, the motivation, objectives and outline of this research are given.

Chapter 2 describes the general research materials, experimental apparatus, and characterization methods used in this study. Meanwhile, a brief introduction of Aspen Plus as the general software used for process simulation in this study is given.

Chapter 3 reports the results of utilization of biomass co-pyrolysis and gasification of co-chars in a two-stage gasification system. Synergistic effect existence between different biomass during the co-pyrolysis process to increase the total gasification efficiency was investigated.

Chapter 4 provides an empirical analysis of a novel small-scale separated-type biomass gasification system including biomass pyrolysis, steam tar reforming, biochar gasification and combustion for power generation. The overall system efficiency was investigated by comparing fast and slow pyrolysis processes.

Chapter 5 assesses the possibility of a novel small-scale biomass hydrogen production system consists of biomass pyrolysis, steam tar reforming, and biochar direct chemical looping hydrogen (CLH) processes with heat recuperation. The hydrogen production efficiency of the system was compared with other hydrogen production methods.

Chapter 6 presents a process design and simulation of a small-scale power generation system using biomass direct chemical looping (BDCL) combustion process with organic Rankine

cycle (ORC) as waste heat recovery unit. Various working fluids were investigated for the ORC process.

Chapter 7 summarizes the highlights of all results in this dissertation and provides the perspectives of the possible future works related with this dissertation study.

References

[1] IEA, Monthly energy review June 2018, International Energy Agency, 2018,

[2] IEA, Key world energy statistics, International Energy Agency, 2017,

[3] BP, Energy outlook 2018, British Petroleum Energy Economics, 2018,

[4] C.-J. Winter, Hydrogen energy — Abundant, efficient, clean: A debate over the energy-system-of-change, International Journal of Hydrogen Energy, 34 (2009) S1-S52.

[5] C. Mansilla, C. Bourasseau, C. Cany, B. Guinot, A.L. Duigou, P. Lucchese, Hydrogen Applications: Overview of the Key Economic Issues and Perspectives, Hydrogen Supply Chain, Elsevier Ltd.2018, pp. 271-292.

[6] N.H. Florin, A.T. Harris, Hydrogen production from biomass, Environmentalist, 27 (2007) 207-215.

[7] M. Ni, D.Y.C. Leung, M.K.H. Leung, A review on reforming bio-ethanol for hydrogen production, International Journal of Hydrogen Energy, 32 (2007) 3238 – 3247.

[8] A. Bhavanam, R.C. Sastry, Biomass gasification processes in downdraft fixed bed reactors: A review, International Journal of Chemical Engineering and Applications, 2 (2011) 425-433.

[9] L. Zhang, C.C. Xu, P. Champagne, Overview of recent advances in thermo-chemical conversion of biomass, Energy Conversion and Management, 51 (2010) 969-982.

[10] S. Ladanai, J. Vinterbäck, Global potential of sustainable biomass for energy, SLU, 2009,

[11] IEA, Electricity from biomass: From small to large scale, IEA Bioenergy, 2013,

[12] T.B. Johansson, K. McCormick, L. Neij, W. Turkenburg, The potentials of renewable energy, International Conference for Renewable Energies., 2004,
[13] REN21, Renewables 2016 global status report, Renewable Energy Policy Network for the 21st Century2016.
[14] S.B. Kontor, Potential of biomass gasification and combustion technology for small- and medium-scale applications in Ghana, International Energy Technology and Management Program Vaasan Ammattikorkeakoulu University of Applied Sciences, 2013,
[15] M. Balat, G. Ayar, Biomass energy in the world, use of biomass and potential trends, Energy Sources, 27 (2005) 931-940.
[16] N.u.R. Chowdhury, Advances and trends in woody biomass gasification, Energy Engineering and Management Tecnico Lisboa, 2014,
[17] WEC, World energy resources, World Energy Council, 2016,
[18] A. Ramos, E. Monteiro, V. Silva, A. Rouboa, Co-gasification and recent developments on waste-to-energy conversion: A review, Renewable and Sustainable Energy Reviews, 81 (2018) 380-398.
[19] J.G. Speight, Handbook of coal analysis. 2nd ed, John Wiley & Sons, Inc.2015.
[20] L. Burhenne, J. Messmer, T. Aicher, M.-P. Laborie, The effect of the biomass components lignin, cellulose and hemicellulose on TGA and fixed bed pyrolysis, Journal of Analytical and Applied Pyrolysis, 101 (2013) 177-184.
[21] Z. Zhang, S. Pang, T. Levi, Influence of AAEM species in coal and biomass on steam co-gasification of chars of blended coal and biomass, Renewable Energy, 101 (2017) 356-363.
[22] K. Kundu, A. Chatterjee, T. Bhattacharyya, M. Roy, A. Kaur, Thermochemical Conversion of Biomass to Bioenergy: A Review, Prospects of Alternative Transportation Fuels, Springer, Singapore, 2017.
[23] V. Dhyani, T. Bhaskar, A Comprehensive Review on The Pyrolysis of Lignocellulosic Biomass, Renewable Energy, 19 (2018) 695-716.
[24] P. Roy, G. Dias, Prospects for pyrolysis technologies in the bioenergy sector: A review, Renew Sust Energ Rev, 77 (2017) 59-69.

[25] D. Neves, H. Thunman, A. Matos, L. Tarelho, A. Gómez-Barea, Characterization and Prediction of Biomass Pyrolysis Products, Progress in Energy and Combustion Science, 37 (2011) 611-630.
[26] D. Chiaramonti, A. Oasmaa, Y. Solantausta, Power generation using fast pyrolysis liquids from biomass, Renewable and Sustainable Energy Reviews, 11 (2007) 1056–1086.
[27] M. Ni, D.Y.C. Leung, M.K.H. Leung, K. Sumathy, An overview of hydrogen production from biomass, Fuel Processing Technology, 87 (2006) 461-472.
[28] E. Kırtay, Recent advances in production of hydrogen from biomass, Energy Conversion and Management, 52 (2011) 1778–1789.
[29] G. Guan, M. Kaewpanha, X. Hao, A. Abudula, Catalytic steam reforming of biomass tar: Prospects and challenges, Renewable and Sustainable Energy Reviews, 58 (2016) 450-461.
[30] V.S. Sikarwar, M. Zhao, P. Clough, J. Yao, X. Zhong, M.Z. Memon, N. Shah, E.J. Anthony, P.S. Fennell, An overview of advances in biomass gasification, Energy and Environmental Science, (2016).
[31] N. Mahinpey, A. Gomez, Review of gasification fundamentals and new findings: Reactors, feedstock, and kinetic studies, Chemical Engineering Science, 148 (2016) 14-31.
[32] A. Inayat, M.M. Ahmad, S. Yusup, M.I.A. Mutalib, Z. Khan, Biomass Steam Gasification for Hydrogen Production: A Systematic Review, Biomass and Bioenergy: Processing and Properties, Springer Link International Publishing2014, pp. 329-343.
[33] L.E. Taba, M.F. Irfan, W.A.M.W. Daud, M.H. Chakrabarti, The effect of temperature on various parameters in coal, biomass and co-gasification: A review, Renewable and Sustainable Energy Reviews, 16 (2012) 5584-5596.
[34] J.A. Ruiz, M.C. Juarez, M.P. Morales, P. Munoz, M.A. Mendivil, Biomass gasification for electricity generation: Review of current technology barriers, Renewable and Sustainable Energy Reviews, 18 (2013) 174-183.
[35] P. Parthasarathy, K.S. Narayanan, Hydrogen production from steam gasification of biomass: Influence of process parameters on hydrogen yield - A review, Renewable Energy, 66 (2014) 570-579.

[36] S.K. Sansaniwal, K. Pal, M.A. Rosen, S.K. Tyagi, Recent advances in the development of biomass gasification technology: A comprehensive review, Renewable and Sustainable Energy Reviews, 72 (2017) 363–384.
[37] M. Kouhia, Biomass gasification, Department of Energy Technology Aalto University School of Engineering, 2011,
[38] P. Basu, Biomass gasification, pyrolysis and torrefaction. 2nd ed, Elsevier Inc.2013.
[39] Y. Kumar, Biomass gasification - a review, International Jounal of Engineering Studies and Technical Approach, 01 (2015) 12-28.
[40] A.A.P. Susastriawan, H. Saptoadi, Purnomo, Small-scale downdraft gasifiers for biomass gasification: A review, Renewable and Sustainable Energy Reviews, 76 (2017) 989-1003.
[41] T.K. Patra, P.N. Sheth, Biomass gasification models for downdraft gasifier: A state of the art review, Renewable and Sustainable Energy Reviews, 50 (2015) 583-593.
[42] Y.A. Situmorang, Z. Zhao, A. Yoshida, A. Abudula, G. Guan, Small-scale biomass gasification systems for power generation (<200 kW class): A review, Renew Sust Energ Rev, 117 (2020).
[43] L. Wang, C.L. Weller, D.D. Jones, M.A. Hanna, Contemporary issues in thermal gasification of biomass and its application to electricity and fuel production, Biomass and Bioenergy, 32 (2008) 573-581.
[44] F.Y. Hagos, A.R.A. Aziz, S.A. Sulaiman, Trends of syngas as a fuel in internal combustion engines, Advances in Mechanical Engineering, (2014).
[45] R.P. Bates, K. Dölle, Syngas use in internal combustion engines - a review, Advances in Research, 10 (2017) 1-8.
[46] B.S.R. J, M. Loganathany, M.S. Shantha, A review of thewater gas shift reaction kinetics, International Journal Of Chemical Reactor Engineering, 8 (2010).
[47] P. Kumar, E. Akpan, H. Ibrahim, A. Aboudheir, R. Idem, Kinetics and reactor modeling of a high temperature water-gas shift reaction (WGSR) for hydrogen production in a packed bed tubular reactor (PBTR), Industrial & Engineering Chemistry Research, 47 (2008) 4086–4097.

[48] T.K. Patra, S. Mukherjee, P.N. Sheth, Process simulation of hydrogen rich gas production from producer gas using HTS catalysis, Energy, 173 (2019) 1130-1140.
[49] B. Moghtaderi, Review of the recent chemical looping process developments for novel energy and fuel applications, Energy & Fuels, 26 (2012) 15-40.
[50] Z. Yu, Y. Yang, S. Yang, Q. Zhang, J. Zhao, X. Hao, G. Guan, Iron-based oxygen carriers in chemical looping conversions: A review, Carbon Resources Conversion, 2 (2019) 23-34.
[51] M. Luo, Y. Yi, S. Wang, Z. Wang, M. Du, J. Pan, Q. Wang, Review of hydrogen production using chemical-looping technology, Renewable and Sustainable Energy Reviews, 81 (2018) 3186-3214.
[52] J. Adanez, A. Abad, F. Garcia-Labiano, P. Gayan, L.F.d. Diego, Progress in chemical-looping combustion and reforming technologies, Progress in Energy and Combustion Science, 38 (2012) 215-282.
[53] L. Devi, K.J. Ptasinski, F.J.J.G. Janssen, A Review of The Primary Measures for Tar Elimination in Biomass Gasification Processes, Biomass and Bioenergy, 24 (2003) 125-140.
[54] G. Guan, C. Fushimi, A. Tsutsumi, M. Ishizuka, S. Matsuda, H. Hatano, Y. Suzuki, High-density circulating fluidized bed gasifier for advanced IGCC/IGFC—Advantages and challenges, Particuology, 8 (2010) 602-606.
[55] B. Gobel, C. Hindsgaul, U.B. Henriksen, J. Ahrenfeldt, F. Folk, N. Houbak, E.B. Qvale, High Performance Gasification with the Two-Stage Gasifier, 12. European Biomass Conference, ETA-Florence & WIP-Munich, 2002, pp. 389-395
[56] U.B. Henriksen, J. Ahrenfeldt, T.K. Jensen, B. Gobel, J.D. Bentzen, C. Hindsgaul, L.H. Sorensen, The Design, Construction and Operation of a 75 kW Two-Stage Gasifier, The 16. International Conference of Efficiency, Cost, Optimization, Simulation, and Environmental Impact of Energy Systems, ECOS 2003, 2003, pp. 1081-1088
[57] T. Bui, R. Loof, S.C. Bhattacharya, Multi-stage reactor for thermal g asification of wood, Energy, 19 (1994) 397-404.

[58] X. Zeng, F. Wang, H. Li, Y. Wang, L. Dong, J. Yu, G. Xu, Pilot Verifiacation of a Low-Tar Two-Stage Coal Gasification Process with a Fluidized Bed Pyrolyzer and Fixed Bed Gasifier, Applied Energy, 115 (2014) 9-16.
[59] G. Esteban-Díez, M.V. Gil, C. Pevida, D. Chen, F. Rubiera, Effect of operating conditions on the sorption enhanced steam reforming of blends of acetic acid and acetone as bio-oil model compounds, Applied Energy, 177 (2016) 579-590.
[60] Z. Qi, C. Jie, W. Tiejun, X. Ying, Review of biomass pyrolysis oil properties and upgrading research, Energy Conversion and Management, 48 (2007) 87-92.
[61] Z. Zhao, Y.A. Situmorang, P. An, N. Chaihad, J. Wang, X. Hao, G. Xu, A. Abudula, G. Guan, Hydrogen production from catalytic steam reforming of bio-oils: a critical review, Chemical Engineering & Technology, 43 (2020) 625-640.
[62] Y. Wang, K. Yoshikawa, T. Namioka, Y. Hashimoto, Performance optimization of two-staged gasification system for woody biomass, Fuel Processing Technology, 88 (2007) 243-250.
[63] M. Kaewpanha, S. Karnjanakom, G. Guan, X. Hao, J. Yang, A. Abudula, Removal of biomass tar by steam reforming over calcined scallop shell supported Cu catalysts, Journal of Energy Chemistry, 26 (2017) 660-666.
[64] W.B. Widayatno, G. Guan, J. Rizkiana, X. Hao, C. Samart, A. Abudula, Steam reforming of tar derived from Fallopia Japonica stem over its own chars prepared at different conditions, Fuel, 132 (2014) 204-210.
[65] P. Breeze, An Introduction to Combine Heat and Power, Combined Heat and Power, Academic Press2018, pp. 1-11.
[66] P. Breeze, Renewable Energy Combined Heat and Power, Combined Heat and Power, Academic Press2018, pp. 77-83.
[67] T. Wang, An overview of IGCC systems, Integrated Gasification Combined Cycle (IGCC) Technologies, Woodhead Publishing2017, pp. 1-80.
[68] M. Rajabi, M. Mehrpooya, Z. Haibo, Z. Huang, Chemical looping technology in CHP (combined heat and power) and CCHP (combined cooling heating and power) systems: A critical review Applied Energy, 253 (2019).

[69] L. Zhu, H. Chen, Z. Zhang, Performance analysis of a new integrated gasification t echnology driven by biomass for hydrogen and e lectricity cogeneration with a dual chemical looping p rocess Energy Technology, 4 (2016) 1-13.
[70] S. Penthor, K. Mayer, S. Kern, H. Kitzler, D. Wöss, T. Pröll, H. Hofbauer, Chemical-looping combustion of raw syngas from biomass steam gasification – Coupled operation of two dual fluidized bed pilot plants, Fuel, 127 (2014) 178-185.
[71] C.-C. Cosmos, Biomass direct chemical looping for hydrogen and power co-production: Process configuration, simulation, thermal integration and techno-economic assessment Fuel Processing Technology, 137 (2015) 16-23.
[72] T. Mendiara, A. Pérez-Astray, M.T. Izquierdo, A. Abad, L.F. de Diego, F. García-Labiano, P. Gayán, J. Adánez, Chemical Looping Combustion of different types of biomass in a 0.5 kWth unit Fuel, 211 (2018) 868-875.
[73] L. Dong, H. Liu, S. Riffat, Development of small-scale and micro-scale biomass-fuelled CHP systems – A literature review Applied Thermal Engineering, 29 (2009) 2119–2126.
[74] A.A. Aliabadi, M.J. Thomson, J.S. Wallace, Efficiency Analysis of Natural Gas Residential Micro-cogeneration Systems, Energy & Fuels, 24 (2009) 1704–1710.
[75] P. Arbabi, A. Abbassi, Z. Mansoori, M. Seyfi, Joint numerical-technical analysis and economical evaluation of applying small internal combustion engines in combined heat and power (CHP), Applied Thermal Engineering, 25 (2017) 694-704.
[76] S. Quoilin, M.V.D. Broek, S. Declaye, P. Dewallef, V. Lemort, Techno-economic survey of Organic Rankine Cycle (ORC) systems, Renewable and Sustainable Energy Reviews, 22 (2013) 168-186.
[77] K. Rahbar, S. Mahmoud, R.K. Al-Dadah, N. Moazami, S.A. Mirhadizadeh, Review of organic Rankine cycle for small-scale applications, Energy Conversion and Management, 134 (2017) 135-155.

CHAPTER 2 : MATERIALS AND EXPERIMENTAL METHODS

2.1 Biomass feedstocks

The biomass feedstocks used in this study are Apple tree branch (ATB), knotweed stem (KWS), seaweed (SW), and rice straw (RSt) collected from Aomori Prefecture, Japan. Prior to experiment, all of them were washed and air dried under sunlight for several days, and then were cut and sieved to a size range of 0.5-2.8 mm. The elemental compositions of biomass were analyzed using a Vario EL cube elemental analyzer (Elementar, Germany). The biomass ash was obtained by calcination of each biomass at 800 ^{o}C for 2 h, and the compositions were determined using an energy dispersive X-ray fluorescence spectrometer (EDX-800HS, Shimadzu, Japan). The moisture content in biomass was analyzed using a moisture analyzer (MX-50, AND, Japan). **Table 2.1** summarized the properties of all biomass samples.

Table 2.1 Elemental composition, moisture and ash contents, and ash composition of biomass samples

Elemental Composition (wt%-d-af)	**ATB**	**KWS**	**SW**	**RSt**
C	43.7	44.79	39.2	35.1
H	6.2	5.88	5	5.3
N	0.5	0.28	1.8	0.4
S	0	0.02	0	0
O*	49.6	49.03	53.9	59.3
Moisture and ash (wt%)				
Moisture	7.8	8.81	13.3	9.3
Ash	1.8	2.87	11.6	14.9
Ash composition (wt%)				
Ca	65.85	44.03	70.76	2.59

K	8.33	50.24	2.38	26.85
Na	n.d.	n.d.	3.72	n.d.
S	4.34	2.69	4.42	3.19
P	8.18	1.68	1.11	2.42
Si	1.75	0.7	5.96	53.21
Fe	0.22	0.62	3.08	2.36
Mg	n.d.	n.d.	6.17	n.d.
Mn	n.d.	n.d.	0.29	0.51
Zn	n.d.	n.d.	n.d.	0.04
Cu	n.d.	n.d.	n.d.	0.04

* by difference

n.d. = not detected

2.2 Experimental setup

Experiments of pyrolysis and steam gasification in this study were conducted in a vertical steel tube-type fixed bed reactor with an inner diameter and a length of 18 mm and 350 mm, respectively. For each experiment, sample of biomass or biochar was place in the middle part of reactor with the position was adjusted by a steel mash. To keep the sample steady inside the reactor, thin pack of quartz wool was placed in the top and bottom side of the sample. The reactor was then placed inside an electrical furnace that provide heat for reactions with heating rate of 10 ^{o}C/min. Argon (Ar) was used as the carrier gas with flow rate of 50 ml/min. The pyrolysis was performed at 500 ^{o}C for 2 h, while gasification is conducted at 750 ^{o}C for 90 min. For steam gasification experiment, the steam was flowed into the fixed-bed reactor from the top with a flow rate of 0.2 g/min. Water was pumped to a vaporization furnace operated at 250 ^{o}C by a peristaltic pump to generate the steam. The produced gas was passed through two cooling baths and a drier cylinder filled with $CaCl_2$ particles for water absorbent before collecting in a gas bag. The tars and water from reacted sample and condensed steam were expected to be trapped in both of cooling baths. The solid residue was collected from the inside of the reactor after experiment, which for pyrolysis was collected as biochar and

for gasification was collected as waste assumed to be only consisted of ash and carbon. Later, the collected gas in the gas bag was analyzed using a gas chromatograph (GC-TCD, Agilent 7890-USA) to determine the gas compositions of CO, CO_2, CH_4, and H_2. **Figure. 2.1** illustrates the schematic diagram of experimental setup described above.

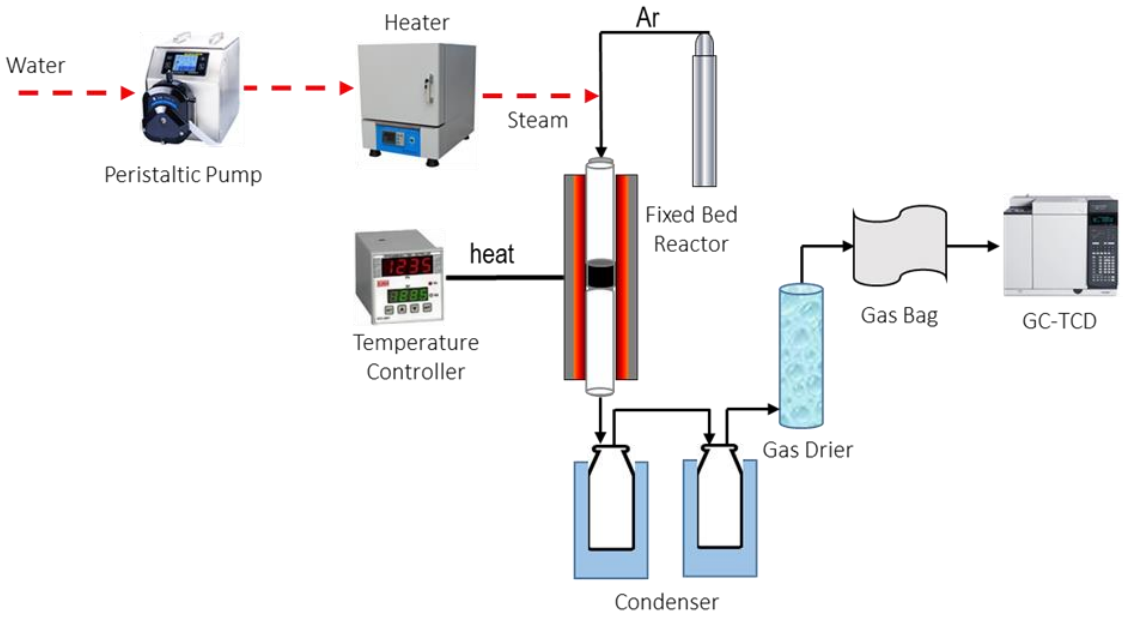

Figure 2.1 Schematic diagram of experimental setup for pyrolysis and gasification

2.3 Characterization

2.3.1 GC-TCD

The gas product collected in the gas bag was analyzed using a gas chromatograph with two thermal conductivity detectors (GC-TCD, Agilent 7890-USA) to determine the gas compositions main product gases from gasification of CO, CO_2, CH_4, and H_2, in which one thermal conductivity detector (TCD) is connected to three columns contained with 1 HayeSep Q column and 2 molecular sieve 5A columns to detect CO_2, CH_4, and CO using He as carrier gas, and the other TCD is connected to a combination of a single molecular sieve 5A and HayeSep Q columns to detect H_2 using Ar as carrier gas. The front inlet operated at temperature of 150 ^oC that injected gas with total flow rate of 23 ml/min, while the back inlet

operated at temperature of 150 ^{o}C and pressure of 18 psi (1.22 atm). The oven operated firstly at temperature of 60 ^{o}C with holding time of 1 min then it was increased to 70 ^{o}C with heating rate of 2.5 ^{o}C/min and no holding time, lastly it was increased to 100 ^{o}C with heating rate of 20 ^{o}C/min and holding time of 1.5 min, so that the total analysis time was 8 min. The both front and back of thermal conductivity detectors (TCD) were operated at temperature of 200 ^{o}C with both of carrier gases flow rate of 30 ml/min. Each columns of molecular sieve 5A and HayeSep Q had length of 6 ft (1.83 m) with outside diameter (OD) of 3.175 mm and inside diameter (ID) of 2 mm.

2.4 Process simulation

Aspen PlusTM software (9.0 version; Aspen Technology Inc.) is used for process simulation in this study. Aspen is stand for **A**dvanced **S**ystem for **P**rocess **En**gineering. Aspen Plus is one of a flowsheet simulation software used to quantitatively model a chemical processing plant produced by AspenTech Inc. that has advantages to simulate and process solid materials. Flowsheet simulator in Aspen Plus allows to predict the behavior of a process using basic engineering relationships and can be used to calculate and determine balance equations of mass, mole, and energy; thermodynamic relationships for reacting and non-reacting components; rate correlations for momentum, heat, and mass transfer; and reaction stoichiometry and kinetic data. Aspen Plus can be used as preliminary study for "what-if" cases, preliminary design process, optimization investigations, and sensitivity analyses [1]. Aspen Plus is also supported with features for performing energy analyses and economic evaluation. In terms of flowsheet notation, there are a stream icon and block icon in Aspen Plus. The stream icon is separated into material, heat, and work streams, while the block icons are categorized to mixers/splitters, separators, exchangers, columns, reactors, pressure changes, manipulators, solids, solids separators, and user models. The block icons used in this study are listed in **Table 2.2**.

Table 2.2 Block icons of Aspen Plus used in this study

Name	**Icon**	**Function**

Mixers/Splitters		
MIX		Mix streams of material, heat, or work
SSplit		Divide streams based on substreams, can be used as cyclone
Separators		
Flash2		Flash drum, separate liquid and gas based on vapor-liquid equilibrium
Sep		Component separator, separate components based on specified flows or split fractions
Exchangers		
Heater		Simple heat exchanger for heater or cooler. Only one input-output stream is required.
HeatX		Co-current or counter current heat exchanger. Two input-output streams are required.
MHeatX		Multistreams heat exchanger.
Reactors		
RYield		Reactor based on yield distribution. This reactor is used when reaction stoichiometry and kinetics are unknown [2]. This model is used for decomposing biomass into simple components (C, H_2, N_2, O_2, S) based on its elemental composition.

REquil		Reactor based on equilibrium reactions at certain specified operating condition.
RGibbs		Reactor for multiphase equilibrium based on Gibbs free energy minimalization at certain specified operating condition.
Pressure changers		
Pump		Pump liquid streams.
Compr		Compressor, turbine, expander for gas streams.
User Models		
Hierarchy		Hierarchy block. Classified 2 different processes which different base method can be used.

References

[1] K.I.M. Al-Malah, Introducing Aspen Plus, Aspen Plus: Chemical Engineering Applications, John Wiley & Sons2016, pp. 1-49.

[2] M.B. Nikoo, N. Mahinpey, Simulation of biomass gasification in fluidized bed reactor using ASPEN PLUS, Biomass and Bioenergy, 32 (2008) 1245-1254.

CHAPTER 3 : STEAM GASIFICATION OF CO-PYROLYSIS CHARS FROM VARIOUS TYPES OF BIOMASS

3.1 Introduction

As described in **Chapter 1**, a two-stage gasification system is recently introduced for solving the tar issue in direct biomass gasification, in which the biomass pyrolysis step was separately performed at first before the char gasification step [1-4]. As such, the generated tar can be treated after the pyrolysis stage and only the biochar is gasified at the following gasification stage. The main advantage of this concept is to minimalize the tar problem in the direct biomass gasification system so that much cleaner syngas can be obtained. Furthermore, combining pyrolysis with steam gasification definitely improve hydrogen production from biomass compared with the existing contemporary thermochemical methods [5]. Therefore, it is important to investigate the biochar gasification characterization for the design of the whole gasification system. Since the biochar has high carbon content with less amount of volatiles, the generated volatiles should have less influence on the biochar gasification rate, leading to high gasification efficiency compared with the gasification of raw biomass [6].

As an abundant and easily available and sustainable energy resources, a wide variety of biomass types exist [7]. It is impossible to use only one type of biomass in a practical energy system since collecting and transporting biomass take high cost and its supply continuity is hard to accomplish. Various kinds of biomass are always used together in the gasification process in order to maintain the supply for biomass resources. Thus, it is important to investigate the co-gasification properties of various biomass and/or biochars, or even with coal. It is found that co-gasification of biomass with coal could reduce sulfur and ash from coal and tar from biomass simultaneously [8-10]. In our previous study [11], co-gasification of land-based biomass with brown seaweed resulted in high syngas production yield since the alkali and alkaline earth metal (AAEM) species in brown seaweed served as catalysts to enhance the gasification of land-based biomass.

Co pyrolysis is other form of combining two or more fuels to take advantage of synergistic effect to improve products quality. For co-pyrolysis, biomass is normally combined with plastics or coal to produce higher quality tar/bio-oils [12, 13] with a very few research cases about co-pyrolysis involving only biomass as a feedstock. Gulab *et al*. [14] investigated about co-pyrolysis of wild aquatic plant of Eichhornia Crassipes with polyethylene using waste Fe and $CaCO_3$ as catalysts to improve bio-oil production and product selectivity to aliphatic and aromatic hydrocarbon. Jun *et al.* [15] used high temperature co-pyrolysis process for producing hydrogen rich syngas from municipal solid waste and wheat straw. While many other investigations regarding co-pyrolysis involving biomass to produce high quality liquid product, there are only a few researches focus on biochar production, yield, composition, even characterization. Whereas co-pyrolysis process to generate co-pyrolysis biochar for the gasification is applicable in the application of two-stage gasification system. Zhang *et al.* [16] conducted co-pyrolysis of biomass and plastic to increase H_2/CO ratio in catalytic gasification and found that a H_2/CO molar ratio of 5.6 can be obtained at a biomass/plastic weight ratio of 1:2. Park *et al.* [17] mixed plastics with wood pellets in a two-stage gasification process, in which cold gas efficiency of 91% was achieved with a plastics/biomass weight ratio of 7:3. In addition, it is found that the synergistic effect in the co-pyrolysis process could not only affect the quality of tar, but also change the morphology or even the properties of biochar [18]. However, the synergistic effect is not always obtained for every co-pyrolysis case. Zhu *et al.* [19] found the absence of synergistic effect when combining coal with wheat straw. Therefore, biomass selection should be important for the obtaining of highly active biochar from the co-pyrolysis of biomass to increase the gas production as well as the lower heating value (LHV) of the syngas produced from the co-pyrolysis biochar gasification. It is well known that various types of biomass such as woody plants, herbaceous plants/grasses, aquatic plants, and manure have different and special characteristics in terms of carbon, moisture, ash contents, fixed carbon and volatiles matters, and inorganic components in their ashes that can affect gasification efficiency [20]. Moreover, it is found that pyrolysis characteristic of biomass is relied on the contents of cellulose and hemicellulose in raw biomass and the type of biomass could dictate the interactive effect

during the co-pyrolysis process [21]. Some kinds of biomass also have auto-catalytic capability in the gasification due to the presence of more AAEM species such as potassium, sodium, calcium, and magnesium in them [22, 23] that is proven to not only promote gas production in the co-gasification of biomass with coal [10] and co-gasification of blended biomass char and coal char [9], but also enhance the activity of the biochar produced from the co-pyrolysis of biomass and coal [24]. Potassium presence in pyrolysis can inhibit the trend of carbonization and promote char gasification reactions efficiently to hydrogen-rich gas at high rates [25]. However, a large amount of such minerals, especially some without the catalytic activity, are also undesirable since they may cause several technological and environmental issues during the biomass processing [26].

Therefore, in this study, four types of biomass with different AAEM contents in their ashes, i.e., apple tree branch (hardwood), knotweed stem (softwood), seaweed (aquatic plant) and rice straw (grass), were selected to prepare co-pyrolysis biochar, and the steam gasification of the obtained co-pyrolysis biochar were investigated. Herein, co-pyrolysis of biomass mixture was conducted firstly to obtain char with high reactivity and steam gasification of the co-pyrolysis char was conducted to obtain hydrogen-rich syngas. Furthermore, proper understanding of synergistic effect induces by combining different types of biomass for the preparation of the highly active co-pyrolysis biochar is expected to improve feedstock sustainability in the two-stage gasification system.

3.2 Experimental

3.2.1. Materials

The biomass used and their characterization are the listed and described in **Section 2.1**.

3.2.2. Pyrolysis and co-pyrolysis for biochar preparation

The pyrolysis and co-pyrolysis experiments were conducted in a vertical steel tube-type fixed bed reactor with experimental setup described in **Section 2.2** and was performed at 500 ^{o}C for 2 h in atmospheric condition with a heating rate of 10 ^{o}C/min. For each experimental run of pyrolysis or co-pyrolysis, about 3 g of biomass or biomass mixture was loaded to the

middle section of the reactor at first and for the co-pyrolysis process, the ratio of two types of biomass was 1:1. The co-pyrolysis biochar collected after the process was later called as co-char in this study. The collected gas in the gas bag was analyzed using a gas chromatograph (GC-TCD, Agilent 7890-USA) to determine the gas compositions of CO, CO_2, CH_4, and H_2 and shown as mmol per gram sample (mmol/g-sample) and mmol/g-biomass in dry and ash free basis (mmol/g-biomass daf). All the gas was assumed to be originated from the biomass, so then the mass of gas can be calculated from their composition. Whereas the biochar collected at the end of the pyrolysis process was weighted, the product yield of pyrolysis is calculated as follows:

$$\text{Mass of bio-oil} = \text{mass of biomass sample} - \text{mass of gas} - \text{mass of biochar} \quad (1)$$

$$\text{Product yield} = \frac{\text{mass of each product (g)}}{\text{mass of biomass sample (g)}} \quad (2)$$

3.2.3. Steam gasification

Steam gasification was performed on the same experimental setup described in **Section 2.2**, in which the steam was flowed into the fixed-bed reactor from the top with a flow rate of 0.2 g/min. For each experimental run, about 0.5 g of biomass, biochar, or co-char was loaded to the tube-type fixed-bed reactor to be gasified at 750 ^{o}C for 90 min. Gas production from the steam gasification of co-char was compared with that of co-gasification of the mixed biochars from the pyrolysis of the individual biomass. In addition, to evaluate the synergetic effect of co-char, the biochars in the co-char from different types of biomass was assumed to be separately gasified, and the sum of product yields was compared with that from the gasification of co-char. Hereafter, the sample of each raw biomass, the biochar from pyrolysis of individual biomass, biochar obtained from co-pyrolysis of biomass mixture, and physical mixture of biochars were called RB_X, BC_X, CC_{XX}, MC_{XX} respectively in this study, where subscript X is the initial letter of the biomass name involved.

Herein, the percentage of each bio-char from the corresponding biomass in the co-char was calculated as follow:

$$EC_{X1} = PY_{C\text{-}X1} \times M_{X1} \quad (3)$$

$$EC_{X2} = PY_{C\text{-}X2} \times M_{X2} \quad (4)$$

$$EC_{X1X2} = EC_{X1} + EC_{X2} \quad (5)$$

$$\%BC_{X1} = \frac{EC_{X1}\ (g)}{EC_{X1X2}\ (g)} \quad (6)$$

$$\%BC_{X2} = 100 - \%BC_{x1} \quad (7)$$

$$\text{Amount of } MC_{X1X2} \text{ for co-gasification (g)} = \%BC_{X1} \times 0.5\ g + \%BC_{X2} \times 0.5\ g \quad (8)$$

where, EC_{X1}, $PY_{C\text{-}X1}$, and M_{X1} are the expected masses of biochars from Biomass X1, biochar yield from pyrolysis of Biomass X1 calculated by Eq. 2, and mass of Biomass X1 in co-pyrolysis process, respectively. As such, the difference of gasification of CC_{XX} and co-gasification of MC_{XX} can be found, and the existence of synergistic effect in the co-char could be indicated by the difference of the two kinds of gasification results. **Fig. 3** further describes the different concepts of co-pyrolysis with gasification of CC_{XX} and co-gasification of MC_{XX}.

3.2.4. Analysis

The gas product collected in the gas bag was analyzed using a gas chromatograph with two thermal conductivity detectors (GC-TCD, Agilent 7890-USA) to determine the gas compositions main product gases from gasification of CO, CO_2, CH_4, and H_2 with the detail described in Section 2.3. Herein, the total gas yield was presented as mmol per gram sample (mmol/g-sample) where the same amount (0.5 g) of samples of RBx, BCx, CCxx, and MCxx was used in each set of experiment. Ash compositions from the single biochar and co-char were determined using an energy dispersive X-ray fluorescence spectrometer (EDX-800HS, Shimadzu, Japan).

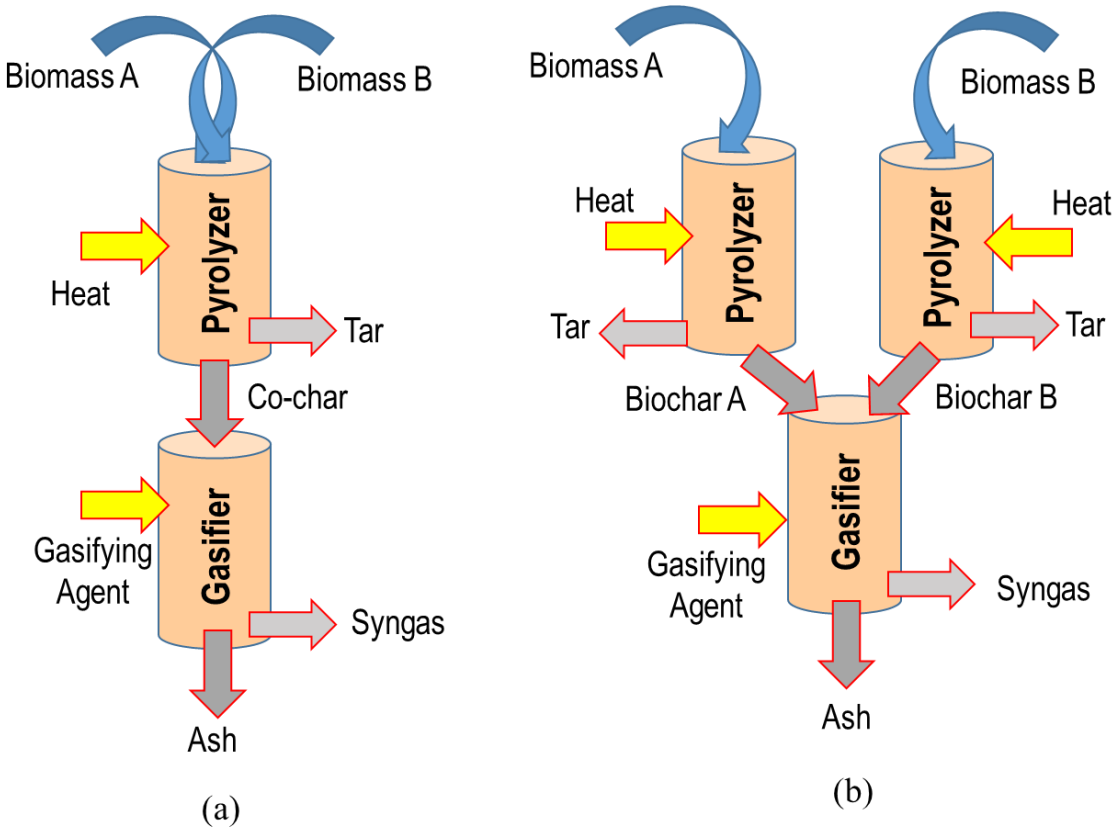

Figure 3.1 Schematic diagram of two-stage gasification concepts of (a) co-pyrolysis with gasification of CC_{XX} and (b) separated pyrolysis with co-gasification of MC_{XX}.

3.3 Results and discussion

3.3.1. Steam gasification of RBx and BCx

Fig. 3.2(a) shows gas yields from the gasification of RB_X and BC_X respectively with a steam flow rate of 0.2 g/min at 750 ^oC for 90 min with the units of mmol/g-sample while **Fig 3.2(b)** shows it in the units of mmol/g-biomass daf. **Table 3.1** summarizes the biochar yield from the pyrolysis of RB_X at 500 ^oC, characteristics of elemental compounds, and ash composition in each BC_X sample. One can see that the gasification of BC_X resulted on a higher gas yield than the gasification of the corresponding RB_X per gram of sample, indicating that biochar was more easily gasified since it had lower volatile compounds compared with the raw

biomass. During the pyrolysis process, volatile matters in raw biomass including water, permanent gases such as CO and CO_2, and tars were released. It is reported that the generation of the volatile compounds in raw biomass during the gasification process could hinder gasification reaction [1, 23, 27]. Thus, separately gasification of biochar could improve the gasification rate of the whole system.

Table 3.1 Biochar yields from the pyrolysis of the RB_x, their elemental analysis results, and ash compositions

	RB_A	**RB_K**	**RB_S**	**RB_R**
Biochar yield (g/g-biomass)	0.27	0.32	0.4	0.38
Elemental composition of biochar (wt% daf)				
	BC_A	**BC_K**	**BC_S**	**BC_R**
C	71.20	73.94	50.01	50.31
H	2.86	2.51	2.12	1.96
N	1.08	0.52	1.84	0.42
S	0.00	0.00	0.29	0.07
O	24.86	23.03	45.75	47.24
Ash composition (wt%)				
Ca	67.04	26.01	59.62	6.88
K	20.50	62.36	4.79	39.18
Na	n.d.	n.d.	6.63	n.d.
S	0.52	0.32	2.38	0.93
P	4.35	1.46	1.47	1.10
Si	3.39	n.d.	3.64	39.90
Fe	0.75	0.13	2.88	0.78
Mg	n.d.	n.d.	7.93	n.d.
Mn	n.d.	n.d.	0.50	0.60
Zn	n.d.	n.d.	n.d.	0.03

n.d. = not detected

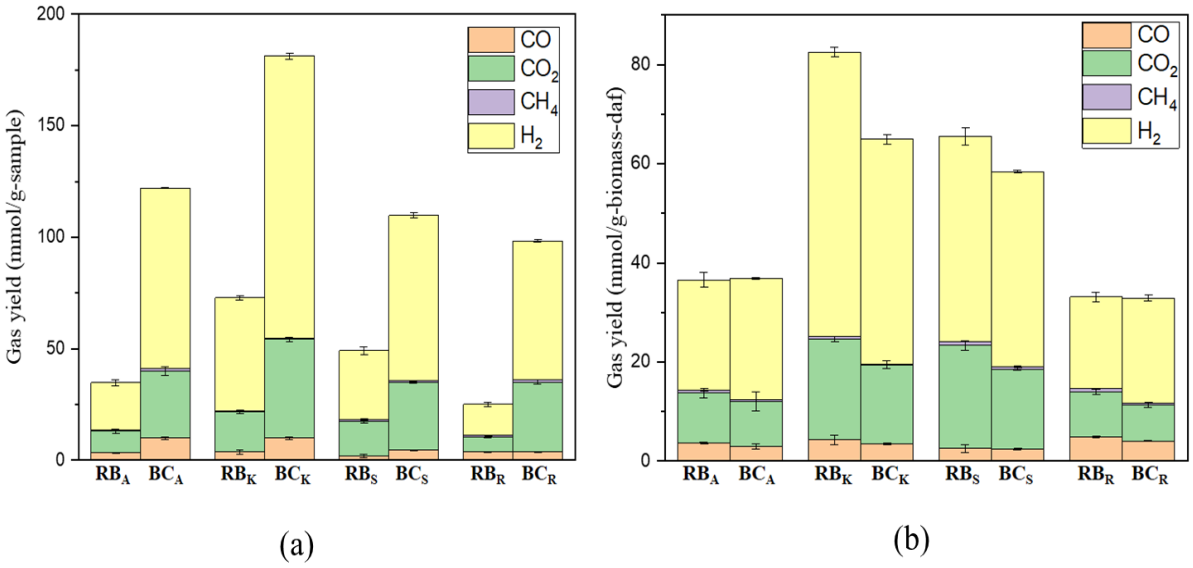

Figure 3.2 Gas yields from the steam gasification of each individual biomass and the corresponding biochar at 750 ^{o}C with steam flow rate of 0.2 g/min for 90 min (a) units of mmol/g-sample and (b) units of mmol/g-biomass daf

Specifically, the gasification of RB_R and BC_R resulted in the lowest gas yields among the four types of biomass. Even though RSt is the popular and the most abundant agricultural biomass residue in the world, it has low energy density, low high heating value (HHV), and high ash content [28, 29]. It is well known that high amount of silica in RSt can hinder the carbon gasification at high temperature. Even after the pyrolysis process, high silica content was still remained, resulting in low gasification efficiencies of RB_R and BC_R [30]. The gas yield of BC_R gasification has similar result with RB_R in the unit of mmol/g-biomass daf even though the biochar yield from pyrolysis and biochar elemental properties are similar to BC_S. In comparison, the gasification of RB_K and BC_K exhibited the highest gas yields. Although biochar yield from pyrolysis of KWS is quite low, the BC_K elemental properties has the highest carbon content among other biochars that resulting in high gas yield of BC_K gasification. In previous study [31, 32], it is found that the high amount of K_2O in KWS can

promote the tar reforming and char gasification. Moreover, the pyrolysis of KWS at 500 ^{o}C produced biochar with the highest reactivity since the highest content of K_2O was intensified after pyrolysis, which made the biochar have auto-catalytic activity to increase gas production yield. In addition, it should be noted that KWS had low ash content. However, compared with RB_K gasification in the unit of mmol/g-biomass daf, the gas yield from BR_K gasification is lower due to weight loss during pyrolysis.

Unlike the land-based biomass, SW contains more sugars, protein, and simple lipid, which are more easily decomposed to generate higher gas amount [11, 33]. Moreover, even though the SW had lower carbon content, the calcium content in SW ash was higher than those in ATB ash, and the higher ash content of SW could promote gasification rate of RB_S when compared with the gasification of land-based biomass such as RB_A. However, it should be noted that the carbohydrates in SW was more easily to be decomposed at low temperatures (200-400 ^{o}C) [33, 34] and during biomass pyrolysis, the elements on the surface of biomass/char change or release together with volatiles [35]. Comparison between Table 1 and Table 2 shows that a little part of calcium was also released after the pyrolysis at 500 ^{o}C, resulting in lower carbon and calcium contents in the BC_S. The gas yield of BC_S gasification is lower than gasification of RBS in the units of mmol/g-biomass daf, Even though BC_S characteristic shows low carbon content and AAEM contents, high biochar yield from SW pyrolysis establishes high gas yield of BC_S gasification per gram biomass. Meanwhile, the pyrolysis of RB_A produced biochar with a high carbon content and a stable calcium content. Thus, the gasification of BC_S resulted in a lower gas yield than that of BC_A at the same amount of biochar sample. In the units of mmol/g-biomass daf, gasification of RB_A and BC_A have similar result due to biochar yield from ATB pyrolysis is the lowest among other feedstocks. It should be noted that the higher carbon content in BC_X effectively enhanced primary and secondary steam reforming reactions during the gasification to produce hydrogen-rich syngas.

3.3.2. Steam gasification of co-char

3.3.2.1. Combination with RSt

To investigate the promoting effect of biochar with higher AAEM species on the gasification of biochar with lower AAEM species in the co-char, several combinations of co-chars were prepared by the co-pyrolysis of RSt with other types of biomass. **Fig. 3.3** compares the gas yields generated from gasification of CC_{RX} with those from the co-gasification of MC_{RX}. **Table 3.2** represents the percentage of each biochar for the co-gasification of MC_{RX} calculated by Eqs. (6) and (7). One can see that only the gasification of CC_{RS} resulted in a higher gas yield than the co-gasification of MC_{RS}. Meanwhile, the gasification of the CC_{RA} and co-gasification of the MC_{RA} had no significant differences whereas the co-gasification of the MC_{RK} even had higher gas yield than the gasification of CC_{RK}.

Table 3.2 Proportion for co-gasification of the MC_{RX}

	MC_{RA}	**MC_{RK}**	**MC_{RS}**
BC_R	60%	54%	48%
Biochar X2	40%	46%	52%

Herein, as stated above, the RSt contains a high amount of silica, which would limit the gasification efficiency. In fact, its bio-char also contained a high content of silica. Suzuki *et al.* [22] confirmed that silica in the RSt tends to react with potassium or other alkaline metal species to form the inactive species of alkali silicate, leading to lower gasification rate. Wang *et al.* [36] also confirmed that the calcium species in the biomass would react with silica to produce stable calcium silicate, which would inhibit the activity of AAEM to certain extent. Similar case was reported by Ellis *et al.* [37] that said $Ca_2Al_2SiO_7$ crystals could be formed during co-pyrolysis of pine sawdust with bituminous coal. The existence of aluminosilicate crystal lower reaction rate during gasification of co-pyrolysis char compared with separated pyrolysis char. Wei *et al.* [38] reported that the RSt existence in co-pyrolysis hindered the activity of calcium and potassium by affecting graphitization degree of the char during the

co-pyrolysis process, inhibiting the gasification reactivity. Risnes *et al.* [39] indicated that the activity of potassium is generally larger than calcium wherefore the inhibition effect of alkali silicate formation is also larger on potassium than calcium. In this study, the ATB, KWS, and SW had high amounts of calcium and potassium in their ashes. Even though these AAEM species should have good catalytic activity for the gasification, when they reacted with silica in the RSt during the co-pyrolysis process, the activity could be also decreased.

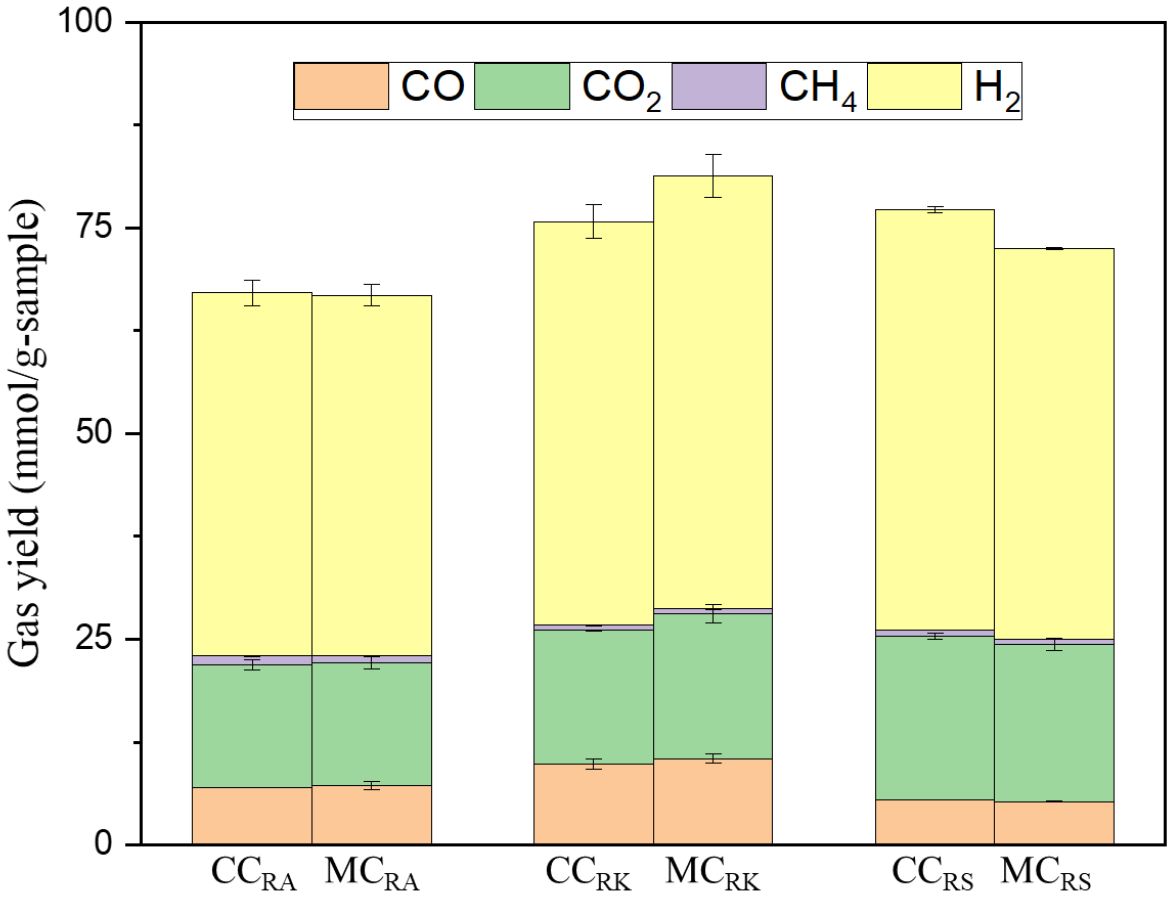

Figure 3.3 Comparison of gas yields from the steam gasification of CC_{RX} with those from the co-gasification of the MC_{RX}

As shown in **Table 3.3**, after the co-pyrolysis, a high potassium content was still remained in CC_{RK} which can lead to the inhibition effect and simultaneously interact with the remaining amount of silica in the co-char. Moreover, the calcium content was too low to have

any effect in the gasification, and as such, the gas yield obtained from the CC_{RK} was 6.8% lower than the co-gasification of MC_{RK}. It should be noted that the interaction between KWS char and RS char in the CC_{RK} would be more intense than the physically mixed biochars used in MC_{RK} since they were formed together during the pyrolysis process. Thus, the inhibition effect in the CC_{RK} should be more vigorous.

Meanwhile, in the ATB + RSt case, the potassium and silica contents originated from RSt itself were still remained high, which may have inhibition effect for the gasification of the CC_{RA}. However, the calcium content as the main AAEM content for ATB was still remained enough high to promote the gasification rate. Thus, no significant difference between the gasification of CC_{RA} and the co-gasification of MC_{RA} where the gas yield difference was only 0.4%. In both ATB and KWS cases, the RSt part was more dominant in the mixture, leading to more intensive silica inhibition. In contrast, in the CC_{RS}, the SW part was more dominant than RSt. Therefore, the highest calcium content of SW was remained in the co-char while the lowest potassium and silica contents were found among other co-chars that combined with RSt, resulting in the best promotion effect in the gasification with about 6.6% higher gas yield difference of CC_{RS} v. MC_{RS}. Furthermore, synergistic effect in CC_{RS} might be occurred because aromatic compound was formed and the strength of C=O and S=O precipitation peaks were enhanced during co-pyrolysis of SW and RSt [35, 40].

Table 3.3 Ash compositions for CC_{RX}

Ash composition (wt%)	**CC_{RA}**	**CC_{RK}**	**CC_{RS}**
Ca	21.71	13.19	34.97
K	34.67	50.07	20.87
S	0.66	0.52	1.77
P	1.84	1.32	1.34
Si	38.24	24.53	21.06
Fe	0.77	0.45	2.55

Mg	n.d.	n.d.	2.77
Mn	0.80	0.45	0.66
Zn	0.07	0.05	0.06
Cu	0.05	n.d.	n.d.

n.d. = not detected

3.3.2.2. Other combinations

Fig. 3.4 compares the gas yields generated from gasification of CC_{AK}, CC_{AS}, and CC_{KS} with those from the co-gasification of MC_{AK}, MC_{AS}, and MC_{KS} whereas **Table 3.4** represents the proportion of each biochar for the co-gasification of MC_{AK}, MC_{AS}, and MC_{KS} calculated by Eqs. (6) and (7). One can see that all of the CC_{XX} had higher gasification efficiencies than the co-gasification of MC_{XX} whereas the CC_{AK} gave the best performance.

Table 3.4 Ash compositions for CC_{RX}

	MC_{AK}	**MC_{AS}**	**MC_{KS}**
Biochar X1	46%	39.4%	44.4%
Biochar X2	54%	60.6%	55.6%

In this study, as shown in **Fig. 3.4**, all the co-chars had the synergistic effect. Especially, the combination of ATB and KWS resulted in the largest gas yields in both cases. In our previous study [11], the synergistic effect was found in the combination of raw brown seaweed and Japanese cedar. Consistently, the synergistic effect was also found in co-pyrolysis of SW with woody biomass of ATB and KWS. Thus, the gasification of the CC_{AS} and CC_{KS} were much easier than those of MC_{AS} and MC_{KS}. Although the difference of CC_{KS} gas yield with the co-gasification of MC_{KS} case was only 1.5% higher and the CC_{AS} v. MC_{AS} case was only 6% higher. Ash composition of CC_{AS} in **Table 3.5** shows that the calcium content was intensified after co-pyrolysis process while the potassium content decreased significantly in CC_{KS}. It may be caused by the better synergistic effect between ATB and SW than that between KWS and SW. Cabuk *et al.* [41] considered that the gasification results could not

solely depend on AAEM content. The interaction between various biomass during the co-pyrolysis could generate synergy effect on the reactivity of the produced co-char. However, due to the higher potassium content remained in CC_{KS} with higher catalytic activity than calcium [22], the combination of KWS and SW resulted in a higher gas yield than the combination of ATB and SW.

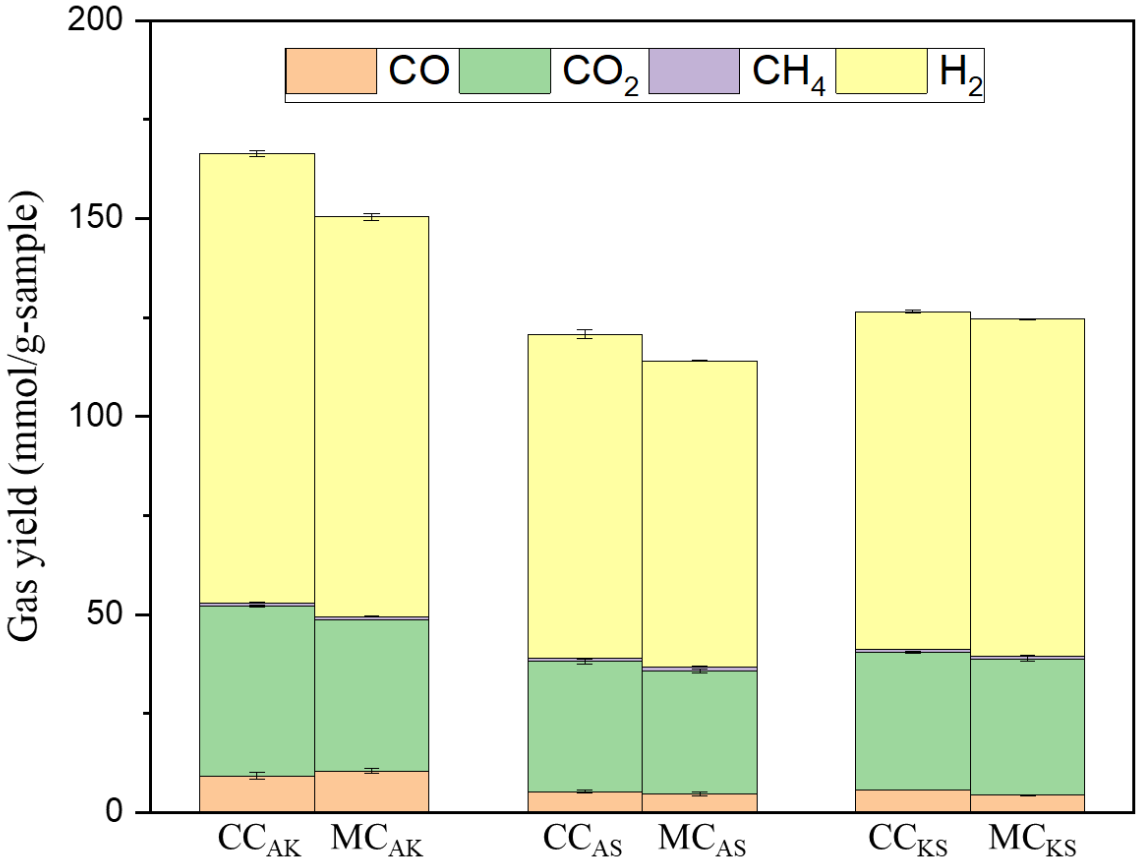

Figure 3.4 Comparison of gas yields from the steam gasification of CC_{AK}, CC_{AS}, and CC_{KS} with those from the co-gasification of the MC_{AK}, MC_{AS}, and MC_{KS}

In contrast, the gas yield from the gasification of CC_{AK} showed an excellent performance with 10.6% higher than that in the MC_{AK} case. Herein, both ATB and KWS were woody biomass with more endurance to the decomposition during the pyrolysis process, which should make more AAEM species maintained in the co-char after the pyrolysis. As shown in

Table 3.5, massive amount of potassium and calcium were found in the ash composition of CC_{AK}, which could lead to an obvious promotion effect. In the co-gasification case, the interaction between the different biochars was less intense so that less amount of gas yield were obtained when compared with the gasification of co-chars. Two-stage gasification system should get substantial benefit by combining various woody biomass together.

Table 3.5 Ash compositions of CC_{AK}, CC_{AS}, and CC_{KS}

Ash composition (wt%)	**CC_{AK}**	**CC_{AS}**	**CC_{KS}**
Ca	39.55	63.71	49.32
K	55.66	6.85	20.44
S	0.36	2.07	1.54
P	2.37	2.16	1.52
Si	**0.31**	**5.38**	**5.19**
Fe	0.36	4.39	4.47
Mg	n.d.	6.67	4.12
Zn	n.d.	0.10	0.06

n.d. = not detected

3.4 Conclusion

Steam gasification of co-pyrolysis char (co-char) from combinations of four different types of biomass with different properties, i.e., Apple tree branch (ATB), knotweed stem (KWS), seaweed (SW), and rice straw (RSt), were investigated. The results were compared with the steam co-gasification of the physically mixed individual biochars from the four types of biomass in order to observe the synergistic effect obtained from co-pyrolysis process.

- The less reactive co-char was always generated for the steam gasification process because of the silica species in the RSt could react with AAEM species in other types of biomass to form alkali silicate compounds.

- Pairing RSt with non-woody biomass such as SW gave a better result than combining with woody biomass.
- In comparison, the gasification of the co-char involving combinations of different woody biomass showed excellent result. The AAEM contents in woody biomass was stably maintained even after pyrolysis process so that the co-char also had higher activity.

Thus, either the positive or negative impacts could be generated during the biomass co-pyrolysis. Especially, the biomass selection should play a significant role in the achieving of efficient two-stage gasification system with feedstock availability including different types of biomass.

References

[1] Y.A. Situmorang, Z. Zhao, A. Yoshida, A. Abudula, G. Guan, Potential power generation on a small-scale separated-type biomass gasification system, Energy, 179 (2019) 19-29.

[2] M. Gassner, F. Marechal, Thermodynamic comparison of the FICFB and Viking gasification concepts, Energy, 34 (2009) 1744-1753.

[3] X. Zeng, F. Wang, H. Li, Y. Wang, L. Dong, J. Yu, G. Xu, Pilot Verifiacation of a Low-Tar Two-Stage Coal Gasification Process with a Fluidized Bed Pyrolyzer and Fixed Bed Gasifier, Applied Energy, 115 (2014) 9-16.

[4] M.H. Adamu, X. Zeng, J.L. Zhang, F. Wang, G. Xu, Property of drying, pyrolysis, gasification, and combustion tested by a micro fluidized bed reaction analyzer for adapting to the biomass two-stage gasification process, Fuel, 264 (2020).

[5] P. Parthasarathy, K.N. Sheeba, Combined slow pyrolysis and steam gasification of biomass for hydrogen generation—a review, International Journal of Energy Research, 39 (2014) 147-164.

[6] T. Yu, A. Abudukeranmu, A. Anniwaer, Y.A. Situmorang, A. Yoshida, X. Hao, Y. Kasai, A. Abudula, G. Guan, Steam gasification of biochars derived from pruned apple

branch with various pyrolysis temperatures, International Journal of Hydrogen Energy, (2019).
[7] E. Madadian, M. Lefsrud, C.A.P. Lee, Y. Roy, Green energy production: The potential of using biomass gasification, Journal of Green Engineering, 4 (2014) 101-116.
[8] B. Digman, H.S. Joo, D.-S. Kim, Recent progress in gasification/pyrolysis technologies for biomass conversion to energy, Environmental Progress & Sustainable Energy, 28 (2009) 47-51.
[9] Z. Zhang, S. Pang, T. Levi, Influence of AAEM species in coal and biomass on steam co-gasification of chars of blended coal and biomass, Renewable Energy, 101 (2017) 356-363.
[10] J. Rizkiana, G. Guan, W.B. Widayatno, X. Hao, W. Huang, A. Tsutsumi, A. Abudula, Effect of biomass type on the performance of cogasification of low rank coal with biomass at relatively low temperatures, Fuel, 134 (2014) 414-419.
[11] M. Kaewpanha, G. Guan, XiaogangHao, Z. Wang, K. Kusakabe, A. Abudula, Steam Co-Gasification of Brown Seaweed and Land-Based Biomass, Fuel Processing Technology, 120 (2014) 106-112.
[12] F. Abnisa, W.M.A.W. Daud, A review on co-pyrolysis of biomass: An optional technique to obtain a high-grade pyrolysis oil, Energy Conversion and Management, 87 (2014) 71-85.
[13] H. Hassan, J.K. Lim, B.H. Hameed, Recent progress on biomass co-pyrolysis conversion into high-quality bio-oil, Bioresource Technology, 221 (2016) 645-655.
[14] H. Gulab, K. Hussain, S. Malik, Z. Hussain, Z. Shah, Catalytic co-pyrolysis of Eichhornia Crassipes biomass and polyethylene using waste Fe and $CaCO_3$ catalysts, International Journal of Energy Research, 40 (2016) 940-951.
[15] Z. Jun, W. Shuzhong, W. Zhiqiang, M. Haiyu, C. Lin, Hydrogen-rich syngas produced from the co-pyrolysis of municipal solid waste and wheat straw, International Journal of Hydrogen Energy, 42 (2017) 19701-19708.

[16] S. Zhang, S. Zhu, H. Zhang, X. Liu, Y. Xiong, High quality H2-rich syngas production from pyrolysis-gasification of biomass and plastic wastes by Ni–Fe@Nanofibers/Porous carbon catalyst, International Journal of Hydrogen Energy, 44 (2019) 26193-26203.
[17] J.H. Park, H.-W. Park, S. Choi, D.-W. Park, Effects of blend ratio between high density polyethylene and biomass on co-gasification behavior in a two-stage gasification system, International Journal of Hydrogen Energy, 41 (2016) 16813-16822.
[18] Q. Jin, X. Wang, S. Li, H. Mikulcic, T. Besenic, S. Deng, M. Vujanovi, H. Tan, B.M. Kumfer, Synergistic effects during co-pyrolysis of biomass and plastic: Gas, tar, soot, char products and thermogravimetric study, Journal of Energy Institute, 92 (2019) 108-117.
[19] W. Zhu, W. Song, W. Lin, Catalytic gasification of char from co-pyrolysis of coal and biomass, Fuel Processing Technology, 89 (2008) 890-896.
[20] P. McKendry, Energy production from biomass (part 1): overview of biomass, Bioresource Technology, 83 (2002) 37-46.
[21] J. Zhu, Y. Yang, Y. Chen, L. Yang, Y. Wang, Y. Zhu, HaijunChen, Co-pyrolysis of textile dyeing sludge and four typical lignocellulosic biomasses: Thermal conversion characteristics, synergetic effects and reaction kinetics, International Journal of Hydrogen Energy, 43 (2018) 22135-22147.
[22] T. Suzuki, H. Nakajima, N. Ikenaga, H. Oda, T. Miyake, Effect of mineral matters in biomass on the gasification rate of their chars, Biomass Conversion and Biorefinery, 1 (2011) 17-28.
[23] A. Nzihou, B. Stanmore, P. Sharrock, A review of catalysts for the gasification of biomass char, with some reference to coal, Energy, 58 (2013) 305-317.
[24] X. Chen, L. Liu, L. Zhang, Y. Zhao, P. Qiu, Gasification reactivity of co-pyrolysis char from coal blended with corn stalks, Bioresource Technology, 279 (2019) 243-251.
[25] X. Lv, J. Xiao, L. Shen, Y. Zhou, Experimental study on the optimization of parameters during biomass pyrolysis and char gasification for hydrogen-rich gas, International Journal of Hydrogen Energy, 41 (2016) 21913-21925.

[26] S. V.Vassilev, C. G.Vassileva, Y.-C. Song, W.-Y. Li, J. Feng, Ash contents and ash-forming elements of biomass and their significance for solid biofuel combustion, Fuel, 208 (2017) 377-409.
[27] G. Guan, C. Fushimi, A. Tsutsumi, M. Ishizuka, S. Matsuda, H. Hatano, Y. Suzuki, High-density circulating fluidized bed gasifier for advanced IGCC/IGFC—Advantages and challenges, Particuology, 8 (2010) 602-606.
[28] J. Park, Y. Lee, C. Ryu, Y.-K. Park, Slow pyrolysis of rice straw: Analysis of products properties, carbon and energy yields, Bioresource Technology, 155 (2014) 63-70.
[29] R. Kizuka, K. Ishii, M. Sato, A. Fujiyama, Characteristics of wood pellets mixed with torrefied rice straw as a biomass fuel, International Journal of Energy and Environmental Engineering, 10 (2019) 357-365.
[30] K.S. Lin, H.P. Wang, C.J. Lin, C.-I. Juch, A process development for gasification of rice husk, Fuel Processing Technology, 55 (1998) 185-192.
[31] M. Lapuerta, J.J. Hernández, A. Pazo, J. López, Gasification and co-gasification of biomass wastes: Effect of the biomass origin and the gasifier operating conditions, Fuel Processing Technology, 89 (2008) 828-837.
[32] W.B. Widayatno, G. Guan, J. Rizkiana, X. Hao, C. Samart, A. Abudula, Steam reforming of tar derived from Fallopia Japonica stem over its own chars prepared at different conditions, Fuel, 132 (2014) 204-210.
[33] S. Wang, X.M. Jiang, N. Wang, L.J. Yu, Z. Li, P.M. He, Research on pyrolysis characteristics of seaweed, Energy & Fuels, 21 (2007) 3723–3729.
[34] M. Schumacher, J. Yanık, A. Sına˘g, A. Kruse, Hydrothermal conversion of seaweeds in a batch autoclave, The Journal of Supercritical Fluids, 58 (2011) 131-135.
[35] S. Xu, B.B. Uzoejinwa, S. Wang, Y. Hu, L. Qian, L. Liu, B. Li, Z. He, Q. Wang, A.E.-F. Abomohra, C. Li, B. Zhang, Study on co-pyrolysis synergistic mechanism of seaweed and rice husk by investigation of the characteristics of char/coke, Renewable Energy, 132 (2019) 527-542.

[36] X. Wang, K. Yao, X. Huang, X. Chen, G. Yu, H. Liu, F. Wang, M. Fan, Effect of CaO and biomass ash on catalytic hydrogasification behavior of coal char, Fuel, 249 (2019) 103-111.
[37] N. Ellis, M.S. Masnadi, D.G. Roberts, M.A. Kochanek, A. Y.Ilyushechkin, Mineral matter interactions during co-pyrolysis of coal and biomass and their impact on intrinsic char co-gasification reactivity, Chemical Engineering Journal, 279 (2015) 402-408.
[38] J. Wei, Y. Gong, Q. Guo, L. Ding, F. Wang, G. Yu, Physicochemical evolution during rice straw and coal co-pyrolysis and its effect on co-gasification reactivity, Bioresource Technology, 227 (2017) 345-352.
[39] H. Risnes, J. Fjellerup, U. Henriksen, A. Moilanen, P. Norby, K. Papadakis, D. Posselt, L.H. Sørensen, Calcium addition in straw gasification, Fuel, 82 (2002) 641-651.
[40] S. Wang, Q. Wang, Y.M. Hu, S.N. Xu, Z.X. He, H.S. Ji, Study on the synergistic co-pyrolysis behaviors of mixed rice husk and two types of seaweed by a combined TG-FTIR technique, Journal of Analytical and Applied Pyrolysis, 114 (2015) 109-118.
[41] B. Cabuk, G. Duman, J. Yanik, H. Olgun, Effect of fuel blend composition on hydrogen yield in co-gasification of coal and non-woody biomass, International Journal of Hydrogen Energy, 45 (2020) 3435-3443.

CHAPTER 4 : POTENTIAL POWER GENERATION ON A SMALL-SCALE SEPARATED-TYPE BIOMASS GASIFICATION SYSTEM

4.1. Introduction

As further development on two-stage gasification system, recently a comprehensive triple-bed combined circulating fluidized bed gasification system was proposed, in which a downer pyrolyzer, a bubbling fluidized bed char gasifier and a riser combustor for combustion of unreacted char are separately set but joined together. In this system, a fast gas-solids separator is used to separate the tar vapor and char at the exit of downer pyrolyzer and the char flows down to the char gasifier. Simultaneously, combustion of unreacted char in the riser combustor is used to provide the heat needed for the pyrolysis of coal/biomass in the downer pyrolyzer. For this purpose, the heat is carried by inert solids medium such as silica sand circulating in the system [1]. As described on **Chapter 1**, liquid product from pyrolysis process called tar has potential to be converted into syngas by steam reforming reaction. Coupling this process into existing triple-bed combined circulating fluidized bed gasification system can increase gas production from the system while improve the system efficiency.

In this study, a small-scale separated-type biomass gasification system composed of an auger-type pyrolyzer, a steam tar reformer, an air-steam char fluidized bed gasifier, and a spent char riser-type combustor with circulating heat carrier particles is proposed to convert biomass into combustible gas which can be applied for gas-engine power generation. Sand is used as heat carrier and bed material for the char fluidized bed gasifier. Different with previous developed two-stage biomass gasification system, this separate-type biomass gasification system applies a self-heating pyrolysis as well as gasification process. To let it suitable for a small-scale gasification, an auger-type pyrolyzer is proposed and a catalytic tar reforming reactor is also integrated. The empirical equations as well as the main experimental data from the published literatures are applied to analyze the elemental, mass, and energy balances of each process by using sets of assumptions at a certain condition to predict final energy efficiency and the potential electricity generated from the system. The models for

determining elemental and mass balances are built by combining experiment results in the literature and basic reaction equations. Energy balance is conducted for calculating heat involved within the system. Comparison of product yields and compositions obtained in the present system with the reported data shows that the prediction gives a reasonable accuracy which could indicate what occur within the system. The model presented in this study could be utilized for preliminary engineering design of comprehensive biomass thermal conversion processes.

4.2. Calculation method

4.2.1. The proposed small-scale separated-type biomass gasification system

Figure 4.1 shows the schematic diagram of the small-scale separated-type biomass gasification system proposed in this study. In this system, the woody biomass and the circulated hot sand (500-600°C) in the system are introduced into the auger-type pyrolyzer. As the biomass is mixed with the hot sand along the auger reactor, it will be decomposed, generating tar volatiles, gases such as H_2, CO, CO_2 and CH_4, and solids char. The tar volatiles and gases will flow upwards to the tar reforming reactor where the tar will be catalytically converted to combustible gases at a temperature over 600 °C. Meanwhile, the char will flow downwards to the fluidized bed gasifier and is self-heatedly gasified with air and steam to syngas at a temperature over 800 °C. The remaining unreacted char (spent char) will overflow into a riser combustor and be burned out completely with excessive air at a temperature over 1000 °C. The generated heat is carried by the sand and recycled to the sand tank, and provided the heat for the biomass pyrolysis. The gas produced in the pyrolyzer, tar reformer, and char gasifier will be collected together and used as the fuel for the gas-engine power generation. Herein, the self-heated gasification and combustion are exothermic reactions, both of them will generate heat, while the pyrolysis is an endothermic process, which requires heat. Even though the steam tar reforming is also endothermic reaction, the energy needed will be supported by external source in this study.

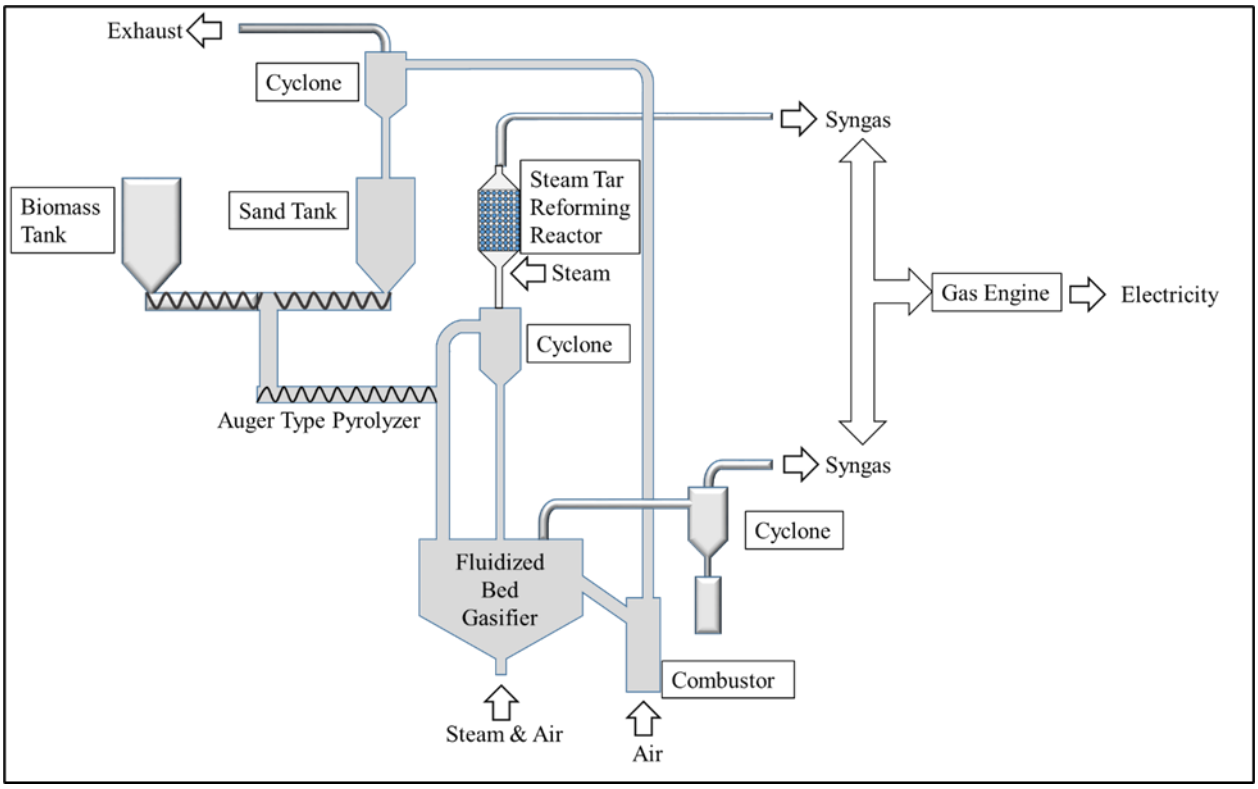

Figure 4.1 Schematic diagram of the separated-type biomass gasification system in this study

4.2.2. Calculation basis

In this study, the woody biomass is considered as the biomass feedstock for the gasification system. Table 1 shows the reported ultimate analysis results of some woody biomass by us and other researchers [2-6]. Herein, as a case study, the apple tree stem is chosen for the main simulation. About 12.5 kg/h (=100 kg/day, 8 h/day) of biomass feeding rate is applied for total calculation. Besides, the following conditions are assumed:

(i) Each process is performed in continuous steady state condition

(ii) No accumulation of each materials in each process

(iii) The separation of each products after the process is done completely

Furthermore, the calculation for each part of this system are described below.

4.2.3. Pyrolyzer

Biomass pyrolysis is a thermal decomposition process in the absence of oxygen, producing condensable volatile matter as tar (also called as bio-oil), non-condensable gas, and carbon-rich material called char within a temperature range of 300-600 °C. In general, the temperature range of 450-550 ^{o}C is the optimum pyrolysis condition for the woody biomass and more tar can be produced [7]. Meanwhile, it is found that the biochar with the highest reactivity could be obtained at 500 ^{o}C [8]. Thus, the temperature condition for the pyrolysis in this study is set at 500^{o}C.

Based on the heating rate and residence time, the pyrolysis can be classified into three types, i.e., slow, intermediate, and fast pyrolysis [9]. In this study, as the biomass is heated using the hot sand in the auger-type pyrolyzer, the pyrolysis type should be determined by the heat transfer rate and the residence time of biomass in the pyrolyzer, which can be adjusted by changing the biomass/sand feeding rate and the motor speed of the auger reactor [10]. As such, the pyrolysis process can be either the slow pyrolysis or the fast pyrolysis or even in between two. In this calculation, only the slow and fast pyrolysis routes will be considered, which will produce different amounts of tar and char, and affect the mass and heat balances of the following tar reforming, char gasification and spent char combustion processes.

To simplify the calculation, it is assumed that the produced tar is only composed of carbon, hydrogen, and oxygen, the gas only contains CO, CO_2, CH_4, and H_2, and the pyrolysis occurs in isothermal condition. Empirical calculation equations developed by Neves et al. [11] (**Table 4.2**) are applied for the simulation of the fast pyrolysis which can characterize some pyrolysis products within the temperature range of 200-1000 °C. Those unpredictable components using these equations are evaluated by using elemental and mass balance equations. Herein, to confirm that this model can predict the system with the fast pyrolysis route with reasonable accuracy, the results obtained by these empirical equations will be compared with the published experiment data [4], in which the ultimate analysis results of the similar wood biomass as the apple tree stem shown in **Table 4.1** is used for the validation of the fast pyrolysis calculation results.

Table 4.1 Ultimate analysis results of the similar wood biomass for the validation of simulation

Data	Biomass	Ultimate Analysis (wt %)					Reference
		C	H	O	N	S	
1	Apple Tree Stem	43.7	6.2	49.6	0.4	0.1	[2, 3]
2	A Kind of Wood	45.48	6.3	47.92	0.3	0	[4]
3	Poplar Wood	48.8	6.5	44.5	0.2	0	[5]
4	*Gmelina arborea* Wood	47.77	6.39	44.84	0.5	0.5	[6]

However, it is reported that the empirical model developed by Neves et al.[11] cannot be used to predict the results from the slow pyrolysis process. Meanwhile, even though many numerical simulations have been conducted for the slow pyrolysis process, it is still difficult to predict the yields of char, tar, and gas obtained from the real process. Especially, there are no results on the slow pyrolysis of apple tree stem. Thus, the data for the slow pyrolysis of apple tree stem based on experiment are collected in this study for the slow pyrolysis simulations. That is, a slow pyrolysis experiment with a heating rate of 10 ^{o}C/min is conducted for the pyrolysis of apple tree branch at first. The gases produced are analyzed using GC-TCD (GC-TCD, Agilent 7890, USA) to determine the gas compositions. Moreover, in the present work, to determine the elemental compositions in char, Eqs. (9)-(11) are used. Tar yield and elemental compositions are calculated based on the experimental results. Moreover, the yields of pyrolytic water produced in the slow pyrolysis process for the simulation is assumed to be 20 wt.% since the water yield in the slow pyrolysis is roughly within 5-22 wt.% regardless of the pyrolysis temperature and heating rate [3, 9-11].

Table 4.2 Equations for the fast pyrolysis simulation

Mass balance	**Eq.**
$Y_F = Y_{char,F} + Y_{tar,F} + Y_{gas,F} + Y_{H2O,F}$	(1)
$Y_{gas,F} = Y_{CO,F} + Y_{CO2,F} + Y_{CH4,F} + Y_{H2,F}$	(2)

$Y_{C,F} = Y_{C,char}.Y_{char,F} + Y_{C,tar}.Y_{tar,F} + Y_{C,CO}.Y_{CO,F} + Y_{C,CO2}.Y_{CO2,F} + Y_{C,CH4}.Y_{CH,F}$	(3)
$Y_{O,F} = Y_{O,char}.Y_{char,F} + Y_{O,tar}.Y_{tar,F} + Y_{O,CO}.Y_{CO,F} + Y_{O,CO2}.Y_{CO2,F} + Y_{O,H2O}.Y_{H2O,F}$	(4)
$Y_{H,F} = Y_{H,char}.Y_{char,F} + Y_{H,tar}.Y_{tar,F} + Y_{H,CH4}.Y_{CH4,F} + Y_{H,H2O}.Y_{H2O,F}$	(5)
Empirical equation	
$\frac{Y_{\mathbf{H_2},F}}{Y_{CO,F}} = 3.10^{-4} + \frac{0.0429}{1+(\frac{T}{632})^{-7.23}}$	(6)
$Y_{CH4,F} = -2.18.10^{-4} + 0.146Y_{CO,F}$	(7)
$Y_{H2,F} = 1.145\times (1 - \exp(-0.11.10^{-2}T))^{9.384}$	(8)
$Y_{C,char} = 0.93 - 0.92 \exp(-0.42.10^{-2}T)$	(9)
$Y_{O,char} = 0.07 + 0.85 \exp(-0.48.10^{-2}T)$	(10)
$Y_{H,char} = -0.41.10^{-2} + 0.10 \exp(-0.24.10^{-2}T)$	(11)
$Y_{char,F} = 0.106 + 2.43 \exp(-0.66.10^{-2}T)$	(12)
$\frac{Y_{C,tar}}{Y_{C,F}} = 1.14$	(13)
$\frac{Y_{O,tar}}{Y_{O,F}} = 0.80$	(14)
$\frac{Y_{H,tar}}{Y_{H,F}} = 1.13$	(15)

4.2.4. Catalytic steam tar reforming

In this study, catalytic steam tar reforming process is considered to convert the tar into the syngas of H_2 and CO. To date, various catalysts such as nickel based catalysts and some inexpensive, abundant, and disposable natural materials have been proven to have high activity for the tar reforming. It is also found that temperature of 650 ^oC gives nickel and CaO based catalyst the highest activity for this reaction [12]. Thus, the tar reforming temperature is chosen at 650 ^oC in this study. As indicated in Eq. (16), tar can be catalytically converted to syngas effectively.

$$C_xH_yO_z + (x\text{-}z)H_2O \rightarrow xCO + [y/2+x\text{-}z]H_2 \quad (16)$$

Herein, it is assumed that (i) only tar component involves in the reaction; (ii) catalytic reaction occurs effectively with a conversion of 70% [12]; (iii) steam/carbon (S/C) ratio used is 1 [13], (iv) no other series or parallel reactions occur, and (v) condition of reaction is isothermal.

4.2.5. Char gasification

Char is a solid carbon rich material as the product of pyrolysis of biomass. Its carbon content usually varies in the range of 63-91%. Other main content is oxygen with a value about 10-30%. Because of its high carbon content, the char contains high energy density. The quality and quantity of char produced from the pyrolysis of certain biomass can be controlled by varying the operating conditions, particularly heating rate and pyrolysis temperature in the pyrolysis process [7, 10]. Especially, it is found that for the char obtained from the pyrolysis of woody biomass at 500 ^oC has a syngas yield as high as about 83% from gasification at 850 ^oC [8]. Thus, 850 ^oC is chosen as the char gasification temperature in this study.

Meanwhile, thermodynamic equilibrium model is used to simulate the gasification process. The advantages of this method are: (i) unnecessary consideration of the transformation mechanism; (ii) independent of gasifier configuration; and (iii) no limit to a certain operating condition [14]. Furthermore, by considering the gasification process as a single overall reaction, the thermodynamic equilibrium model is useful to predict exit gas compositions at certain working parameters [15].

Herein, for the oxygen-steam char gasification, it is assumed that (i) temperature of the products is equal to the gasification temperature; (ii) oxygen is completely consumed; (iii) the gas mixture is equilibrium and homogenous; (iv) the residence time is long enough for all reactions considered to reach the equilibrium state; (v) ash is not involved in the simulation; (vi) pressure is atmospheric [14]; (vii) nitrogen and sulphur substances in char are not involved in this process simulation but they go to the combustor with the spent char; (viii) no tar is produced in the gasification process; (ix) the gases produced are only composed

of CO, CO_2, H_2, and CH_4; (x) equivalence ratio (ER) is 0.4 mol/mol; (xi) steam to char ratio (SCR) is 0.35 mol/mol. As such, the overall gasification reaction can be summarized as:

$$CH_yO_z + m\ O_2 + n\ H_2O = x_1\ CO + x_2\ CO_2 + x_3\ H_2 + x_4\ CH_4 + x_5\ H_2O + x_6\ C \qquad (17)$$

where *y* and *z* are the number of atoms of hydrogen and oxygen for each atom of carbon in the char. *m* and *n* molar amounts of oxygen and steam per mole of char as the gasifying agents. x_1, x_2, x_3, x_4, x_5, and x_6 molar amounts of corresponding products of gasification, respectively [14]. The m and n values can be calculated by the following equations:

$$m = ER \times (1 + \frac{y}{4} + \frac{z}{2}) \qquad (18)$$

$$n = SCR \times (12 + y + 12z) \qquad (19)$$

The element balances of carbon, hydrogen, and oxygen are given as below:

$$x_1 + x_2 + x_4 + x_6 = 1 \qquad (20)$$

$$y + 2n = 2x_3 + 4x_4 + 2x_5 \qquad (21)$$

$$z + n + 2m = x_1 + 2x_2 + x_5 \qquad (22)$$

Two reactions considered to give the equilibrium constants are

$$CO + H_2O \rightarrow CO_2 + H_2 \qquad (23)$$

$$C + 2H_2 \rightarrow CH_4 \qquad (24)$$

It is obvious that both equilibrium reactions here do not involve oxygen, and the steam role in water gas shift reaction is limited. Hence, it can be considered that the gasifying agents do not affect the equilibrium reactions significantly in this study [16]. Equilibrium constants as the function of partial pressure for these two reactions can be expressed as follows respectively:

$$K_1 = \frac{(P_{CO_2}/P_{total})(P_{H_2}/P_{total})}{(P_{CO}/P_{total})(P_{H_2O}/P_{total})} = \frac{x_2 x_3}{x_1 x_5} \qquad (25)$$

$$K_2 = \frac{P_{CH_4}/P_{total}}{(P_{H_2}/P_{total})^2} = \frac{x_4}{x_3} x_{total} \quad (26)$$

where K and P are the equilibrium constant and pressure, respectively. x_{total} is the total mole of gas product from Eq. (17).

Equilibrium constant can be determined by calculating the Gibbs free energy as the function of temperature, where the standard Gibbs function is dependent on the standard enthalpy change. Zainal et al. [17] have derived a mathematical correlation among the thermodynamic parameters involved. Thusly, the equilibrium constants as a function of temperature can be written as follows [18].

$$\ln K_1 = 2.04 \ln T - 2.7\ 10^{-4}\ T\ - 58200/T^2 + \frac{5926.04}{T} - 19.22 \quad (27)$$

$$\ln K_2 = -6.927 \ln T + 0.0037\ T - 3.61\ 10^{-7} T^2 + \frac{35050}{T^2} + \frac{6975.51}{T} + 34.95 \quad (28)$$

Carbon conversion is defined as that how many mole of carbon substance in the feed of gasification are converted into gas. Lim & Lee [16] set up an empirical formula as the function of ER and the temperature to predict the carbon conversion of gasification process is as follows:

$$f_c = x_1 + x_2 + x_4 = 0.901 + 0.439\ (1 - \exp(-ER + 0.0003\ T) \quad (29)$$

In this study, MATLAB routine is developed to solve all equations involved simultaneously.

4.2.6. Combustion of spent char

Spent char (including the nitrogen and sulphur in the original biomass) as the residue from gasification process is burnt out in order to generate heat for the biomass pyrolysis. In this study, it is assumed that the spent char is mainly composed of carbon, nitrogen, and sulphur. About 20% excess of air is introduced into the combustor to completely burn out the spent char and only ash remains at the end of process. It is assumed that only CO_2, NO_2, and SO_2 are contained in the exhausted gas. Emission of CO_2 and NO_x in the exhaust gas is calculated

by assuming that the system is operating for 365 days a year with a capacity 100 kg/day (see section 4.2.2).

4.2.7. Heat balance in each process and the total system

Heat balance is determined by calculating the heat contained in each material involved in the reactions based on the mass balance of each process. Meanwhile, the heat of reaction is calculated based on the heat of formation of each component involved in each process. In the pyrolysis and gasification processes, when the complex organic compounds such as coal, biomass, and char are involved, the heat of combustion can be used for the calculation based on the ultimate analysis compositions. In this case, higher heating value (HHV), which is the heat released per unit mass of the fuel reacted with oxygen with water component in condensed state in the combustion, is considered. Smith et al. [18] suggested to use the following equations to estimate the heat released from the complex organic compound based on the ultimate analysis compositions:

$$\Delta H_c^0 = -HHV + 33.3\ w_O + 38.05\ w_N - 264.3\ w_H \tag{30}$$

$$\Delta H_f = -H_c^0 + \frac{w_C}{12.01}\Delta H_{f,CO_2(g)}^0 + \frac{1}{2}\left(\frac{w_H}{1.008}\right)\Delta H_{f,H_2O(l)}^0 + \frac{w_S}{32.06}\Delta H_{f,SO_2(g)}^0 \tag{31}$$

where ΔH_f is heat of formation and ΔH_c is heat of combustion of organic complex compound. The $\Delta H_{f,CO_2(g)}^0$, $\Delta H_{f,H_2O(l)}^0$, and $\Delta H_{f,SO_2(g)}^0$ are heats of formation of CO_2, water, and SO_2, respectively. w_C, w_H, w_O, w_N, and w_S are elemental weight fraction obtained from the ultimate analysis of the organic complex compound. In this study, the organic complex compounds are biomass and char.

To predict HHVs of biomass and char, the following empirical equation is proposed [19]:

$$HHV = 14658\ w_C + 56878\ w_H + 2940\ w_S - 658\ w_{ash} - 5153\ (w_O + w_N) \tag{32}$$

where w_C, w_H, w_O, w_N, w_S, and w_{ash} are the weight fractions of C, H, O, N, S, and ash, respectively, and all are on dry basis.

Enthalpies of biomass and char at certain temperature related to the standard condition (25 °C, 1 atm) are determined based on the heat of formation and heat capacity (C_p) of the compound. The heat capacities of biomass and char can be calculated by Kirov's equation [19] as follows:

For fixed carbon: $C_p = 0.145 + 4.70.10^{-4}\ T - 2.63.10^{-7}\ T^2 + 5.25.10^{-11}\ T^3$ (33)

For ash: $C_p = 0.18 + 7.78.10^{-5}\ T$ (34)

For primary volatile matter: $C_p = 0.381 + 4.5.10^{-4}\ T$ (35)

For secondary volatile matter: $C_p = 0.699 + 3.39.10^{-4}\ T$ (36)

where C_p is the heat capacity in Btu/lb_m°F and T is temperature in °F. Secondary volatile matter is described as the portion of volatile matter based on 10% of dry-ash free, and the primary volatile matter is considered as the remains of the total volatile matter. Total heat capacity of biomass or char is calculated by multiply each heat capacity mentioned above with each weight fraction obtained from the proximate analysis.

Enthalpy of tar is also calculated by Eqs. (30) and (31) as those used for the calculation of enthalpies of biomass and char. Hyman and Kay [20] proposed a correlation to evaluate the heat capacity of tar produced from gasification as follows:

$$C_p = \frac{1}{D}(4.94.10^{-3}\ T) \quad (37)$$

where D is specific gravity at 298 K and T is temperature (K). Using typical specific gravity value of tar of 1.17 [21], Eq. (37) can be simplified to:

$$C_p = 0.00422\ T \quad (38)$$

Enthalpy of gas is calculated using the basic correlation between the standard heat of formation of gas and the heat capacity of gas as a function of temperature [18]. Briefly, it can be calculated using the following equation:

$$\Delta H^{ig} = \Delta H_0^{ig} + \int_{T0}^{T} C_p^{ig} dT \quad (39)$$

where ΔH^{ig} (J/mol) and ΔH_0^{ig} (J/mol) are enthalpies of the gas and the standard heat of formation of a certain gas at ideal state, respectively. The values of ΔH_0^{ig} are obtained from the literature [18]. The change of heat capacity as a function of temperature is calculated by Eq. (40):

$$\frac{C_p^{ig}}{R} = A + BT + CT^2 + DT^{-2} \quad (40)$$

where R is ideal gas constant and T (K) is temperature. A, B, C, and D are constant values for certain gas and the data are obtained from the literature [18].

Finally, the heat of reaction is calculated by Eq. (41) .

$$Q_{reaction} = \Delta H_{product} - \Delta H_{reactant} \quad (41)$$

4.2.8. Silica sand circulating amount

In this study, silica sand is applied in the system as the heat carrier to transfer energy generated from the exothermic reaction to the endothermic one. It is important to know how large amount of energy needs to be absorbed and carried by the sand. In the proposed system, gasification and combustion are the exothermic reactions which play as the energy donor for the pyrolysis process. Here, a simple equation used to determine the silica sand amount required can be written as below:

$$m_{sand} = \frac{Q_{absorb}}{C_{p_{sand}} \times (T_{combustion} - T_{pyrolysis})} \times 1000 \quad (42)$$

where m_s (kg) is mass of sand required for the system, Q_{absorb} (kJ) is total energy generated by the gasification and combustion processes, C_{psand} (J/kg.°C) is the heat of capacity of the sand used, $T_{combustion}$ (°C) is temperature of the combustion process, and $T_{pyrolysis}$ (°C) is temperature of the pyrolysis process. In this study, silica sand has a heat capacity of 730 J/kg°C [22]. In the practical process, heat loss usually occurs. Herein, as a case study, it is

assumed that only 95% of total energy generated in gasification and combustion will be absorbed by the sand. Similarly, it is also assumed that only 95% of energy will be transferred from the sand to biomass.

4.2.9. Power generation potential

The purpose of this supposed biomass gasification system is to generate power by the fuel gases obtained from the total process. That is to say, the produced gases from the biomass pyrolysis, tar reforming, and char gasification processes contain combustible gases, which is expected to be used as fuel for the gas engine to generate power. In this study, the estimated power generated is calculated using the following equation.

$$\text{Estimated power generated} = \frac{\text{Total gas} \times \text{HHV}_{gas} \times \eta_{\text{gas engine}}}{3600} \quad (43)$$

where HHV_{gas} is the HHV of total gas collected and $\eta_{\text{gas engine}}$ is the efficiency of gas engine which is assumed to be about 40%. The total gas includes the gases produced in the pyrolysis, tar reforming, and char gasification processes. HHV_{gas} is calculated as follows:

$$HHV_{gas} = m_{H_2}HHV_{H_2} + m_{CO}HHV_{CO} + m_{CH_4}HHV_{CH_4} \quad (44)$$

where m_{H_2}, m_{CO}, and m_{CH_4} are masses of H_2, CO, and CH_4 in the total gas collected.

4.2.10. Cold Gas Efficiency

Cold gas efficiency is one important parameter to evaluate gasification system performance. It is defined as the ratio of energy containing in gas produced to energy containing in fuel supplied to the system, and can be calculated as follows:

$$CGE = \frac{HHV_{gas}}{HHV_{biomass}} \times 100\% \quad (45)$$

HHV_{gas} is the total gas HHV which is calculated by Eq. (43) while $HHV_{biomass}$ is the biomass HHV which is calculated by Eq. (32).

4.2.11. Sensitivity analysis

Some parameters considered in this simulation could affect the final results of cold gas efficiency and potential power generation from the system. In general, as one value is selected as the assumption, any change of other parameters could change the final results. Herein, the sensitivity analysis with one-factor-at-time (OFAT) method is applied on the prediction of steam tar reforming conversion, ER and SCR values in the gasification process, and the gas engine efficiency. Firstly, certain ranges are chosen for those parameters which can reflect the shifting values of the cold gas efficiency and the potential power generation. That is, the steam tar reforming conversion is assumed to be ranged from 50 to 100% on the basis of many experiments about the tar conversion (generally in the range of 69-92%) in the catalytic steam tar reforming [12]. ER of gasification process is ranged from 0.2 to 0.5 when the SCR is set at 0.35 (the same as the assumption in section 4.2.5). Here, when ER is less than 0.2, negative values of syngas composition are generated and meanwhile, when ER is set at a value higher than 0.5, no spent char is formed in the gasification process. For SCR, the value is assumed to be ranged from 0 to 1 when ER set at 0.4 (the same as the assumption in section 4.2.5). Meanwhile, the gas engine efficiency is ranged from 35%-45% since some gas engines fueled by the syngas on the market have efficiency from about 37% to 44% [23, 24].

4.3. Results and discussion

4.3.1. Pyrolyzer

Figure 4.2 compares the calculation results based on the empirical equations in **Table 4.2** and the reported experimental data. One can see that the yield distributions of gas, tar, char and pyrolytic water of the calculation results are similar to the experimental data (**Figure 4.2(a)**). Moreover, the gas compositions (**Figure 4.2(b)**), elemental compositions in tar (**Figure 4.2(c)**) as well as in char (**Figure 4.2(d)**) are also the similar. It indicates that the calculation results are reliable when compared with experiment data. As a result, for the fast pyrolysis of woody biomass, 15.5 wt% gas (consisted of 0.23 wt% H_2, 33.05 wt% CO, 4.69

wt% CH_4 and 62.03 wt% CO_2) , 42.7 wt% tar, 19.5 wt% char and 22.2 wt% pyrolytic H_2O could be produced at 500 °C whereas 35.25 MJ/h heat is required in the fast pyrolysis process (as shown in **Table 4.7**). It should be noted that the pyrolytic water content is a little higher than the maximum value (20 wt%) described in the literature [11], but still in an acceptable amount. In contrast, as shown in **Table 4.3**, in the slow pyrolysis process based on experiment, it is found that 12.6 wt% gas (consisted of 0.25 wt% H_2, 23.11 wt% CO, 11.33 wt% CH_4 and 65.32 wt% CO_2) , 40.6 wt% tar, 26.8 wt% char and 20 wt% pyrolytic H_2O are obtained whereas 31.76 MJ/h heat is needed (**Table 4.7**). One can see that more tar is produced and less char are produced and more energy is needed in the fast pyrolysis process. These significant difference in the two pyrolysis process will also affect the following results on the tar reforming, char gasification and spent char combustion. Also, the sand circulating rate will also be different based on these two pyrolysis routes.

Table 4.3 Mass balance in the slow pyrolysis process via experiment

Product yield (wt.%)							
Gas	12.6	Tar[a]	40.6	Char	26.8	Pyrolytic water[b]	20.0
Composition (wt.%)							
H_2	0.25	C	40.15	C	81.05	H_2O	100
CO	23.11	H	7.45	H	2.58		
CH_4	11.33	O	52.40	O	14.59		
CO_2	65.31			N	1.43		
				S	0.36		

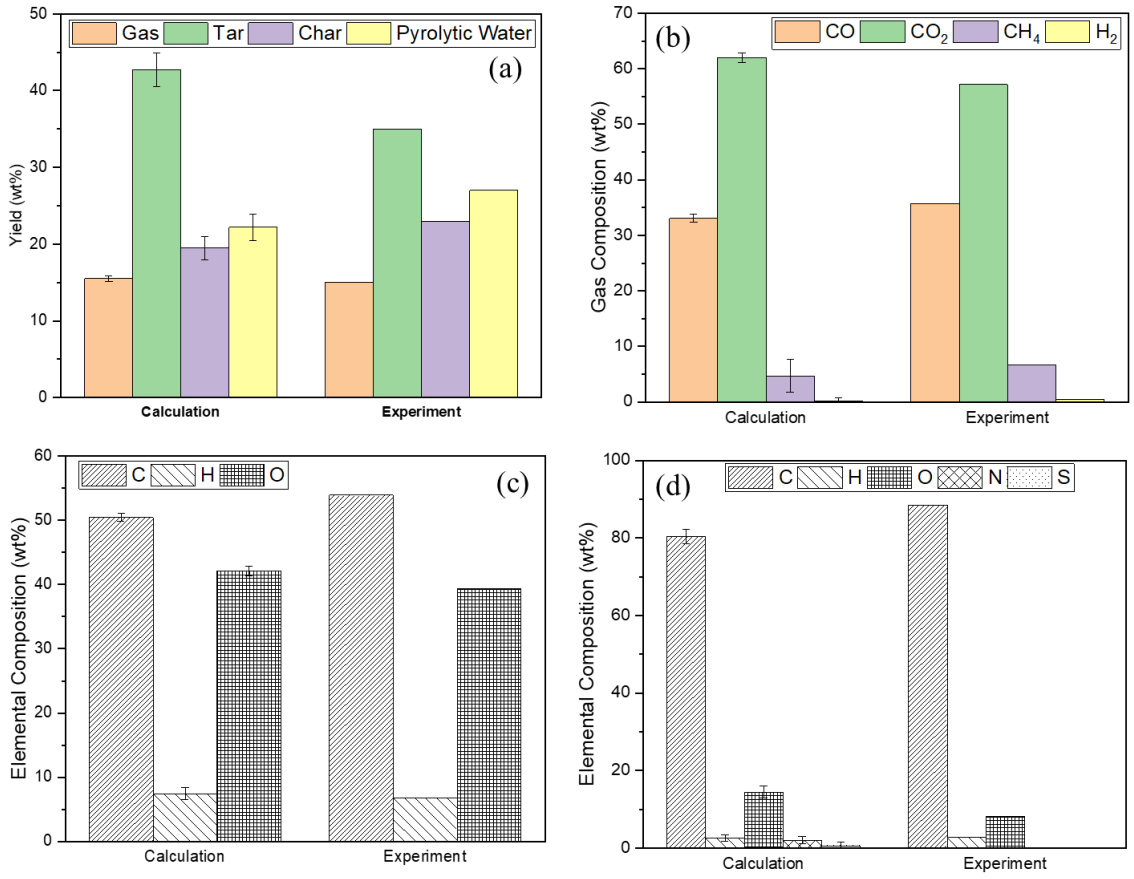

Figure 4.2 Comparison of calculation results with the reported experimental data [13] for the fast pyrolysis process (a) yields, (b) gas compositions, (c) tar elemental compositions, and (d) char elemental compositions

4.3.2. Steam tar reformer

Table 4.4 shows the mass as well as heat balance calculation results based on the tar amounts obtained in the two different pyrolysis routes. As indicated in section 4.2.4, it is assumed that catalytic reaction occurs with a conversion of 70%, and as such, 14.8 wt% and 15.8 wt% tar residues are still remained in the final products corresponding to the fast and slow pyrolysis routes, respectively. However, more syngas (59.5 wt% vs. 57.5 wt% in the products) can be obtained from the tar produced in the fast pyrolysis route since more tar is reformed in this case. It should be noted that the syngas amount obtained in this steam tar reforming is total amount of gas produced in the pyrolysis process and gas produced in the followed tar

reforming reaction based on the gasification system design as shown in **Figure 4.1**. Meanwhile, corresponding to the fast pyrolysis route, the total steam and heat required to support the reforming reaction are also higher since more tar is processed. It is found that external energy required to the steam tar reforming process are about 6.7 kW (24.1 MJ/h) and 4.5 kW (16.4 MJ/h) corresponding to the fast and slow pyrolysis routes, respectively.

Table 4.4 Comparison of mass and heat balance results in the steam tar reforming process based on the tar amounts obtained in the two pyrolysis routes

Fast Pyrolysis						Slow Pyrolysis					
Products Yield (wt.%)											
Syngas		Tar residue		Pyrolytic water		Syngas		Tar residue		Pyrolytic water	
59.5		14.8		25.7		57.5		15.8		26.7	
Composition (wt.%)											
H_2	6.15	C	50.45	H_2O	100	H_2	4.82	C	39.01	H_2O	100
CO	68.41	H	7.44			CO	58.45	H	7.67		
H_2O	25.44	O	42.11			H_2O	36.73	O	53.33		
Total steam required: 2.6 kg/h						Total steam required: 1.9 kg/h					
Heat required: 24.10 MJ/h						Heat required: 16.40 MJ/h					

4.3.3. Char gasification

Table 4.5 shows the mass and heat balance results on the char gasification based on the char amounts obtained from the two different pyrolysis routes. Since more char can be produced from the slow pyrolysis process, more syngas (21.1 kg/h vs.14.4 kg/h) is produced with higher energy generated (31.64 MJ/h vs. 21.97 MJ/h) in the followed char gasification process. Herein, the high energy generated is significantly important to supply the energy for the pyrolysis energy requirement. Meanwhile, in order to convert more char to syngas, more air and steam are also required accompanying with the slow pyrolysis route. It should be noted that the syngas compositions (0.65 wt% H_2 and 15.97 wt% CO) are almost the same

for the two cases since it is assumed that the obtained chars in the two routes have the same compositions (see section 4.2.5).

Table 4.5 Comparison of mass and heat balance results in the char gasification processes based on the char amounts obtained in the two pyrolysis routes

Fast pyrolysis				Slow pyrolysis			
Products yield (kg/h)							
Produced gas		Spent char		Produced gas		Spent char	
14.4		0.4		21.1		0.4	
Composition (wt.%)							
H_2	0.65	C	19.64	H_2	0.65	C	26.31
CO	15.97	N	12.86	CO	15.97	N	11.79
CH_4	1.06	S	3.214	CH_4	1.06	S	2.947
CO_2	18.91	Ash	64.29	CO_2	18.91	Ash	58.95
H_2O	1.22			H_2O	1.22		
N_2	62.19			N_2	62.19		
Total air: 11.4 kg/h				Total air: 16.6 kg/h			
Total steam: 0.8 kg/h				Total steam: 1.2 kg/h			
Heat generated: 21.97 MJ/h				Heat generated: 31.64 MJ/h			

4.3.4. Combustion

Table 4.6 shows the mass and heat balance results on the spent char combustion process corresponding to the two different pyrolysis routes. Consistent with the char gasification results, more char produced from the slow pyrolysis route results in more exhaust gas (2.6 kg/h vs. 2.0 kg/h) with higher heat energy generated (3.2 MJ/h vs. 2.0 MJ/h) in the spent char combustion process. Referring to the char gasification process, even though both pyrolysis routes produce the same amount of spent char, the slow pyrolysis route leads to higher carbon content (see **Table 4.5**). As such, in order to burn higher carbon content in the spent char, more air is required. Relating to combustion of higher carbon content, more CO_2 are also

generated from the slow pyrolysis route, which means higher CO_2 emission (1.13 ton/year vs. 0.82 ton/year) released to the air. Since the same N content is contained in the spent char of the same biomass feedstock, both pyrolysis routes generate the same amount of NO_x that is, about 0.48 ton/year.

Table 4.6 Comparison of mass and heat balance results on the spent char combustion process based on the spent char amounts obtained in char gasification processes corresponding to the two pyrolysis routes

Fast pyrolysis		Slow pyrolysis	
Products yield (kg/h)			
Exhaust gas		Exhaust gas	
2.0		2.6	
Composition (wt.%)			
CO_2	13.81	CO_2	15.74
NO_2	8.10	NO_2	6.32
SO_2	1.23	SO_2	0.96
O_2	3.26	O_2	3.27
N_2	73.59	N_2	73.71
Ash: 0.025 kg/h			
Total air: 1.9 kg/h		Total air: 2.4 kg/h	
CO_2 emission: 0.82 ton/year		CO_2 emission: 1.13 ton/year	
NO_x emission: 0.48 ton/year		NO_x emission: 0.48 ton/year	
Heat generated: 2.0 MJ/h		Heat generated: 3.2 MJ/h	

4.3.5. Recycled sand amount

As shown in **Table 4.7**, the total energy generated from gasification and combustion processes corresponding to the fast and slow pyrolysis routes are about 23.97 and 32.94 MJ/h respectively. To carry such heat amount by the silica sand, about 65.67 and 90.26 kg/h recycled sand amounts are needed, which could theoretically provide 68% and 104% of the

necessary heats for the fast and slow biomass pyrolysis processes, respectively. After considering 5% heat loss in heat transfer process when energy is absorbed and released by the sand, the needed sand amount does not change significantly. As a result, about 62.38 and 85.75 kg/h of sand are required for the fast and slow biomass pyrolysis processes, respectively. However, since the energy carried by the sand is less and also considering heat loss during the heat transfer between sand and biomass, the energy coverage drops to 61% and 94% for the fast and slow pyrolysis routes, respectively. That is to say, energy is needed to be provided from the outside of the system in the fast pyrolysis route either with or without the heat loss. In contrast, in the slow pyrolysis route, the energy generated in the char gasification as well as the spent char combustion processes can supply enough energy required by the slow pyrolysis process, and the extra heat could be provided for the catalytic steam tar reforming process if there is a good thermal recovery system design. However, considering the 5% heat loss, a little amount of external energy is also needed to be supplied for the slow pyrolysis route.

Table 4.7 Energy required for pyrolysis process, total energy generated, recycled sand amount and pyrolysis heat coverage by the generated heat in the systems based on the two pyrolysis routes

	Fast pyrolysis	Slow pyrolysis
Energy required (MJ/h)	35.25	31.76
Total energy generated (MJ/h)	23.97	32.94
Recycled sand amount (kg/h)[a]	65.67	90.26
Pyrolysis heat coverage[a]	68%	104%
Recycled sand amount (kg/h)[b]	62.38	85.75
Pyrolysis heat coverage[b]	61%	94%

4.3.6. Power generation potential

As shown in **Table 4.8**, the total amounts of fuel gas collected in the gasification systems based on the fast and slow pyrolysis routes are 22.6 kg/h (consisted of 2.15 wt% H_2, 32.12

wt% CO, 0.70 wt% CH_4, 17.32 wt% CO_2, 7.89 wt% H_2O and 39.81 wt% N_2) and 27.9 kg/h (consisted of 1.47 wt% H_2, 24.66 wt% CO, 1.16 wt% CH_4, 17.75 wt% CO_2, 7.87 wt% H_2O and 47.09 wt% N_2) with 151.2 MJ/h and 145.7 MJ/h HHVs, respectively, by which 16.8 and 16.3 kWe power generation with the cold gas efficiencies of 73.8% and 71.7% could be reached respectively. Even though the slow pyrolysis route can generate higher amount of gas, higher remaining nitrogen dominates the compositions so that the gas HHV, the power generation potential and the cold gas efficiency are lower since the nitrogen amount has no contribution to HHV.

Compared to the Viking Two-Stage Gasification System developed by Technical University of Denmark (DTU) with a cold gas efficiency of about 90% based on a lower heating value (LHV) [25], the cold gas efficiency of this proposed system is lower. Nevertheless, compared with the two-stage gasification developed by Wang et al. [26] with a cold gas efficiency of 66%, the cold gas efficiency of this proposed system is higher. Moreover, compared with the small-scale downdraft fixed bed reactor developed by Chawdhury et al. [27], which has a cold gas efficiency of about 59% for wood pellets and 67% for woodchips, this proposed system has a much higher cold gas efficiency. Herein, it should be noted that although our separated-type biomass gasification system also applies the similar staged gasification concept as Viking Gasification System, the ways for the handling tar and char gasification are different. The Viking Gasification System used the partial oxidation process for tar treatment and the char was gasified by air, which could generate more high-heat-value gases such as CO and CH_4. This is the reason why our system has a little lower cold gas efficiency. On the other hand, comparing with the systems of Wang et al. [26] and Chawdhury et al. [27], a self-heating pyrolysis is used by circulating the hot sand inside our system, which is the main reason why our system has a higher cold gas efficiency than theirs.

Table 4.8 Total produced fuel gas amount, HHV, power generation potential, and cold gas efficiency of the systems based on the two pyrolysis routes

Fast pyrolysis	Slow pyrolysis
Total produced fuel gas amount (kg/h)	

	22.6		27.0
Composition (wt.%)			
H_2	2.15	H_2	1.47
CO	32.12	CO	24.66
CH_4	0.70	CH_4	1.16
CO_2	17.32	CO_2	17.75
H_2O	7.89	H_2O	7.87
N_2	39.81	N_2	47.09
HHV: 151.2 MJ/h		HHV: 147.0 MJ/h	
Power generation potential: 16.8 kWe		Power generation potential: 16.3 kWe	
Cold gas efficiency: 73.8%		Cold gas efficiency: 71.7%	

4.3.7. Sensitivity analysis

Figure 4.3 shows the sensitivity analysis on the 4 different parameters which have direct impact on the cold gas efficiency and potential power generation by the system. Figure 3(a) shows that when the steam tar conversion is changed to 50% from 70%, the cold gas efficiency and the power generation drop 18.7% and 13.7% for the fast and slow pyrolysis routes, respectively. Meanwhile, when it is changed to 100%, the cold gas efficiency and the power generation rise about 28% and 21% for the fast and slow pyrolysis routes, respectively. As shown in Figure 3(a), in the case of the tar conversion is less than 66%, the slow pyrolysis route could result in a higher cold gas efficiency and more power generation than the fast pyrolysis one and vice versa. Thus, the steam tar conversion has great effect on the cold gas efficiency and potential electricity generated by the system. Figure 3(b) shows the sensitivity of the cold gas efficiency and the power generation to the different gas engine efficiencies. One can see that only the power generation is changed linearly with the change of gas engine efficiency. That is, when the gas engine efficiency is decreased to 35% from 40%, the electricity generated drops 12.5% and when it is increased to 45%, the electricity generated rises 12.5% linearly for both the fast and slow pyrolysis routes. Thus, the power generation

is more sensitive to the gas engine efficiency but the cold gas efficiency has almost no sensitive to the gas engine efficiency. Figure 3(c) shows the sensitivity of cold gas efficiency and the power generation to the different ER in the char gasification process with the same SCR value of 0.35. One can see that as the ER is decreased to 0.2 from 0.4, the cold gas efficiency and the power generation rise 8.5% and 12.1% for the fast and slow pyrolysis routes, respectively. While it change to 0.5, both of the cold gas efficiency and the power generation drop about 4.6% and 6.5% for fast and slow pyrolysis routes, respectively. Thus, the ER also has some effect on the cold gas efficiency and the power generation. Figure 3(d) shows the sensitivity of cold gas efficiency and electricity generated to the different SCR at the same ER of 0.4. One can see that both the cold gas efficiency and the power generation decrease with the increase in the SCR for both the fast and slow pyrolysis routes. From the above results, it can be concluded that the change of either ER or SCR does not significantly change the overall result of the system. On the other hand, the change of steam tar reforming conversion or gas engine efficiency could result in a significant effect on the system performance.

4.4. Conclusions

In this study, simulations of a small-scale separated-type biomass gasification system composed of a screw pyrolyzer, a steam tar reformer, an air-steam char fluidized bed gasifier, and a spent char combustor with heat carrier particles circulating based on the fast and slow biomass pyrolysis routes are performed. During the simulations, empirical equations from the published literatures are successfully applied to analyze the elemental, mass, and energy balances of each process by applying sets of assumptions at a certain condition to predict final energy efficiency of the system. As a result, 12.5 kg/h of wood biomass feeding to this system has power generation ability of 16.8 kWe and 16.3 kWe with cold gas efficiencies of 73.8% and 71.7% for the fast and slow pyrolysis routes respectively. The sensitivity analysis indicates that the change of either ER or SCR does not significantly change the overall result of the system, but the change of steam tar reforming conversion or gas engine efficiency

could result in a significant effect on the system performance. It is expected that the calculation methods presented in this study could be utilized for preliminary engineering design of comprehensive biomass thermal conversion processes.

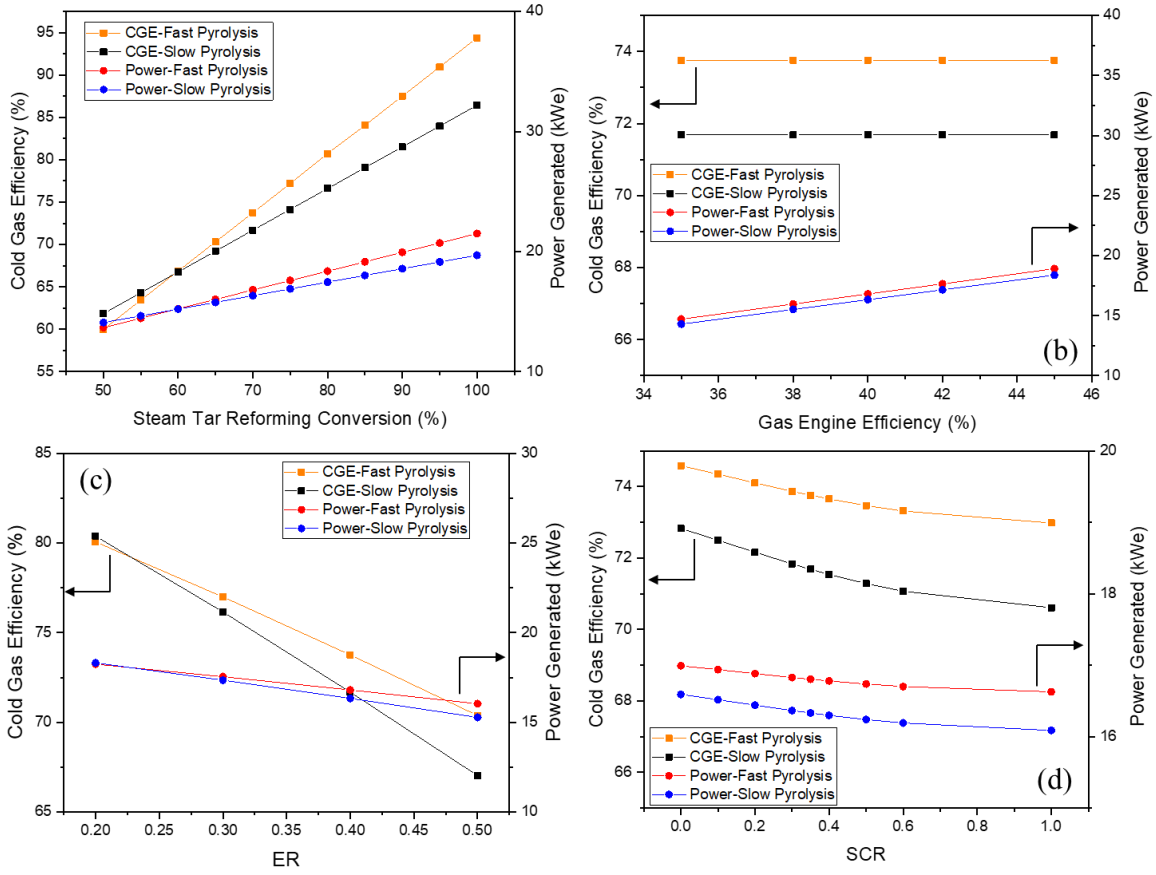

Figure 4.3 Sensitivity analysis of the cold gas efficiency and the potential power generation to (a) steam tar reforming conversion, (b) gas engine efficiency, (c) ER, and (d) SCR

References

[1] G. Guan, C. Fushimi, A. Tsutsumi, M. Ishizuka, S. Matsuda, H. Hatano, Y. Suzuki, High-density circulating fluidized bed gasifier for advanced IGCC/IGFC—Advantages and challenges, Particuology, 8 (2010) 602-606.

[2] N. Chaihad, S. Karnjanakom, I. Kurnia, A. Yoshida, A. Abudula, P. Reubroycharoen, G. Guan, Catalytic upgrading of bio-oils over high alumina zeolites, Renewable Energy, 136 (2018) 1304-1310.
[3] M. Kaewpanha, G. Guan, XiaogangHao, Z. Wang, K. Kusakabe, A. Abudula, Steam Co-Gasification of Brown Seaweed and Land-Based Biomass, Fuel Processing Technology 120 (2014) 106-112.
[4] L. Fagbemi, L. Khezami, R. Capart, Pyrolysis Products from Different Biomasses: Application to The Thermal Cracking of Tar, Applied Energy, 69 (2001) 293-306.
[5] K.H. Kim, I.Y. Eom, S.M. Lee, D. Choi, H. Yeo, I.G. Choi, J.W. Choi, Investigation of Physicochemical Properties of Biooils Produced from Yellow Poplar Wood (Liriodendron Tulipifera) at Various Temperatures and Residence Times, Journal of Analytical and Applied Pyrolysis 92 (2011) 2-9.
[6] E. Okoroigwe, Z. Li, T. Stuecken, C. Saffron, S. Onyegegbu, Pyrolysis of *Gmelina arborea* Wood for Bio-oil/Bio-char Production: Physical and Chemical Characterisation of Products, Journal of Applied Sciences, 12 (2012) 369-374.
[7] R.E. Guedes, A.S. Luna, A.R. Torres, Operating Parameters for Bio-Oil Production in Biomass Pyrolysis: A Review, Journal of Analytical and Applied Pyrolysis, 129 (2018) 134-149.
[8] Y. Xin, H. Cao, Q. Yuan, D. Wang, Two-step gasification of cattle manure for hydrogen-rich gas production: Effect of biochar preparation temperature and gasification temperature, Waste Management 68 (2017) 618-625.
[9] V. Dhyani, T. Bhaskar, A Comprehensive Review on The Pyrolysis of Lignocellulosic Biomass, Renewable Energy 19 (2018) 695-716.
[10] P. Roy, G. Dias, Prospects for Pyrolysis Technologies in The Bioenergy Sector: A Review, Renewable and Sustainable Energy Reviews, 77 (2017) 59-69.
[11] D. Neves, H. Thunman, A. Matos, L. Tarelho, A. Gómez-Barea, Characterization and Prediction of Biomass Pyrolysis Products, Progress in Energy and Combustion Science 37 (2011) 611-630.

[12] G. Guan, M. Kaewpanha, X. Hao, A. Abudula, Catalytic steam reforming of biomass tar: Prospects and challenges, Renewable and Sustainable Energy Reviews, 58 (2016) 450-461.
[13] N. Gao, S. Liu, Y. Han, C. Xing, A. Li, Steam Reforming of Biomass Tar for Hydrogen Production Over Nio/Ceramic Foam Catalyst, International Journal of Hydrogen Energy 40 (2015) 7983-7990.
[14] Q. Eri, W. Wu, X. Zhao, Numerical Investigation of the Air-Steam Biomass Gasification Process Based in Thermodynamic Equilibrium Model, Energies, 10 (2017).
[15] S. Sharma, P.N. Sheth, Air–Steam Biomass Gasification: Experiments, Modeling and Simulation, Energy Conversion and Management, 110 (2016) 307-318.
[16] Y. Lim, U. Lee, Quasi-Equilibrium Thermodynamic Model with Empirical Equations for Air–Steam Biomass Gasification in Fluidized-Beds, Fuel Processing Technology 128 (2014) 199-210.
[17] Z.A. Zainal, R. Ali, C.H. Lean, K.N. Seetharamu, Predicition of Performance of a Downdraft Gasifier Using Equilibrium Modeling for Different Biomass Materials, Energy Conversion and Management, 42 (2001) 1499-1515.
[18] J.M. Smith, H.C.V. Ness, M.M. Abbott, Introduction to Chemical Enginnering Thermodynamics, 6th ed., McGraw Hill2001.
[19] G.V. Reklaitis, Introduction to Material and Energy Balances, John Wiley & Sons, Inc.1983.
[20] D. Hyman, W.B. Kay, Heat Capacity and Content of Tars and Pitches, Ind. Eng. Chem., 41 (1949) 1764-1768.
[21] W. Eisermann, P. Johnson, W.L. Conger, Estimating Thermodynamic Properties of Coal, Char, Tar and Ash, Fuel Processing Technology, 3 (1980) 39-53.
[22] www.engineeringtoolbox.com, Specific Heat of Common Substances, 2018 [accessed 20 September 2018],
[23] ClarkEnergy, Syngas Cogeneration / Combined Heat & Power, https://www.clarke-energy.com/synthesis-gas-syngas/, 2019 [accessed 31 March 2019],

[24] MWM, Gas engine TCG 2020, https://www.mwm.net/mwm-chp-gas-engines-gensets-cogeneration/gas-engines-power-generators/gas-engine-tcg-2020/, 2019 [accessed 31 March 2019],

[25] B. Gobel, C. Hindsgaul, U.B. Henriksen, J. Ahrenfeldt, F. Folk, N. Houbak, E.B. Qvale, High Performance Gasification with the Two-Stage Gasifier, 12. European Biomass Conference, ETA-Florence & WIP-Munich, 2002, pp. 389-395

[26] Y. Wang, K. Yoshikawa, T. Namioka, Y. Hashimoto, Performance optimization of two-staged gasification system for woody biomass, Fuel Processing Technology 88 (2007) 243-250.

[27] M.A. Chawdhury, K. Mahkamov, Development of a Small Downdraft Biomass Gasifier for Developing Countries, J. Sci. Res. , 3 (2011) 51-64.

CHAPTER 5 : A NOVEL SYSTEM OF BIOMASS-BASED HYDROGEN PRODUCTION BY COMBINING STEAM BIO-OIL REFORMING AND CHEMICAL LOOPING PROCESS

5.1. Introduction

Cogeneration, trigeneration, and polygeneration have been proposed to increase the efficiency of the whole biomass conversion system. Meanwhile, by using such integrating processes, several products can be coproduced [1]. In general, the hybrid process combining two or more processes could fully utilize the feedstock of the system to generate single or multiple products simultaneously with improved efficiency, which can also increase product yields while decrease wastes or by-products. A hybrid process composed of the pyrolysis combined with the catalytic steam reforming of bio-oil and separate gasification of biochar was proposed as a potential and promising method for the small-scale power generation from biomass without facing tar problems in gasifier [2]. It is reported that nickel (Ni)-based catalysts can be used to obtain syngas with high H_2/CO from bio-oil through the steam reforming reaction and combined with additional water-gas shift reaction, H_2 production can be increased more [3, 4], while biochar gasification produces cleaner syngas with higher efficiency.

In addition to the conventional thermochemical process, another concept called chemical looping is also known as a promising way for H_2 production from solid fuels such as coal, biomass, and biochar. This method can effectively use carbonaceous materials as the reducing agent with a redox loop of metal oxide as the oxygen carrier and steam as oxidizer and hydrogen source. Especially, it can produce pure H_2 with other gases such as CO and CO_2 separately obtained from biomass decomposition by coupling several reactors without using any additional gas treatment and separation processes [5, 6]. Nevertheless, there are limitations in the exploration of chemical looping process using solid fuels as reducing agents. For example, they always have low reactivity with the oxygen carriers due to the low solid-solid contact efficiency in short residence time inside the reactor. Moreover, the selection of

an oxygen carrier with suitable properties such as high catalytic and mechanical stability at high temperature and the resistance ability against carbon deposition at high pressure is the key issue in the chemical looping process [7]. The more common way for chemical looping application is production of the syngas from biomass/coal gasification or natural gas/methane [8-10]. Recently, the work of Li *et al.* [6] and Zeng *et al.* [11] showed the promising feasibility of direct utilization of solid fuels as the reducing agent in chemical looping process. Thus, it should be more interesting by using solid carbon resources as the feedstock in a practical chemical looping process.

In this study, a novel system combining the pyrolysis of biomass and catalytic steam reforming of bio-oil with a chemical looping process using the generated biochar from biomass pyrolysis as the reducing agent was proposed and simulated for the H_2 production from biomass. The hybrid system was designed for the full utilization of products from biomass pyrolysis to produce single H_2 product. Based on the evaluation of mass and energy balances in the overall system, the optimized self-supported energy circulation was achieved. The effects of operating parameters including the steam to carbon ratio for catalytic steam bio-oil reforming and temperatures in the reducing reactor and the steam reactor of the chemical looping unit on the performance of the overall system were investigated. It is expected to obtain a new way for the effective production of H_2 from biomass.

5.2. Methodology

5.2.1. Process Description

Figure 5.1 describes the schematic diagram of the proposed novel system for H_2 production from biomass including the biomass pyrolysis, catalytic steam reforming of bio-oil, and chemical looping unit using biochar from the biomass pyrolysis as the reducing agent. Herein, woody biomass is chosen as the model biomass feedstock for the system since it is the most promising resource among various biomass. It is found that various woody biomass have almost the similar properties [12]. Herein, apple tree branch is chosen as the model woody biomass with intrinsic characteristics as shown in **Table 5.1**, where the high heating value

(HHV) was calculated with the Institute of Gas Technology (IGT) method [12, 13]. In the system, the biomass is introduced into the biomass pyrolysis reactor at first. After the pyrolysis, the generated biochar and the gaseous products including bio-oil are separated. The bio-oil is catalytically reformed by steam to form syngas whereas the biochar is introduced into the reducing reactor (RR) of the chemical looping unit, which also includes other two coupling reactors, i.e., a steam reactor (SR), and an air reactor (AR), integrated with each other, for the H_2 production. The syngas generated from the catalytic steam reforming of bio-oil is used for heating biomass pyrolysis process before compressed and entering a pressure swing adsorption (PSA) unit to obtain the purified H_2 product. The tail gas from the PSA system is firstly dried and then burned in the furnace. The exhaust gas from combustion chamber is used to generate steam and provide heat for the steam reforming reaction.

Table 5.1 Characteristics of woody biomass (apple tree branch) as biomass feedstock

Ultimate Analysis (wt%-daf)		**Proximate Analysis (wt%-dry basis)**	
C	43.7	Moisture	7.8
H	6.2	FC	19.8
N	0.5	VM	78.2
S	0.0	Ash	2
O	49.6		
HHV (MJ/hr)		1732.48	

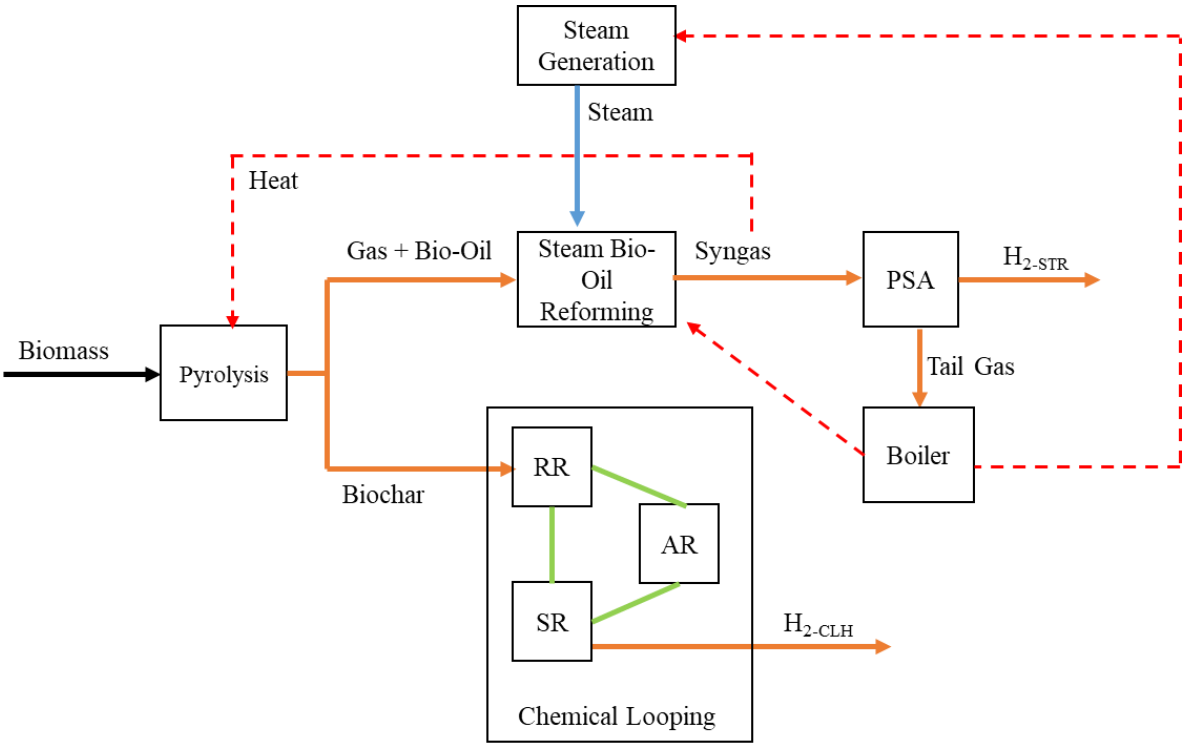

Figure 5.1 Schematic diagram of the novel hydrogen production system with biomass pyrolysis, catalytic steam reforming of bio-oil and a chemical looping unit.

5.2.1.1. Biomass pyrolysis

Pyrolysis is one of the thermochemical processes to decompose biomass in the absence of oxygen at a temperature range from 350 to 700 ^{o}C, by which biochar, bio-oil (in gas state at the pyrolysis temperature), and non-condensable gases such as CO, CO_2, CH_4, and H_2 are generated together from biomass. Biomass pyrolysis can be categorized into two different processes, i.e., slow and fast pyrolysis based on the heating rate. The slow pyrolysis always generates much more biochar from biomass whereas the fast pyrolysis will produce more bio-oil [14].

Various reactors have been developed for the fast pyrolysis of biomass, which include the fluidized bed reactor, recirculating bed reactor, ablative reactor, and cone reactor. Among them, the fluidized bed reactor is the most favorable and commercially available one for the bio-oil production, by which the tar yield can reach about 70-75%. On the other hand, the

fixed bed reactor is the most widely used one for biochar production. In addition, the auger or screw type reactor is one pyrolysis reactor which can produce both biochar and bio-oil with the yields between those from the fluidized bed reactor and the fixed bed reactor. This type of reactor gains popularity recently because it has a simple design, is easy to operate, requires only a small amount of carrier gas, and consumes less energy. The result of pyrolysis process is mainly dependent on the amount of feedstock processed at the specific temperature within certain residence time of reaction. The main advantage of auger type reactor is that the residence time can be controlled by tuning the rotation speed of the screw inside the reactor [15]. In the present study, the auger type reactor is chosen for the biomass pyrolysis at 500 ^{o}C. Flow and temperature controllers are applied in the input and inside of pyrolyzer, respectively, to ensure the biomass pyrolysis process occurring at a stable condition during the simulation.

5.2.1.2. Catalytic steam bio-oil reforming, H_2 Separation, and heat circulation units

Bio-oil is a condensable product of biomass pyrolysis, which contains various hydrocarbons such as alcohol, ketones, acids, polycyclic aromatic hydrocarbons (PAH). It is difficult to use it as a fuel directly due to its low heat value, high viscosity, and corrosive. Steam reforming is considered as the most effective process to produce hydrogen. Methane or natural gas is the most common feedstock for hydrogen production through the steam reforming process [16]. Steam reforming of bio-oil is also considered as the most effective and promising route to convert it to H_2 or syngas for clean applications [17]. It is found that CO produced during this process can further react with excess steam by water-gas shift reaction to produce more H_2 as follows [3, 18]:

$$C_xH_yO_z + (x\text{-}z)H_2O \rightarrow xCO + [y/2+x\text{-}z]H_2 \quad (1)$$

$$CO + H_2O \rightarrow CO_2 + H_2 \quad (2)$$

Theoretically, about 6 kg of H_2 can be obtained from 100 kg of woody biomass via the biomass pyrolysis process combined with the steam reforming of bio-oil. It is reported that the commercial Ni-based catalysts has good activity for the steam reforming of bio-oil and the deactivated catalysts can be also easily regenerated for the reuse [19]. In this study, the

simulation on the steam reforming of bio-oil was based on the operation temperature of 850 ^{o}C with a pressure of 1 bar and a steam to carbon (S/C) ratio of 6 since the bio-oil conversion was as high as 95% over the Ni-based catalysts at this condition [20].

PSA is a common separation technology with low cost to obtain H_2 with purity over than 99.99% from the syngas produced from the steam reforming process [21]. In the PSA separation process, the adsorption occurs at a high pressure whereas the desorption performs at atmospheric pressure. Adsorption pressure is usually in the range of 7-35 bar, depending on the pressure of the gas entering the PSA unit [22, 23]. Separation process in PSA normally occurs at atmospheric temperature. PSA with elevated temperature of 200-450 ^{o}C can be applied for certain condition that allowing the feed gas entering PSA without pre-cooling and achieve higher H_2 recovery [24]. However, in this study, the hot syngas is considered to be used to heat biomass pyrolysis process. Thus, the separation at a low temperature is selected. Moreover, as shown in **Table 5.2**, PSA separation with a feed pressure of 7 bar can obtain high purity H_2 with average recovery about 70.8% [22, 23, 25-27]. Consequently, the PSA separation operated at 7 bar and 35 ^{o}C to achieve H_2 purity of 99.5% and recovery efficiency of 70.8% is then selected.

Table 5.2 Results on PSA unit for the hydrogen purification and recovery using various pressure ratios and various adsorbents reported in the literatures

Gas Type	**Adsorbent**	**PF/PR[b] (bar)**	**H_2 Purity (%)**	**H_2 Recovery[c] (%)**	**Ref.**
SMROG[a]	AC/Zeolite	7.0/1.0	99.996	52.1	[22]
SMROG[a]	AC	7.0/1.0	99.999	62.7	[23]
SMROG[a]	AC	5.0/0.5	99.981	81.6	[25]
Coal Gasification	AC/Zeolite	8.0/1.0	99.430	71.2	[26]
Coal Gasification + WGS	AC	7.0/1.0	99.980	78.55	[27]
Coal Gasification + WGS	Zeolite	7.0/1.0	87.820	78.55	

[a] SMROG: steam methane reforming off-gas

[b] PF: feed pressure

[b] PR: recovery pressure

[c] H_2 recovery: percentage of H_2 amount can be separated from other gases

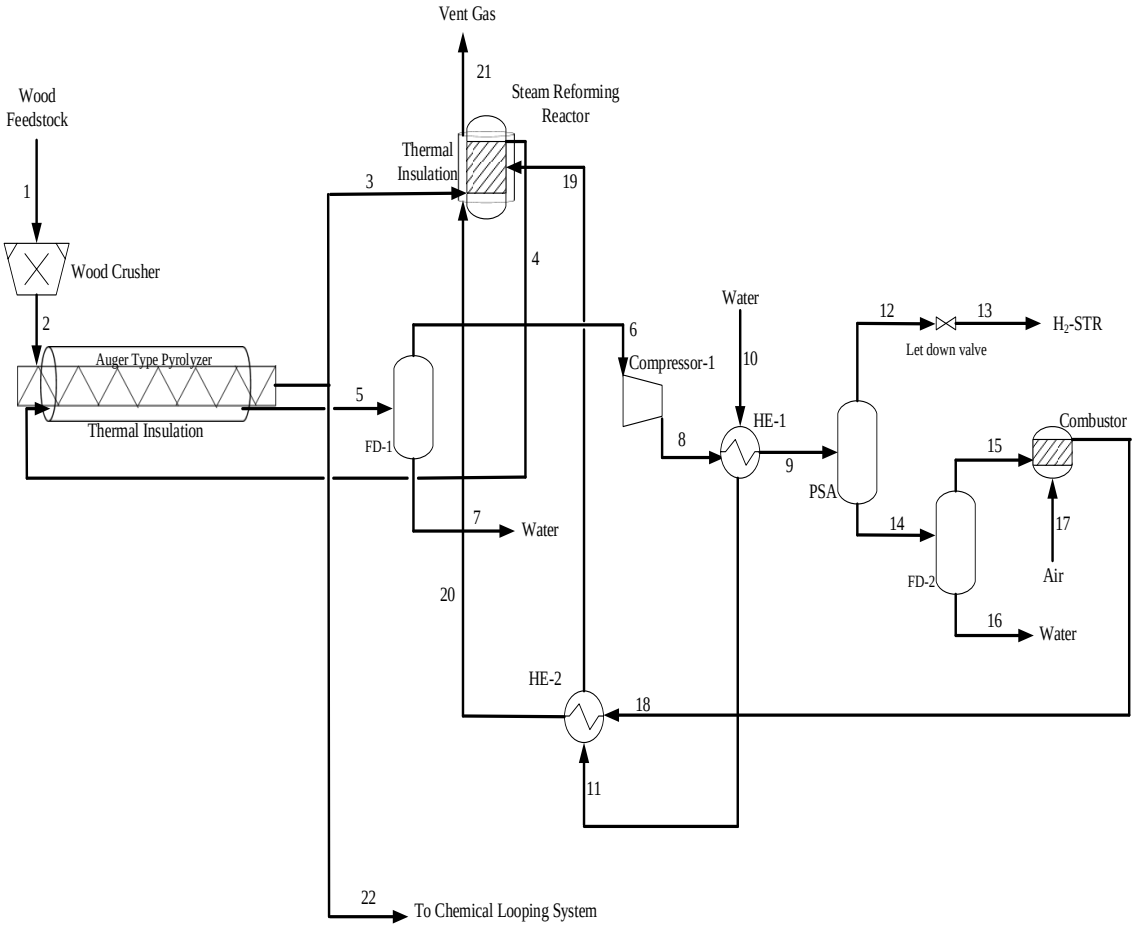

Figure 5.2 Detailed schematic diagram of biomass pyrolysis, steam tar reforming, PSA, and heat circulation units.

Before entering the PSA separation unit, firstly the water in the syngas is partly separated in flash drum. Then, the syngas is pressurized to 7 bar, which will result in a temperature increase. Then, the compressed syngas is cooled down to the operating temperature of the

PSA while pre-heat the water for steam generation. The tail gas from PSA separation still has heating value that can be utilized further. Herein, the tail gas is firstly dried and then burned out in the boiler adiabatically and used to generate steam and heat for the reforming reactor with thermal insulation and the cooled flue gas is then vented out. **Figure 5.2** shows the schematic diagram of the above-stated system with biomass pyrolysis, steam bio-oil reforming, and heat circulation units. Temperature control is also essential in heat circulation in order to make the syngas enter PSA process at a proper temperature while it provides the heat for biomass pyrolysis. The heat supply for the steam reforming also should be controlled by monitoring the combustion of the tail gas.

5.2.1.3. Chemical looping system for H_2 production from biochar

The chemical looping unit can use carbonaceous materials as the reducing agent in the redox cycle of a solid oxygen carrier for the H_2 production. Herein, the solid oxygen carrier provides oxygen source to replace the "gasifying agent" normally supplied by air or cryogenic separation of air in a gasification system. Meanwhile, the oxygen carrier also works as heat carrier and/or catalyst in this unit. The main advantage of the chemical looping unit for H_2 production (CLH) is that it can generate pure H_2 with only a simple separation process. As shown in **Figure 5.3**, the CLH used in this study has three coupling reactors of RR, SR and AR. In the RR, the oxygen carrier is reduced by the biochar with the generation of CO_2 and H_2O at first. Then, the reduced oxygen carrier enters the SR and is partly oxidized by steam to produce H_2. Thereafter, the partly oxidized oxygen carrier is moved into the AR and completely oxidized by air and finally the completely oxidized oxygen carrier is circulated back to the RR for the next reducing cycle. Since iron oxide is the most common compound applied in the CLH for the H_2 production [7, 28], it is also used as the oxygen carrier in this study. Herein, the main reactions occur in the RR are expressed as Eqs. (3) to (8), in the SR as Eqs. (9) and (10), and in the AR as Eq. (11), respectively [7, 29, 30].

$$Fe_2O_3 + 1/2C \rightarrow 2FeO + 1/2\ CO_2 \quad (3)$$

$$Fe_2O_3 + CO \rightarrow 2FeO + CO_2 \quad (4)$$

$$Fe_2O_3 + 3/2C \rightarrow 2Fe + 3/2CO_2 \quad (5)$$

$$Fe_2O_3 + 3CO \rightarrow 2Fe + 3CO_2 \quad (6)$$

$$Fe_2O_3 + H_2 \rightarrow 2FeO + H_2O \quad (7)$$

$$Fe_2O_3 + 3H_2 \rightarrow 2FeO + 3H_2O \quad (8)$$

$$3Fe + 4H_2O \rightarrow Fe_3O_4 + 4H_2 \quad (9)$$

$$3FeO + H_2O \rightarrow Fe_3O_4 + H_2 \quad (10)$$

$$2Fe_3O_4 + 1/2O_2 \rightarrow 2Fe_2O_3 \quad (11)$$

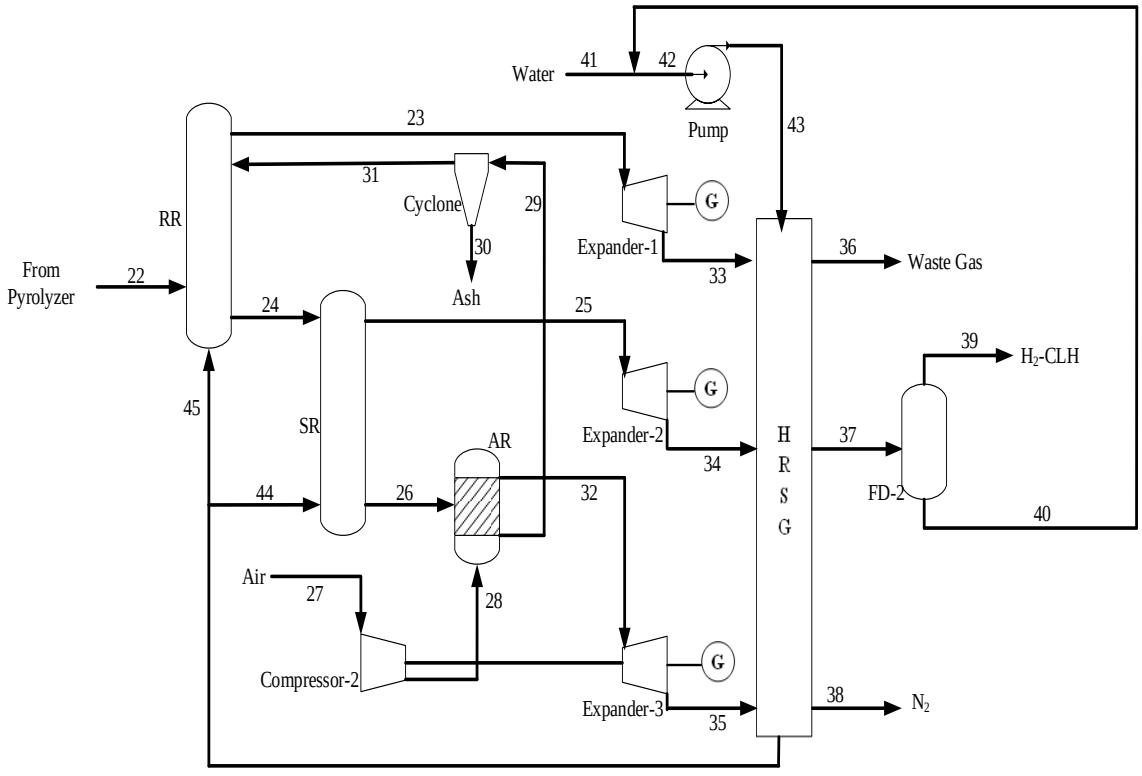

Figure 5.3 Detailed schematic diagram of biochar chemical looping unit for hydrogen production.

Moreover, during the simulation, the RR is assumed to be operated at 10 bar and 900 ^{o}C, where the iron ore Fe_2O_3 is reduced into a mixture of FeO and Fe. The SR operated at 10 bar

and 700 ^{o}C is used to convert steam into H_2, where the FeO and Fe are partially oxidized to Fe_3O_4. Then, Fe_3O_4 is flowed into the AR and completely oxidized with stoichiometric air back to Fe_2O_3 at 10 bar and 1200 ^{o}C. Each produced gas flow from each reactor is considered to be expanded from 10 to 1 bar for the power generation, which provides the power for the compressors, pumps, and others. The remaining heat contained in the gases is absorbed by water to generate steam, which is introduced into the SR. In addition, the water contained in the produced gas from the SR is separated from the H_2 and reused as the steam in the SR. It is essential to control and monitor the temperature of the steam produced in heat recovery steam generation (HRSG) unit since it is the key to hold heat circulation within CLH process in order to achieve the auto-thermal state.

5.2.2. Process simulation

Aspen PlusTM software (9.0 version; Aspen Technology Inc.) is used to simulate the process at a steady state condition using IDEAL as the base method. The feeding rate of woody biomass (i.e., apple tree branch in this study) is assumed to be 100 kg/h. Iron species including Fe_2O_3, Fe_3O_4, FeO, and Fe are considered to be existed in the chemical looping unit. All the reactors are assumed to be operated at an isobaric condition and all the processes have no pressure drops and no accumulation occurred.

The biomass pyrolysis process is simulated by integrating RYield reactor for biomass decomposition and a series of separators to separate the volatiles and biochar parts. REquil and RGibbs are used to generate gases from a partial proportion of the volatiles. The volatiles and biochar parts are presented as the composition of C, H, N, S, O, and H_2O, while the produced gases are assumed to be CO, CO_2, CH_4, and H_2. The model for simulating pyrolysis process is modified from the model developed by Kabir *et al.* [31], which is shown in **Figure 5.4**. In our previous work [12], the results from the pyrolysis of woody biomass were successfully predicted by using the empiric equations developed by Neves *et al*. [32], which are also used as the basic reference in this simulation. The steam reforming of bio-oil is simulated using the single RGibbs reactor and assumed to reach the equilibrium. The PSA

process is simulated by using the separator block to separate CO, CO_2, CH_4, and H_2O from H_2.

The RR and SR in the chemical looping unit are assumed to be operated as the counter current moving bed reactor to achieve high conversions. As such, an interconnected series of multiple RGibbs reactors (5 stages) are used to simulate the moving reactor following the model developed by Li *et al.* [6] and Zeng *et al.* [11]. For the simulation of RR, the oxygen carrier particle is considered to be dropped from the top side (1^{st} stage) and the biochar is introduced into the middle part of the reactor (4^{th} stage). A small amount of steam is introduced from the bottom side (5^{th} stage) as the promoter and carrier gas for the produced gas to move upward, which also helps to increase the pressure inside the reactor. The S/C ratio used is 8% of carbon content in biochar introduced to the reactor. The ash and reduced oxygen carrier are discharged from the reactor from the 5^{th} stage whereas the produced gas is moved out from the 1^{st} stage. The complete conversion of biochar is assumed to be achieved in the RR where only CO_2 and H_2O are produced. The SR is simulated using the similar method as that for the RR, in which the oxygen carrier is dropped from the 1^{st} stage, the steam is introduced from the 5^{th} stage, the partially oxidized oxygen carrier is discharged from the 5^{th} stage and the produced gas is discharged from the 1^{st} stage. The AR is modeled as the single RGibbs reactor for combustion, in which the air is compressed to 10 bar before introduced into it.

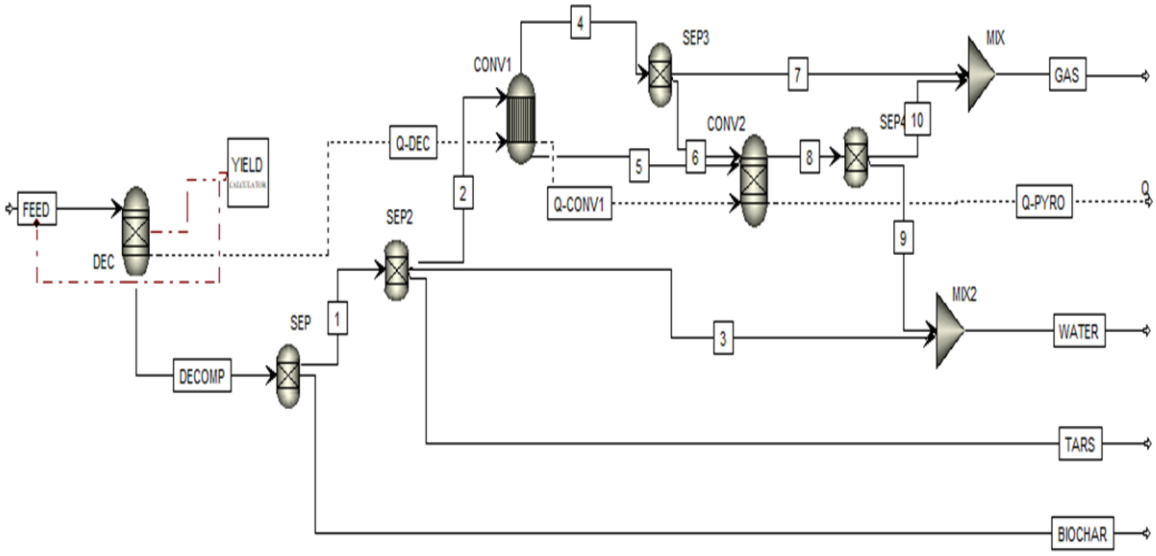

Figure 5.4 Aspen Plus model for pyrolysis simulation

In this study, the minimum amount of Fe_2O_3 required for the CLH unit is firstly simulated to achieve the lowest generation amounts of CO and H_2 in the exhaust gas from the RR. Then, about 51% of excess Fe_2O_3 is added as the heat carrier to make the CLH unit is in auto-thermal state. All key assumptions used for the operating conditions and blocks used for each process in this simulation are summarized in **Table 5.3**.

Table 5.3 Key parameters and main process simulation assumptions.

General parameters	
Ambient condition	25 ^oC, 1 bar
Reaction	All the reactions reach equilibrium at specified condition Kinetics of all the reactions are not considered
Process	Steady state, no accumulation, no heat loss, and no pressure drops
All Pressure Changers	Mechanical efficiency is 0.99, Isentropic efficiency is 0.85 [29]

Heat exhangers	Minimum temperature approach is 8 ^{o}C
Process simulation	
Pyrolysis	RYield, REquil, RGibbs, Sep, 500 ^{o}C, 1 bar All N and S components carried out in biochar stream [12]
Steam Tar Reforming	Rgibbs, 850 ^{o}C, 1 bar, catalyst: Nickel (C11-NK from Sud Chemie)
PSA	Separator block, 35 ^{o}C, 7 bar
Boiler	RGibbs, 1 bar, Heat duty is 0 (adiabatic)
Chemical Looping	RGibbs, 10 bar The operation temperature of RR: 900 ^{o}C, CO and H_2 concentrations: below 0.5 wt% The operation temperature of SR: 700 ^{o}C, The operation temperature of AR: 1200 ^{o}C, air feeding: stochiometric Oxygen carrier: Fe_2O_3, excess 51%
Waste Heat Recovery	Heater, MheatX

5.2.3. Performance indicators for evaluation

The performance of this novel system is evaluated by the total H_2 production, H_2 production efficiency, and power generation as follows:

$$\text{Total } H_2 = H_{2\text{-STR}} + H_{2\text{-CLH}} \tag{12}$$

$$H_2 \text{ production efficiency} = \frac{\text{Total } H_2 \text{ (kg/h)}}{\text{Mass of feed (kg/h)}} \times 100\% \tag{13}$$

$$\text{net power} = \sum W_{exp} - \sum W_{cp} - \sum W_{pump} \tag{14}$$

where $H_{2\text{-STR}}$ and $H_{2\text{-CLH}}$ are H_2 produced by the steam reforming of bio-oil and CLH units, respectively; W_{exp}, W_{cp}, and W_{pump} are the work generated by the expanders and the works required by the compressors/blower and pumps, respectively. The H_2 production efficiency describes as the total amount of H_2 produced from a certain amount of feedstock, which can indicate the effectiveness of the system. The effects of changing parameters such as S/C ratio in the bio-oil reforming of bio-oil process and temperatures at RR and SR on these indicators are also considered.

5.3. Results and discussion

5.3.1. Effect of S/C ratio

The S/C ratio in the steam reforming reaction is one of the key parameters. The increase in S/C ratio will lower the CO/H_2 ratio in the produced gas at certain temperatures. Moreover, the increase in S/C ratio will increase the conversion and reduce the carbon (coke) formation. For the bio-oil reforming, it is reported that the S/C ratio of around 4 on weight or 6-8 on moles corresponds to high conversion as well as high CO/H_2 ratio in the produced gas [33]. **Table 5.4** summarizes the experimental results regarding to the steam reforming of bio-oil with different temperatures, S/C ratios, and reactor types [20, 34-38]. Herein, the S/C ratio in the range of 5.8-9 at 850 ^oC using a commercial Ni-based catalyst (C11-NK from Sud Chemie) was found to achieve about 95% conversion of bio-oil to syngas. Lower S/C also can achieve the similar reaction conversion, however, the catalysts used have not been proven commercially.

Table 5.4 Various reported results for steam reforming of bio-oil with Ni-based catalysts for base assumptions in this simulation.

Oil/Tar	Temperature (^oC)	S/C (mol/mol)	Conversion	Catalyst	Reactor	Ref.

Hardwood	850	5.8	95% (5% on catalyst deactivation)	Ni (C11-NK from Sud Chemie)	Fluidized bed	[20]
Sawdust	550	6.1	95%	Ni-CNT	Fixed bed	[34]
Pine Sawdust	850	7-9	95%	Ni (C11-NK from Sud Chemie)	Fluidized bed	[35]
Sawdust	800	5	96%, 4% on coking formation	Ni-dolomite	Fluidized bed	[36]
Sawdust (aq. fraction)	750	4	96%	C12A7/ Mg	Fixed bed	[37]
Wood (air gasification)	800-850	3.8	95-97%	Ni-dolomite	Packed bed	[38]

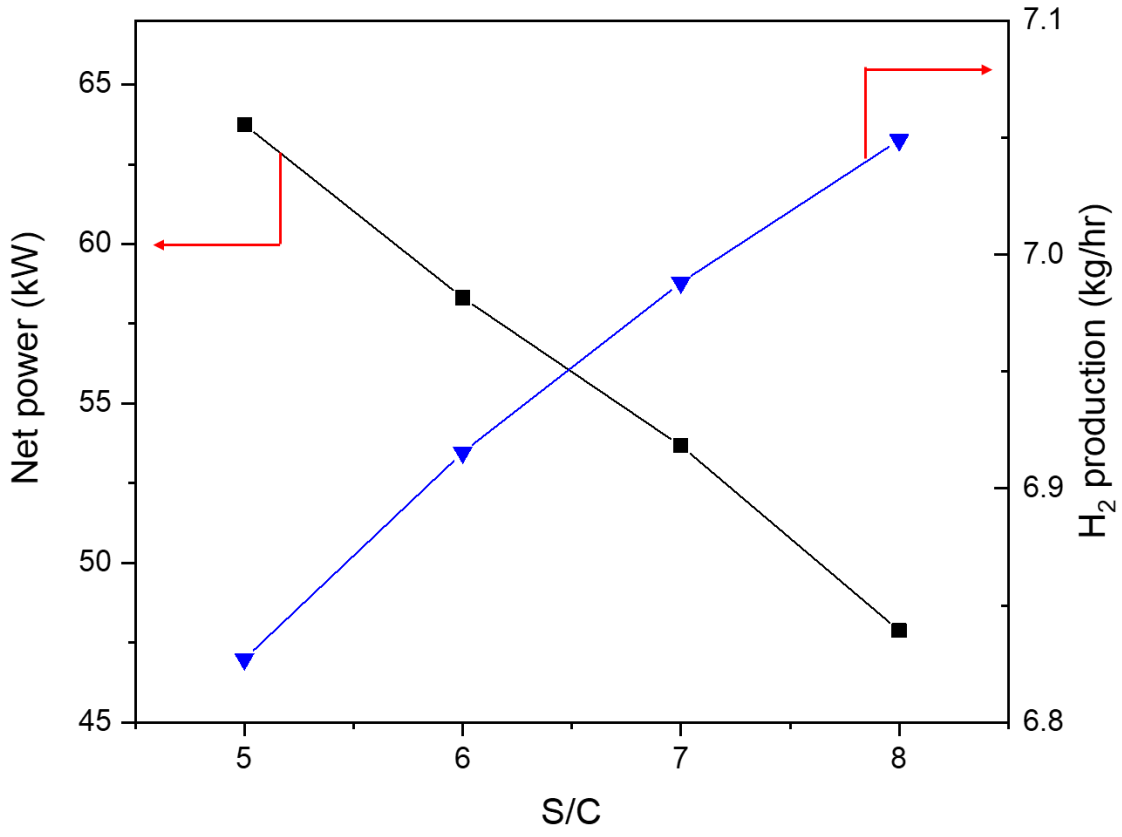

Figure 5.5 Effect of S/C ratio on hydrogen production and net power requirements in the system.

Figure 5.5 shows the effect of S/C ratio on the total H_2 production and net power in the system. Hydrogen production increases with the increase in the S/C ratio. However, the total net power is decreased since the amount of steam consumption is increased, which affects the work of the Compressor-1 for the PSA unit. Meanwhile, the increase in the S/C ratio causes the energy demand increase for the endothermic reaction, which decreases the temperature of flue gas vented out from the thermal insulation of the reforming reactor. As a result, the S/C ratio of 6 is selected as the optimum condition for this process. Referring to **Table 5.4**, the minimum reliable S/C ratio to produce H_2 at the highest conversion should be over than 5.8.

5.3.2. Effect of RR operation temperature

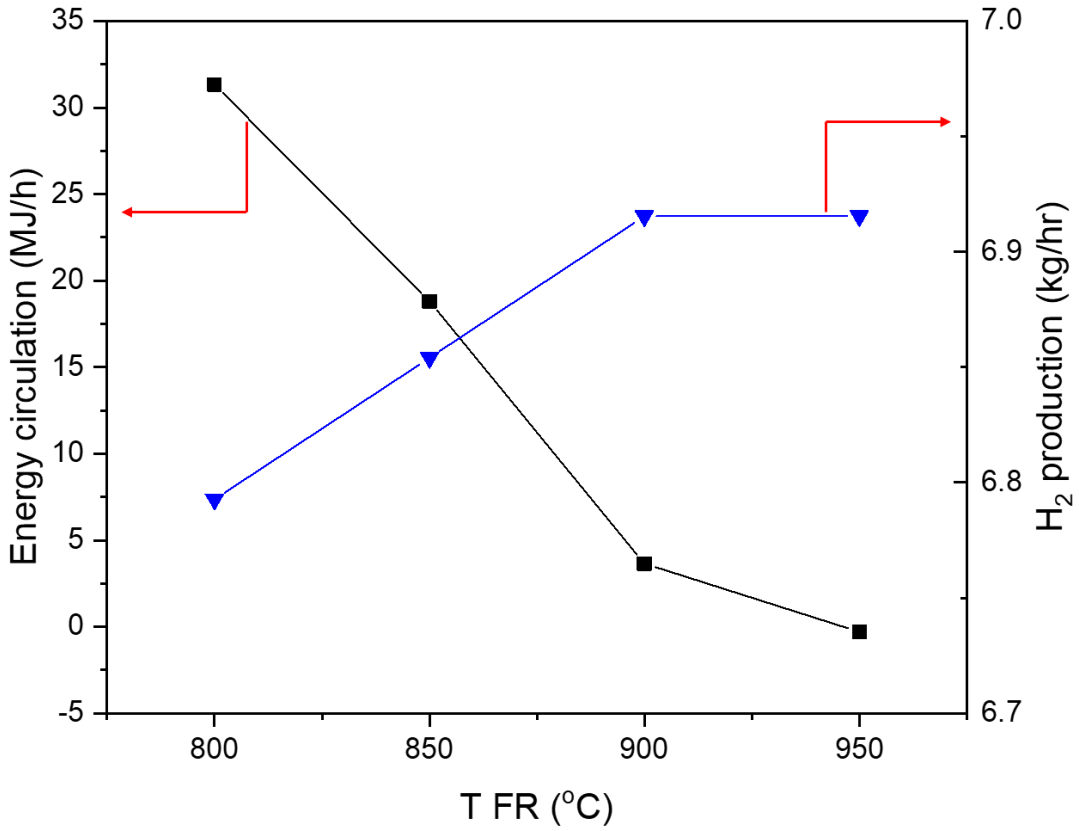

Figure 5.6 Effect of RR operation temperature on hydrogen production and net power requirements in the system. The "-" in energy circulation means that the system is not auto-thermal and requires energy, "+" means that the system is auto-thermal and generates energy.

For the oxygen carrier of Fe_2O_3, the temperature in the range of 850-950 ^oC is normally used for the reducing of it to Fe/FeO in the RR when using coal or biomass as the reducing agents [6]. **Figure 5.6** shows the effect of the RR operating temperature from 800-950 ^oC on the H_2 production and the energy circulation in the CLH system. High temperature is required to support the kinetics of reaction between biochar and iron ore because it is a solid-solid reaction in the moving bed reactor with a short residence time. Even though the kinetics of reactions are not considered in this simulation, the high temperature is still applied to ensure

that the kinetics are enough for the complete conversion of biochar to CO_2 and H_2O. Shen *et al.* [39] and Gu *et al.* [40] found that the temperature range of 720-740 ^oC was enough for the complete conversion of original biomass with a low CO concentration in the flue gas. For the biochar with higher carbon content than biomass, higher temperatures than 740 ^oC are used in this study. From **Figure 5.6**, it can be seen that the total H_2 production is low at a temperature lower than 900 ^oC even though the energy circulation within the system is high due to the heat transfer by the circulation of Fe_2O_3 originated from the AR with the temperature of 1200 ^oC. The CLH system is designed to be auto-thermal by utilizing the extra oxygen carrier as the heat carrier. The higher RR temperature is, the lower the energy circulation becomes, as such, at 950 ^oC, the energy circulation is not enough to support the system to be auto-thermal. Therefore, the operating temperature of the RR is determined as 900 ^oC rather than 950 ^oC to obtain higher H_2 production with higher total energy circulation.

5.3.3. Effect of SR operating temperature

As stated above, in the SR, H_2 is produced by converting steam through the oxidation of Fe/FeO from the RR to Fe_3O_4. The operation temperature range of 700-900 ^oC is usually used for this reaction [6]. **Figure 5.7** shows the effect of the SR operating temperature in the range of 650-800 ^oC on the H_2 production and the energy circulation in the CLH system. Iron oxidation with steam is an exothermic reaction with the equilibrium achieved at a low temperature. By increasing the temperature from 100 to1000 ^oC, H_2 concentration in the product decreases from 99.9 to 64.6 vol.% according to the reaction as shown in Eq. (9). For the reaction of Eq. (10), the increase in temperature from 600 to1000 ^oC decreases H_2 concentration from 62.0% to 11.4 vol.% [41]. Since the reduced iron ore which originates from the RR is totally in the form of FeO (see Eq. (10)), the change in temperature of the SR significantly affects H_2 production, and the lower the temperature is, the higher the H_2 production becomes. However, at the temperature below 700 ^oC, the energy circulation is not enough to maintain the CLH system auto-thermally. At the temperature of 650 ^oC, the total CLH unit becomes an endothermic process that requires external heat or more Fe_2O_3 circulation in it as the heat carrier. With the same amount of Fe_2O_3 circulation, the

temperature of 700 ^{o}C is determined as the SR operating condition to obtain the highest H_2 production and enough energy circulation for the auto-thermal CLH system.

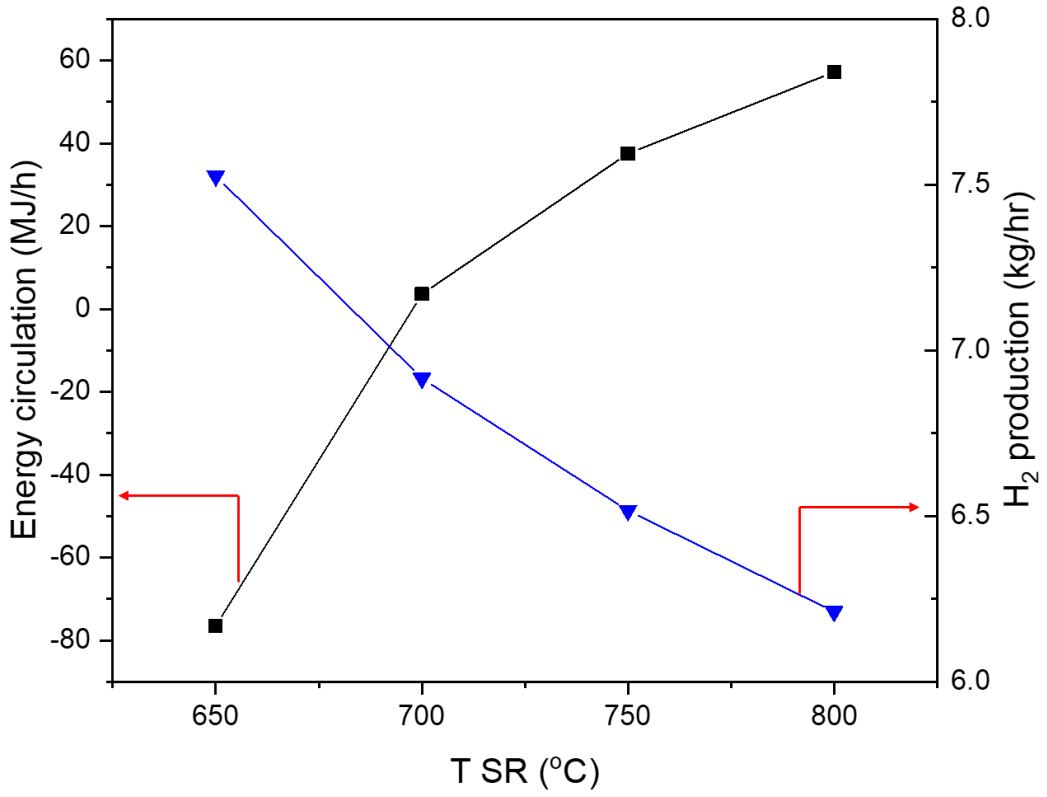

Figure 5.7 Effect of SR operation temperature on H_2 production and net power requirements in the system. The "-" in energy circulation means that the system is not auto-thermal and requires energy, "+" means that the system is auto-thermal and generates energy.

5.3.4. Overall performance

The overall system can generate a total of 6.9 kg/h of H_2 per 100 kg/h of biomass feeding rate with a net power of 58.3 kW in the optimum operating condition in **Table 5.3**. The biomass pyrolysis process generates 20.9% of gas, 24.8% of biochar, 37.1% of tar, and 17.2% of water. **Table 5.5** summarizes and compares the reported several results for the biomass pyrolysis in the auger-type reactor for similar woody biomass at the same temperature of 500 ^{o}C [42-45] which shows that the residence time of pyrolysis reaction can be assumed to be

in the range of 180-300 s. The bio-oil with the generated gases and water is flowed into the steam bio-oil reforming reactor which produces 4.2 kg/h of H_2 after purified by the PSA unit. Meanwhile, the biochar is streamed to the CLH unit, where 2.7 kg/h of H_2 is produced. In the CLH unit, in order to convert the biochar completely, about 525.5 kg/h of Fe_2O_3 particles are circulated, which includes 51% excess as the heat carrier. The total amount of water required as the steam for the overall process is 355.6 kg/h, including 132.6 kg/h for the steam bio-oil reforming process, 2.2 kg/h as the promoter in the RR, and 220.8 kg/h introduced to the SR. After H_2 is separated from the CLH unit, about 196.7 kg/h of water is also obtained, which is recycle-used as the steam for the SR. As such, only 26.3 kg/h of additional make-up water is required to be supplied into CLH unit from outside. **Table 5.6** shows the detailed streams of the biomass pyrolysis, steam tar reforming, CLH process described in **Figure 5.2** and **Figure 5.3**, and **Table 5.7** summarizes the net power for overall system.

Table 5.5 Comparison of the results in this simulation with other reported results on woody biomass pyrolysis in the auger-type reactor at 500 ^oC

Pyrolysis Results in Auger-Type Pyrolyzer (T = 500 ^oC)						
Residence Time (s)	72	180	300	420	480	
Oil/Tar (wt%)	33.8	37.4	36.8	49	18.5	37.07
Char (wt%)	22.6	25.7	23.6	22	30.3	24.75
Gas (wt%)	17.6	18	22.6	29	35.7	20.91
Water (wt%)	26	11-19		(water in oil 33-43%)	15.5	17.27
Ref.	[42]	[43]		[44]	[45]	*This Work*

Table 5.6 Detailed streams for overall process at S/C, T RR, and T SR of 6, 900 ^{o}C, and 700 ^{o}C, respectively

Stream	Materials	Flow rate (kg/h)	Temperature (^{o}C)	Pressure (bar)
1	Dried wood feedstock	100.00	25	1
2	Crushed wood	100.00	25	1
3	Gas + tar + water	75.25	500	1
4	Hot syngas	206.03	850	1
5	Cold syngas	206.03	83	1
6	Dried syngas	172.92	83	1
7	Produced water	33.11	83	1
8	Compressed syngas	172.92	337	7
9	Cooled compressed syngas	172.92	35	7
10	Water	132.63	25	1
11	Hot water	132.63	99	1
12	Hydrogen	4.20	35	7
13	Hydrogen STR	4.20	35	1
14	Tail gas	168.72	35	1
15	Dried tail gas	72.07	35	1
16	Produced water 2	96.65	35	1
17	Air	118.00	25	1
18	Flue gas	190.07	1516	1
19	Steam	132.63	300	1
20	Flue gas 2	190.07	1305	1
21	Vent gas	190.07	28	1
22	Biochar	24.75	500	1
21	Hot waste gas	76.06	900	10

22	Fe + FeO + ash	476.37	900	10
23	Hot produced gas	199.42	700	10
24	Fe_3O_4 + ash	497.77	700	10
25	Air	127.50	25	1
26	Compressed air	127.50	343	10
27	Fe_2O_3 + ash	527.34	1200	10
28	Ash	1.84	1200	10
29	Fe_2O_3	525.50	1200	10
30	Hot N_2	97.92	1200	10
31	Expanded waste gas	76.06	458	1
32	Expanded produced gas	199.42	236	1
33	Expanded N_2	97.92	433	1
34	Waste gas	76.06	33	1
35	Produced gas	199.42	33	1
36	Waste N_2	97.92	33	1
37	Hydrogen CLH	2.71	33	1
38	Recycled water	196.71	33	1
39	Make-up water	26.29	25	1
40	Total water	223.00	32	1
41	Pumped water	223.00	32	10
42	Steam 2	220.80	285	10
43	Steam 3	2.20	285	10

Table 5.7 Simulation results of net power from the overall system.

Works of Pressure Changers (kW)			
Positive		Negative	
Expander-1	12.39	Compressor-1	24.70
Expander-2	58.08	Compressor-2	11.74

Expander-2	24.35	Pump	0.07
Total	94.82	Total	36.51
Net power		**58.31**	

Table 5.8 Comparison of the results between this novel system and other CLH systems.

No.	**Fuel**	**Fuel Amount (kg/h)**	**Methods**	**H_2 Production (kg/h)**	**H_2 Production Efficiency (%)**	**Ref.**
1	Biomass (Poplar Wood)	3,573	Direct	156	4.37	[6]
2	Coal	13,265	Direct	1,958	14.76	[11]
3	Biomass (Microalgae)	2,106	via Gasification (Syngas)	180	8.55	[29]
4	Biomass (Microalgae)	100,000	via Gasification (Syngas)	2,270	2.27	[30]
5	Coal	360	via Gasification (Syngas)	33.2	9.22	[46]
6	Black Liquor	348,120	via Gasification (Syngas)	4,130	11.86	[47]
6	Biochar (Apple Tree)	24.75	Direct	2.78	10.95 (Total eff: 6.9)	This Work

Table 5.8 compares the H_2 production efficiency of this simulation with some typical H_2 production processes with the CLH units using various fuels and methods [6, 11, 29, 30, 46, 47]. The CLH process in this simulation can achieve H_2 production efficiency of 10.95%, which is calculated from 2.71 kg/h of H_2 produced from 24.75 kg/h of biochar. The biochar has the similar characteristics as the coal, which can achieve higher H_2 production efficiency than the raw biomass. Coal as the feed for chemical looping process can reach H_2 production efficiency up to 15% or even more compared to raw biomass that limited at around 5%. However, using biochar as reducing material for chemical looping increases H_2 production efficiency from raw biomass even though it is not as good as coal. Moreover, even compared with other reported results for biomass to H_2 through the CLH process, a total H_2 production efficiency of 7.0% by this novel system is still better. Applications of both the steam reforming of bio-oil and CLH process can increase H_2 production efficiency by around 53% compared to the biomass direct chemical looping (BDCL) process.

Table 5.9 compares the H_2 production efficiency of this novel system with those reported data using other methods for H_2 production [35, 48-52]. A previous theoretical analysis result indicated that the maximum H_2 production efficiencies should be 12.6, 11.5%, and 17.1 wt.% for the biomass pyrolysis with steam reforming of bio-oil, biomass gasification with water-gas shift reaction, and direct reaction between biomass and steam using externally supplied heat, respectively [35]. Moreover, as shown in **Table 5.9,** for this novel system, all the processes can hardly reach the theoretical maximum H_2 production. However, compared with other reported results for H_2 production, this novel system still shows higher H_2 production efficiency.

Table 5.9 Comparison of the results between this novel system with other reported ones for H_2 production.

Biomass	**Methods**	**Status**	**H_2 Production Efficiency (%)**	**Ref.**
Wood Pyrolysis Liquid	Steam Tar Reforming	Experiment, S/C 9, 850 ^oC, Catalyst	3.0	[35]
Biomass	Supercritical Water Gasification	Experiment, Continuous Reactor 600 ^oC, 35 MPa, Catalyst	6.42	[48]
Pine Wood	Air-Steam Gasification	Experiment, Downdraft Reactor	4.52	[49]
Pine Wood	Oxygen-Steam Gasification	Experiment, Downdraft Reactor	7.40	[50]
Pine Sawdust	Steam Gasification + Steam Reforming	Experiment, Continuous Fixed Bed, 900 ^oC	7.99	[51]
Rice Straw	Steam Gasification	Simulation, Fluidized Bed, 800 ^oC	6.2	[52]
Apple Tree Branch	Pyrolysis + Steam Reforming + CLH	Simulation	6.9	This Work

5.4. Conclusions

The present study evaluates the feasibility and performance of a novel system for H_2 production from biomass, in which a biomass pyrolysis process, a catalytic steam bio-oil

reforming process, a CLH process using biochar generated from the biomass pyrolysis, and other auxiliary processes including H_2 separation and thermal energy circulation processes. It is found that this novel system has a higher H_2 production efficiency than other reported ones. Especially, this novel system recoveries the waste heat to maintain the system auto-thermally. This system also generates positive net power from the pressure changing processes, which can provide power for the compressors, pumps, and others. Moreover, compared with the biomass direct chemical looping process (BDCL) to H_2 production, separating the bio-oil and biochar after the pyrolysis process and combining the steam bio-oil reforming process with the chemical looping process using biochar for H_2 production can increase H_2 production efficiency from biomass by more than 50%. Thus, this proposed system has a promising potential for the effective H_2 production from biomass. For the success of implementing this novel system, detailed design and economic analysis need to be further performed.

References

[1] K. Jana, A. Ray, M.M. Majoumerd, M. Assadi, S. De, Polygeneration as a future sustainable energy solution – A comprehensive review, Applied Energy, 202 (2017) 88-111.

[2] G. Guan, C. Fushimi, A. Tsutsumi, M. Ishizuka, S. Matsuda, H. Hatano, Y. Suzuki, High-density circulating fluidized bed gasifier for advanced IGCC/IGFC—Advantages and challenges, Particuology, 8 (2010) 602-606.

[3] G. Guan, M. Kaewpanha, X. Hao, A. Abudula, Catalytic steam reforming of biomass tar: Prospects and challenges, Renewable and Sustainable Energy Reviews, 58 (2016) 450-461.

[4] M. Ni, D.Y.C. Leung, M.K.H. Leung, K. Sumathy, An overview of hydrogen production from biomass, Fuel Processing Technology, 87 (2006) 461-472.

[5] PaoloChiesa, GiovanniLozza, AlbertoMalandrino, MatteoRomano, VincenzoPiccolo, Three-reactors chemical looping process for hydrogen production, International Journal of Hydrogen Energy, 33 (2008) 2233-2245.
[6] F. Li, L. Zeng, L.-S. Fan, Biomass direct chemical looping process: Process simulation, Fuel, 89 (2010) 3773–3784.
[7] M. Luo, Y. Yi, S. Wang, Z. Wang, M. Du, J. Pan, Q. Wang, Review of hydrogen production using chemical-looping technology, Renewable and Sustainable Energy Reviews, 81 (2018) 3186-3214.
[8] J.A.Medrano, I.Potdar, J.Melendez, V.Spallina, D.A.Pacheco-Tanaka, M.v.S. Annaland, F.Gallucci, The membrane-assisted chemical looping reforming concept for efficient H_2 production with inherent CO_2 capture: Experimental demonstration and model validation, Applied Energy, 215 (2018) 75-86.
[9] T.-L. Hsieh, D. Xu, Y. Zhang, S. Nadgouda, D. Wang, C. Chung, Y. Pottimurthy, M. Guo, Y.-Y. Chen, M. Xu, P. He, L.-S. Fan, AndrewTong, 250 kWth high pressure pilot demonstration of the syngas chemical looping system for high purity H_2 production with CO_2 capture, Applied Energy, 230 (2018) 1660-1672.
[10] S.G. Nadgouda, M. Guo, A. Tong, L.-S. Fan, High purity syngas and hydrogen coproduction using copper-iron oxygen carriers in chemical looping reforming process, Applied Energy, 235 (2019) 1415-1426.
[11] L. Zeng, F. He, F. Li, L.-S. Fan, Coal-Direct Chemical Looping Gasification for Hydrogen Production: Reactor Modeling and Process Simulation, Energy & Fuels, 26 (2012) 3680-3690.
[12] Y.A. Situmorang, Z. Zhao, A. Yoshida, A. Abudula, G. Guan, Potential power generation on a small-scale separated-type biomass gasification system, Energy, 179 (2019) 19-29.
[13] G.V. Reklaitis, Introduction to Material and Energy Balances, John Wiley & Sons, Inc.1983.

[14] T. Kan, V. Strezov, T. J.Evans, Lignocellulosic biomass pyrolysis: A review of product properties and effects of pyrolysis parameters, Renewable and Sustainable Energy Reviews, 57 (2016) 1126-1140.
[15] P. Brassard, S. Godbout, V. Raghavan, Pyrolysis in auger reactors for biochar and bio-oil production: A review, Biosystem Engineering, 161 (2017) 80-92.
[16] C. Song, Q. Liu, N. Ji, Y. Kansha, A. Tsutsumi, Optimization of steam methane reforming coupled with pressure swing adsorption hydrogen production process by heat integration, Applied Energy, 154 (2015) 392-401.
[17] G. Esteban-Díez, M.V. Gil, C. Pevida, D. Chen, F. Rubiera, Effect of operating conditions on the sorption enhanced steam reforming of blends of acetic acid and acetone as bio-oil model compounds, Applied Energy, 177 (2016) 579-590.
[18] R. Trane, S. Dahl, M.S. Skjøth-Rasmussen, A.D. Jensen, Catalytic steam reforming of bio-oil, International Journal of Hydrogen Energy, 37 (2012) 6447-6472.
[19] Z. Qi, C. Jie, W. Tiejun, X. Ying, Review of biomass pyrolysis oil properties and upgrading research, Energy Conversion and Management, 48 (2007) 87-92.
[20] S. Czernik, R. Evans, R. French, Hydrogen from biomass-production by steam reforming of biomass pyrolysis oil, Catalysis Today, 129 (2007) 265-268.
[21] D.-K. Moon, D.-G. Lee, C.-H. Lee, H_2 pressure swing adsorption for high pressure syngas from an integrated gasification combined cycle with a carbon capture process, Applied Energy, 183 (2016) 760-774.
[22] A.M. Ribeiro, C.A. Grande, F.V.S. Lopes, J.M. Loureiro, A.E. Rodrigues, A parametric study of layered bed PSA for hydrogen purification, Chemical Engineering Science, 63 (2008) 5258-5273.
[23] A.M. Ribeiro, C.A. Grande, F.V.S. Lopes, J.M. Loureiro, A.E. Rodrigues, Four beds pressure swing adsorption for hydrogen purification: Case of humid feed and activated carbon beds, Aiche Journal, 55 (2009) 2292-2302.
[24] X. Zhu, Y. Shi, S. Li, N. Cai, Two-train elevated-temperature pressure swing adsorption for high-purity hydrogen production, Applied Energy, 229 (2018) 1061-1071.

[25] F.V.S. Lopes, C.A. Grande, A.E. Rodrigues, Activated carbon for hydrogen purification by pressure swing adsorption: Multicomponent breakthrough curves and PSA performance, Chemical Engineering Science, 66 (2011) 303-317.
[26] S. Ahn, Y.-W. You, D.-G. Lee, K.-H. Kim, M. Oh, C.-H. Lee, Layered two- and four-bed PSA processes for H_2 recovery from coal gas, Chemical Engineering Science, 68 (2012) 413-423.
[27] C.-t. Chou, F.-h. Chen, Y.-J. Huang, H.-s. Yang, Carbon dioxide capture and hydrogen purification from synthesis gas by pressure swing adsorption, Chemical Engineering Transaction, 32 (2013) 1855-1860.
[28] Z. Yu, Y. Yang, S. Yang, Q. Zhang, J. Zhao, X. Hao, G. Guan, Iron-based oxygen carriers in chemical looping conversions: A review, Carbon Resources Conversion, 2 (2019) 23-34.
[29] I.N. Zaini, A. Nurdiawati, M. Aziz, Cogeneration of power and H_2 by steam gasification and syngas chemical looping of micralgae, Applied Energy, 207 (2017) 134-145.
[30] A. Nurdiawati, I.N. Zaini, M. Amin, D. Sasongko, M. Aziz, Microalgae-based coproduction of ammonia and power employing chemical looping process, Chemical Engineering Research and Design, 146 (2019) 311-323.
[31] M.J. Kabir, A.A. Chowdhury, M.G. Rasul, Pyrolysis of municipal green waste: A modelling, simulation and experimental analysis, Energies, 8 (2015) 7522-7541.
[32] D. Neves, H. Thunman, A. Matos, L. Tarelho, A. Gómez-Barea, Characterization and Prediction of Biomass Pyrolysis Products, Progress in Energy and Combustion Science 37 (2011) 611-630.
[33] R. Trane, S. Dahl, M.S.S. Rasmussen, A.D. Jensen, Catalytic steam reforming of bio-oil, International Journal of Hydrogen Energy, 37 (2012) 6447-6472.
[34] T. Hou, L. Yuan, T. Ye, L. Gong, J. Tu, M. Yamamoto, Y. Torimoto, Q. Li, Hydrogen production by low-temperature reforming of organic compounds in bio-oil over a CNT-promoting Ni catalyst, International Journal of Hydrogen Energy, 34 (2009) 9095-9107.

[35] D. Wang, S. Czernik, D. Montané, M. Mann, E. Chornet, Biomass to hydrogen via fast pyrolysis and catalytic steam reforming of the pyrolysis oil or its fractions, Industrial & Engineering Chemistry Research, 36 (1997) 1507-1518.
[36] H. Li, Q. Xu, H. Xue, Y. Yan, Catalytic reforming of the aqueous phase derived from fast-pyrolysis of biomass, Renewable Energy, 34 (2009) 2872-2877.
[37] Z. Wang, Y. Pan, T. Dong, X. Zhu, T. Kan, L. Yuan, Y. Torimoto, M. Sadakata, Q. Li, Production of hydrogen from catalytic steam reforming of bio-oil using C12A7-O^--based catalysts, Applied Catalyst A: General, 320 (2007) 24-34.
[38] D. Wang, S. Czernik, E. Chornet, Production of hydrogen from biomass by catalytic steam reforming of fast pyrolysis oils, Energy & Fuels, 12 (1998) 19-24.
[39] L. Shen, J. Wu, J. Xiao, Q. Song, R. Xiao, Chemical-looping combustion of biomass in a 10 kW_{th} reactor with iron oxide as an oxygen carrier, Energy & Fuels, 23 (2009) 2498-2505.
[40] H. Gu, L. Shen, J. Xiao, S. Zhang, T. Song, Chemical-looping combustion of biomass/coal with natural iron ore as oxygen carrier in a continous reactor, Energy & Fuels, 25 (2010) 446-455.
[41] G. Słowiński, A. Smoliński, Thermodynamic feasibility of hydrogen-rich gas production supported by iron based chemical looping process, Hindawi Journal of Chemistry, 2016 (2016).
[42] P. Kim, S. Weaver, K. Noh, N. Labbe, Characteristics of bio-oils produced by an intermediate semipilot scale pyrolysis auger reactor equipped with multistage condensers, Energy & Fuels, 28 (2014) 6966-6973.
[43] N. Puy, R. Murillo, M.V. Navarro, J.M. López, J. Rieradevall, I. Aranguren, T. García, J. Bartrolí, A.M. Mastral, Valorisation of forestry waste by pyrolysis in an auger reactor, Waste Management, 31 (2011) 1339-1349.
[44] A. Veses, M. Aznar, J.M. López, M.S. Callén, R. Murillo, T. García, Production of upgraded bio-oils by biomass catalytic pyrolysis in an auger reactor using low cost materials, Fuel, 141 (2015) 17-22.

[45] L. Bosong, L. Wei, Z. Qi, W. Tiejun, M. Longlong, Pyrolysis and catalytic upgrading of pine wood in a combination of auger reactor and fixed bed, Fuel, 129 (2014) 61-67.
[46] W. Xiang, S. Chen, Z. Xue, X. Sun, Investigation of coal gasification hydrogen and electricity co-production plant with three-reactors chemical looping process, International Journal of Hydrogen Energy, 35 (2010) 8580-8591.
[47] A. Darmawan, M.W. Ajiwibowo, M.K. Biddinika, M. Aziz, Black liquor-based hydrogen and power co-production: Combination of supercritical water gasification and syngas chemical looping, Applied Energy, 252 (2019).
[48] T.G. Madenoğlu, N. Boukis, M. Sağlam, M. Yüksel, Supercritical water gasification of real biomass feedstocks in continuous flow system, International Journal of Hydrogen Energy, 36 (2011) 14408-14415.
[49] P. Lv, Z. Yuan, L. Ma, C. Wua, Y. Chen, JingxuZhu, Hydrogen-rich gas production from biomass air and oxygen/steam gasification in a downdraft gasifier, Renewable Energy, 32 (2007) 2173-2185.
[50] Y. Kalinci, A. Hepbasli, I. Dincer, Biomass-based hydrogen production: A review and analysis, International Journal of Hydrogen Energy, 34 (2009) 8799–8817.
[51] N. Gao, S. Liu, Y. Han, C. Xing, A. Li, Steam Reforming of Biomass Tar for Hydrogen Production Over Nio/Ceramic Foam Catalyst, International Journal of Hydrogen Energy 40 (2015) 7983-7990.
[52] L. Shen, Y. Gao, J. Xiao, Simulation of hydrogen production from biomass gasification in interconnected fluidized beds, Biomass and Bioenergy, 32 (2008) 120-127.

CHAPTER 6 : A SMALL-SCALE POWER GENERATION SYSTEM BASED ON BIOMASS DIRECT CHEMICAL LOOPING PROCESS WITH ORGANIC RANKINE CYCLE

6.1. Introduction

As described in **Chapter 1**, the CLC is usually used as a combined heat and power (CHP) generation process [1], in which a redox loop of solid metal oxide as the oxygen carrier with carbonaceous materials (biomass) as the reducing agent occurs to separately generate flue gas with atmospheric N_2. Chemical looping with two separated reactors are always used in this process. In the reducing reactor (RR), the metal oxide is reduced by the fuel to produce CO_2 and H_2O. While, in the air reactor (AR), the reduced metal oxide is oxidized to its initial state by oxygen in the air. The CLC process is normally combined with CO_2 capture process since it is easy to recover almost 100% of CO_2 from the flue gas of the first reactor without consuming any extra energy for separation of it from H_2O [2, 3].

As a solid material, biomass is less reactive than the gaseous one such as methane or syngas and the solid-solid reaction between it and the metal oxide hardly occurs in any appreciable rate than the gas-solid reaction. However, the direct biomass-based chemical looping process could simplify the process and increase the efficiency compared to generate syngas through gasification process at first [4]. Li *et al.* [5] and Zeng *et al.* [6] developed a simulation model for the CLH process directly using biomass or coal in the moving bed reactor with Fe_2O_3 as oxygen carrier for co-production of hydrogen and power, which indicated the possibility of this process The research group at Chalmers University of Technology experimentally investigated this process by using coal and petroleum coke as solid fuels and ilmenite as the oxygen carrier in fluidized bed reactors, and found that it can be continuously operated for 90 h [7-9]. Meanwhile, they also tested the performance of NiO as the oxygen carrier for the solid CLC process [10, 11]. Combination of chemical looping combustion of direct biomass with organic Rankine cycle (ORC) as a waste heat recovery (WHR) system has a potential to be proposed as novel process for small-scale CHP system.

In this study, a small-scale biomass-based power generation system using the direct biomass chemical looping combustion (BDCLC) process and the ORC as the WHR system was proposed and simulated. Based on the mass and energy balances, the performance of the overall system was optimized. In addition, the effect of the pressure in the BDCLC unit and the selection of working organic fluid for the ORC-WHR system on the power generation were investigated. It is expected to set up a novel small-scale biomass-based power generation system.

6.2. Methodology

6.2.1. Process description

Figure 6.1 describes the schematic diagram of the proposed small-scale biomass-based power generation system including a direct biomass CLC unit and an ORC-WHR unit. Herein, apple tree branch was chosen as the model woody biomass, whose basic properties are shown in **Table 6.1** [12]. In the system, the biomass is firstly introduced to the RR of the CLC unit together with the circulated oxygen carrier of metal oxide. While the reduced metal oxide is oxidized back to its initial state in the AR by air, the produced gas from the RR is expanded to generate power. The metal oxide is circulated back to the RR and the exhaust gas from the AR is also expanded to generate power. The remained heat in the produced gas as well as the exhaust gas is recovered by the organic fluid in the WHR unit which is also used to produce power. The total power output of the overall system includes the power generated by gas expansion and the WHR unit.

Table 6.1 Basic properties of apple tree branch as the woody biomass feedstock

Proximate Analysis (wt%-dry basis)		**Ultimate Analysis (wt%-daf)**	
Moisture	7.8	C	43.7
FC	19.8	H	6.2
VM	78.2	N	0.5

Ash	2	S	0
		O	49.6

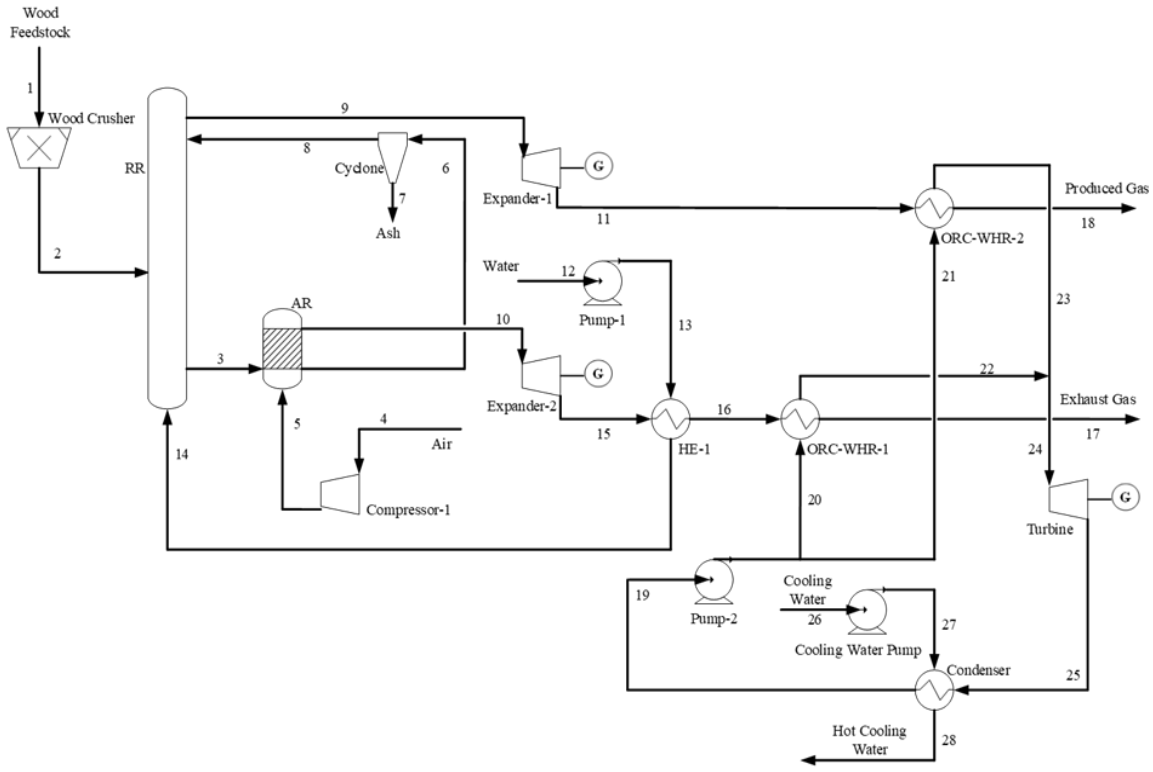

Figure 6.1 Schematic diagram of the small-scale biomass-based power generation system with a BDCLC unit and an ORC-WHR unit.

6.2.2. Process simulation

Aspen PlusTM software (9.0 version; Aspen Technology Inc.) is used to simulate the CLC process using IDEAL as the base method and the ORC-WHR process using SRK-Twu with two different hierarchy blocks as the property package. All reactions are assumed to reach the equilibrium, all the reactors are operated at an isobaric condition, all the processes have no accumulation occurred and work at the steady state condition, and all parameters assumed in this study stay constant during the simulation and analysis.

6.2.2.1.BDCLC Process

The RR in the CLC unit is simulated as a counter current moving bed reactor to achieve high conversions. As such, a model of the moving bed reactor developed by Li *et al.* [5] and Zeng *et al.* [6] with 5-stage interconnected series of RGibbs reactors is used in this simulation. The iron ore is selected as the metal oxide (oxygen carrier) since it is cheap, easy available, and non-toxic with low tendency to agglomeration, high strength, and high resistance to carbon formation although only 0.5 mol of O_2 can be transferred by per 3 mol of Fe_2O_3 [13, 14]. Iron species including Fe_2O_3, FeO, and Fe are considered to be existed in the CLC unit and the following reactions are assumed to occur along the process [15].

$$Fe_2O_3 + 1/2\ C \rightarrow 2\ FeO + 1/2\ CO_2 \quad (1)$$

$$Fe_2O_3 + CO \rightarrow 2\ FeO + CO_2 \quad (2)$$

$$Fe_2O_3 + 3/2\ C \rightarrow 2\ Fe + 3/2CO_2 \quad (3)$$

$$Fe_2O_3 + 3\ CO \rightarrow 2\ Fe + 3\ CO_2 \quad (4)$$

$$Fe_2O_3 + H_2 \rightarrow 2\ FeO + H_2O \quad (5)$$

$$Fe_2O_3 + 3\ H_2 \rightarrow 2\ FeO + 3\ H_2O \quad (6)$$

$$2\ FeO + O_2 \rightarrow Fe_2O_3 \quad (7)$$

$$2\ Fe + 3/2\ O_2 \rightarrow Fe_2O_3 \quad (8)$$

For the simulation of reduction process in the moving bed reactor, the metal oxide particles are dropped from the top side (1st stage), the biomass as reducing agent is introduced at the middle part of the reactor (4th stage), and a small amount of steam as the promoter is input from the bottom side (5th stage). The steam with the S/C 8% of carbon content in biomass also acts as the carrier gas for the produced gas to move upward and helps to increase the pressure inside the reactor. The solid product consists of the ash and reduced metal oxide is discharged from the bottom part of the reactor (5th stage) whereas the produced gas is moved out from the 1st stage. The complete conversion of biomass is assumed to be achieved so that the produced gas only consists of CO_2 and H_2O. The oxidation of metal oxide in the AR is

modeled as the single RGibbs reactor, in which the stoichiometric air is compressed to the operating condition before introduced into AR so that only N_2 exists in the exhaust gas. Then, the exhaust gas is used to generate the steam as the promoter in the RR.

6.2.2.2. ORC-WHR Process

As shown in **Figure 6.2**, the Rankine cycle is thermodynamic cycle consists of four sub-processes: isentropic pressurizing of a working fluid by a pump (1), isobaric heating in evaporator (2), isentropic expansion by a turbine (3), and isobaric-isothermal condensation in a condenser (4) to produce saturated liquid [16-18]. In the simulation, the working fluid is firstly pumped to the optimum working pressure which is set to be lower than critical pressure of each working fluid considered. The heat in the produced gas from BDCLC process is absorbed by the working fluid in the heat exchanger. The working fluid is then expanded to room pressure by a turbine and condensed to the saturated liquid by one-through cooling water.

The working fluid for Rankine cycle is basically categorized into three parts depending on the slope of the T-S curve: dry (positive), isentropic (infinite), and wet (negative). For the ORC application, the dry and isentropic working fluid are most appropriate while the steam is categorized as the wet working fluid [19]. The main criteria for selecting the working fluid for ORC system are [20].

- low heat capacity in the liquid form,
- low specific volume
- high temperature stability, do not deteriorate or decompose at high temperature,
- non-toxic and non-flammable substance is preferable,
- zero Ozone Depleting Potential (ODP) and low Greenhouse Warning Potential (GWP), and
- high availability and low cost.

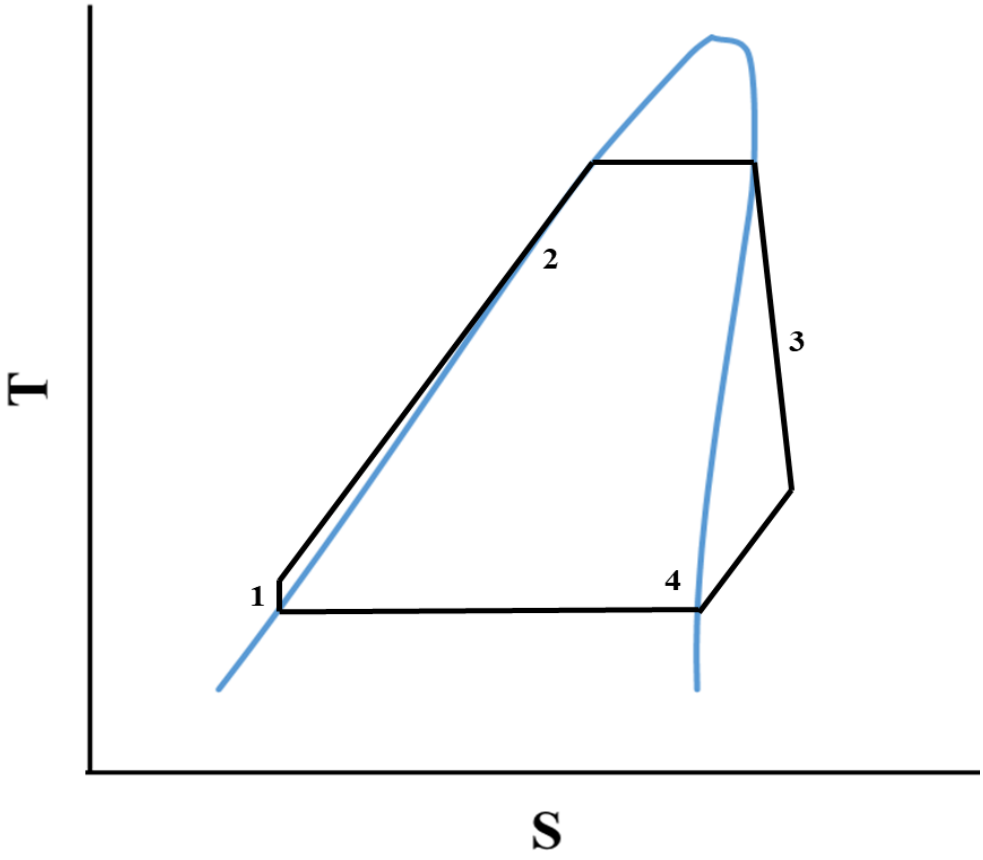

Figure 6.2 T-S diagram of Rankine cycle.

For biomass-based CHP applications, octamethyltrisiloxane (OMTS) is the most selected working fluid for the ORC-WHR system. However, thermal and total heat recovery efficiency of OMTS is considerably low [21]. As such, other working fluids (**Table 6.2**) are considered in this simulation and water/steam is considered as the comparison point.

Table 6.2 Working fluids selected for this simulation.

Working fluids	**Tc (°C)**	**Pc (bar)**	**Types [19]**
Toluene	318.6	41.00	dry
n-pentane	196.5	33.75	dry

cyclohexane	280.1	40.53	dry
Acetone	235	47.00	isentropic
Benzene	288.9	49.24	isentropic
Water/Steam	373.9	217.8	wet

Tc: critical temperature

Pc: critical pressure

6.2.3. Assumptions and performance evaluation

The thermal energy input of the biomass for the system is set at 1000 kW, which is equivalent to a biomass feeding rate of 208 kg/h. The amount of Fe_2O_3 circulated in the BDCLC unit is adjusted to be 1.5 times mol of carbon in the biomass feed to ensure the full conversion of biomass in the RR. No solid loss is assumed in the cycle, and thus no make-up Fe_2O_3 is required. The BDCLC unit is operated at a pressure of 30 bar. Herein, the temperature of the RR is 900 ^oC and the AR is set to be operated at the same temperature as the RR. Since the reduction reaction in the RR is endothermic reaction and oxidation reaction in the AR is exothermic reaction, the BDCLC unit is set to make the whole system work auto-thermally. The heat produced in the AR is assumed to be absorbed by only the exhaust gas which makes the temperature of the exhaust gas higher than the operating condition of the AR. The expander drops the pressure of the produced gas to 1.3 bar and exhaust gas to 1.6 bar. Then, the exhaust gas is used firstly to generate the steam at 250 ^oC for FR promoter and carrier gas before flowing into ORC-WHR unit.

The working pressure for the ORC-WHR is changed based on the working fluid used. Two evaporators are operated for absorbing the heat from the produced and exhaust gas separately without mixing. The amount of working fluid circulated in the ORC-WHR unit is adjusted to the point that makes the minimum temperature approach in the evaporator at 10 ^oC while the working fluid leaves the evaporator at its saturated vapor condition. For the condensation, cooling water is used as the cooling agent to make the working fluid back to the saturated liquid condition at 1 bar before being pumped into the next cycle. It is assumed that no fluid

loss occurs in the cycle and thus the make-up flow for the working fluid is not required. The amount of cooling water used is adjusted so that the working fluid is condensed and the hot cooling water leaves the condenser at 60 ^{o}C. All the key assumptions and operating conditions of the equipment in this simulation are summarized in **Table 6.3**.

The performance of this biomass-based power generation system is evaluated by the total power generated by the BDCLC and ORC-WHR units, efficiency of ORC-WHR unit, electrical efficiency of the system, exergy destruction, and exergy efficiency as follows:

$$\text{net power (kW)} = \sum W_{exp} + W_{turbine} - \sum W_{comp} - \sum W_{pump} \quad (9)$$

$$\eta_{ORC\text{-}WHR} = \frac{W_{turbine} - W_{pump2} - W_{pump3}\ (kW)}{m_{hc}.Cp_{hc}(T_{in} - T_{out})\ (kW)} \times 100\% \quad (10)$$

$$\eta_{system} = \frac{\text{net power (kW)}}{\text{Biomass thermal input (kW)}} \times 100\% \quad (11)$$

$$Ex_{d} = \left(\sum Ex_{in} - \sum Ex_{out}\right) \quad (12)$$

$$Ex_{eff} = \left(1 - \frac{Ex_{d}}{\sum Ex_{in}}\right) \times 100\% \quad (13)$$

where W_{exp}, $W_{turbine}$, W_{cp}, and W_{pump} are the work generated by the expanders and turbine and the works required by the compressors/blower and pumps, respectively; $\eta_{ORC\text{-}WHR}$ and η_{system}, are efficiencies of ORC-WHR unit and electrical overall system, respectively; m_{hc} and cp_{hc} are flow rate and heat capacity of the heat carrier, respectively; T_{in} and T_{out} are temperatures of heat carrier entering and leaving the evaporator, respectively; and Ex_{in}, Ex_{out}, Ex_{d} and Ex_{eff} are the exergy flow entering the equipment, the exergy flow leaving the equipment, the exergy destruction and the exergy efficiency, respectively. Herein, the heat carriers are the produced gas from the Expander-1 and the exhaust gas from HE-1. All works by the pressure changers and the heat capacities of heat carriers are calculated and determined by Aspen software. The exergy flow of each stream in the system is calculated as follows [22]:

$$Ex_{in/out} = Ex_{ph} + Ex_{ch} \quad (14)$$

$$Ex_{ph} = \sum n_i(h-h_0) - T_0(s-s_0) \quad (15)$$

$$s = s_0 + C_p \ln(T-T_0) - R \ln \frac{P}{P_0} \quad (16)$$

$$Ex_{ch} = \sum_{i=1} n_i\left(Ex_{ch,i} + RT_0 \ln x_i\right) \quad (17)$$

where Ex_{ph} and Ex_{ch} are physical and chemical exergy, respectively; n_i, h, and s are molar flow rate, enthalpy, and entropy of each stream, respectively; Cp, R, T, and P are heat capacity, gas ideal constant, temperature, and pressure, respectively, and subscription 0 means the value of parameter at the standard condition (1 atm, 25 ^oC); x_i is molar fraction of each component; $Ex_{ch,i}$ is the standard chemical exergy of the component at the dead state, which are summarized in Table 6.4 [23, 24]

Table 6.3 Essential assumptions for the simulation in this study

General assumptions	
Ambient condition	25 ^oC, 1 bar
Reaction	Kinetics of all the reactions are not considered
Process	Steady state condition, no accumulation, no heat loss
Process simulation	
RR	Multiple RGibbs, 30 bar, 900 ^oC Fe_2O_3/C: 1.5 (mol/mol)
AR	RStoic, 30 bar, Heat duty is the same as total duty in RR
Expanders, Turbines	Isentropic efficiency: 90%, mechanical efficiency: 98% [25]
Compressors, Pumps	Isentropic efficiency: 80%, mechanical efficiency: 98% [25]
Heat Exchangers	Minimum temperature approach: 10 ^oC, Pressure drop: 0.3 bar

Table 6.4 Standard chemical exergy for all substances involved in the system [23, 24]

Standard Chemical Exergy	**kJ/kmol**	**Standard Chemical Exergy**	**kJ/kmol**
CO	275,430	O_2	3,970
CO_2	20,140	Fe_2O_3	20,370
H_2O (g)	11,710	FeO	133,750
H_2O (l)	3,120	Fe	377,740
H_2	238,490	Benzene (g)	3,301.3
N_2	720	Benzene (l)	3,296.2

For the biomass feedstock, the physical exergy can be neglected while the standard chemical exergy can be calculated as follows [26]:

$$Ex_{ch,biomass} = \dot{m}\beta HHV_{biomass} \quad (10)$$

$$\beta = \frac{1.044 + 0.016\ (H/C) - 0.3493\ (O/C)\left(1+0.0531\ \left(\frac{H}{C}\right)\right) + 0.0493\ (N/C)}{1 - 0.4124\ (O/C)} \quad (11)$$

where $\dot{m}$ is mass flow rate of biomass; and C, H, O, N are the mass fractions of carbon, hydrogen, oxygen and nitrogen of biomass in ultimate analysis, respectively. The factor β can be applied in the condition of $[O/C] \leqslant 2$. In this study, the value of $\dot{m}$ x $HHV_{biomass}$ is 1000 kW or equal with 3600 MJ/h. The effects of changing parameters such as the Fe_2O_3/C ratio, the BDCLC operating temperature and pressure and the types of working fluids in ORC-WHR unit on these indicators are also considered.

6.3. **Results and** d**iscussion**

6.3.1. Effect of working fluid

Figure 6.3 shows the $\eta_{ORC\text{-}WHR}$ from different working fluids used for simulation in this study. The analysis of ORC-WHR unit is conducted using the BDCLC condition at 900 ^oC and 30 bar, by which the produced gas and exhaust gas entering the WHR heat exchanger at temperatures of 329 ^oC and 403 ^oC, respectively. One can see that better performances are

achieved by using benzene and acetone. Rahbar *et al.* [20] reported that benzene, toluene, and cyclohexane are more suitable for the high temperature (250-400 ^{o}C) WHR and n-pentane for the medium temperature (150-250 ^{o}C) WHR. Especially, the isentropic fluids such as benzene and acetone are more suitable for the ORC-WHR system [27]. Herein, benzene and acetone have the highest possible working pressure and the highest latent heat among others. Since toluene has a higher critical temperature it is more suitable for the high temperature heat recovery. However, the performance of toluene is limited by its lower critical pressure that those of benzene and acetone. The higher working pressure of the fluid is, the higher work can be produced by the turbine. Meanwhile, the higher the latent heat is, the lower amount of the fluid is required to absorb the heat from the heat carrier. Moreover, as the isentropic fluids, benzene and acetone have similar thermodynamic trends as the wet fluid like water, which usually results in good efficiency for the Rankine cycle system. In comparison, the dry fluids such as toluene, n-pentane and cyclohexane have low efficiency at high turbine-inlet temperature [28]. Thus, benzene and acetone lead to higher efficiencies of the ORC-WHR unit.

In comparison, the steam has superior performance when compared to the hydrocarbon working fluids. It should be noted that the steam is effective at very high pressure since it has very high critical pressure with quite low critical temperature, which makes it have low saturated temperature at low pressure. In the same condition of analysis with other working fluids, condensation can be found in the turbine expansion after the steam absorbs the heat until it reaches a saturated vapor state, which may harm the turbine operation. As such, even though the steam can lead to very high efficiency, it is not suitable for the low and medium grade WHR, especially for the BDCLC operation in this study.

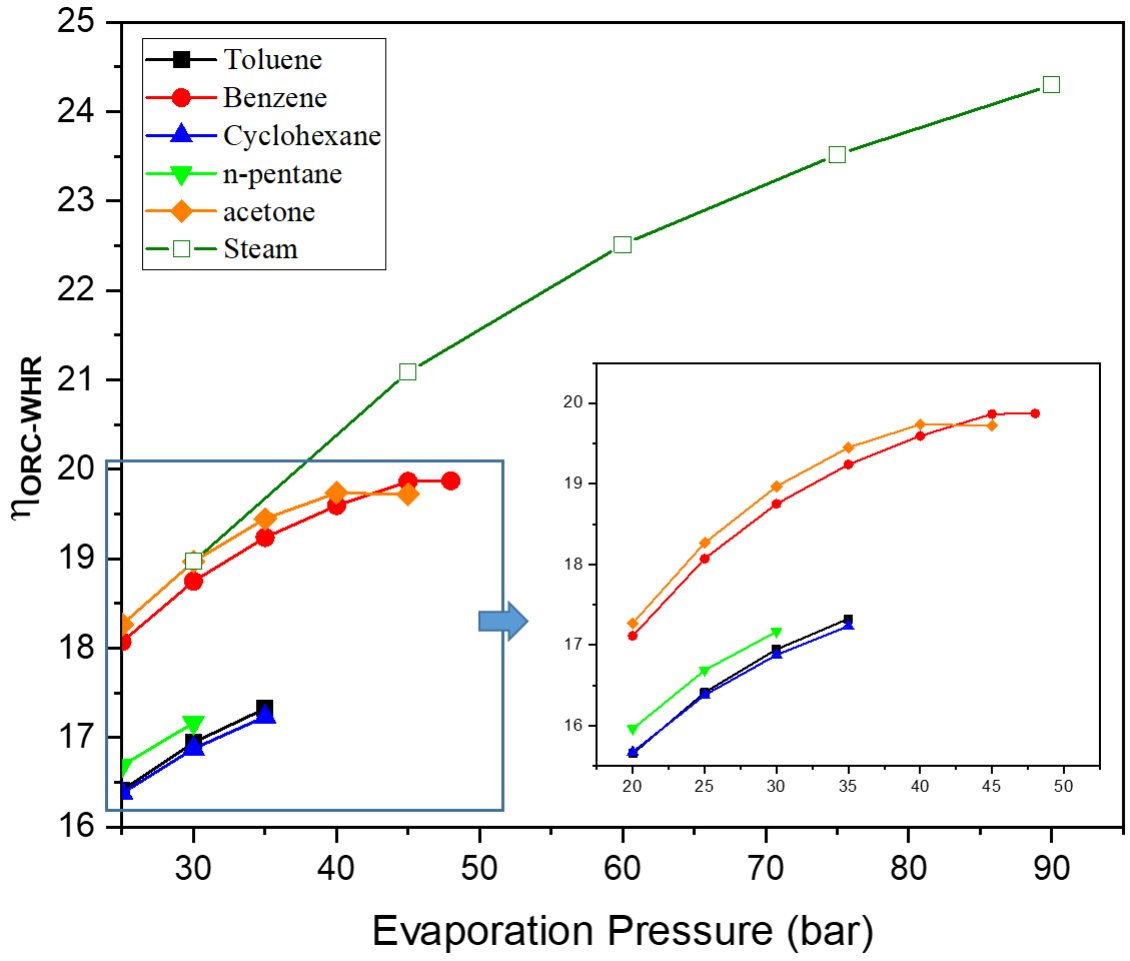

Figure 6.3 The effect of different working fluids on ηORC-WHR. The inset shows the ηORC-WHR by using hydrocarbon working fluids.

6.3.2. Effect of Fe2O3/C ratio

In the RR, Fe_2O_3 is reduced by the carbon containing in biomass as well as the CO and H_2 gases generated by the biomass decomposition to FeO and/or Fe according to reactions (1) to (6), resulting in the production of CO_2 and H_2O. In the AR, the FeO and/or Fe are oxidized back to Fe_2O_3. By this chemical looping, it is easier to capture the CO_2 from the biomass thermochemical process.

Fig. 6.4 shows the effect of Fe_2O_3/C molar ratio (C: carbon amount in biomass) on the carbon conversion in the RR with the operating conditions of 30 bar and 900 ^oC. In the case without the Fe_2O_3 introducing into the reactor, the carbon in biomass cannot be completely decomposed to CO and CO_2 by the heat. At a lower Fe_2O_3/C ratio, the unconverted carbon is firstly converted to CO and then, by increasing the amount of Fe_2O_3 circulated in the system, the CO is converted further to CO_2. At 900 ^oC and 30 bar, the simulation results indicate that the Fe_2O_3/C molar ratio of 2.02 is the minimum value to ensure the full biomass conversion in the moving bed reducer, and by the end of process, about 305 kg/h of CO_2 can be captured in this condition.

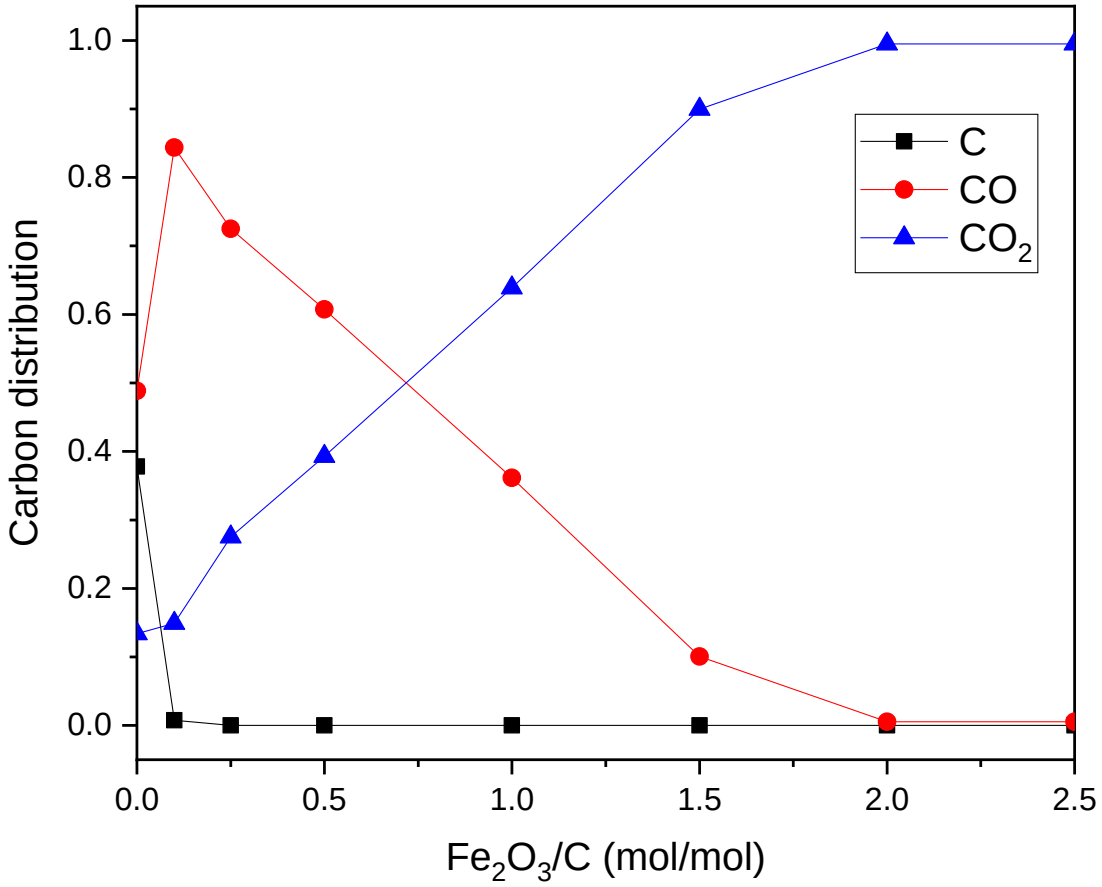

Figure 6.4 Effect of Fe_2O_3/C ratio on the carbon conversion in the RR at 900 ^oC and 30 bar.

6.3.3. Effect of BDCLC temperature

Fig. 6.5a illustrates the effect of RR operating temperature on the carbon conversion of biomass at a pressure of 30 bar and an Fe_2O_3/C ratio of 2.02. The full conversion of biomass is achieved at the temperature over 700 ^oC. It is reported that the temperature of 740 ^oC is enough to obtain a produced gas with a low CO concentration from the biomass feedstock. Thermodynamically, a higher reaction temperature favors the endothermic carbon-Fe_2O_3 reaction and results in more CO formation in the RR [13]. However, from the standpoint of kinetic reaction, a high temperature is required to ensure the solid-solid reaction between biomass and Fe_2O_3 occurred in a short residence time. Thus, even though the kinetics of reactions are not considered in this simulation, the high temperature is still applied to ensure the reaction in the RR occurred well kinetically to achieve the complete conversion of biomass.

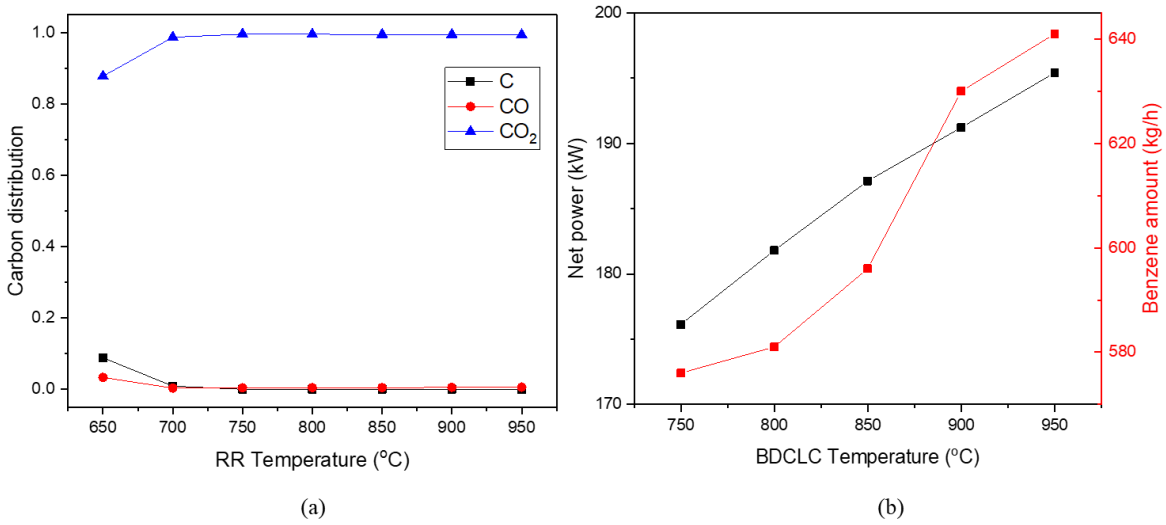

Figure 6.5 The effect of temperature of (a) RR on the carbon conversion and (b) of BDCLC unit on the net power as well as the required benzene flow rate

Fig. 6.5b shows the effect of BDCLC operating temperature on the net power produced by the overall system as well as the amount of benzene required to absorb the heat in the ORC-WHR unit. It is obvious that the net power produced and the amount of benzene required increase by increasing the temperature. The higher the operating temperature is, the higher

the work produced from expander and the higher the heat can be recovered in the ORC-WHR unit. Although the high temperature is favorable for achieving a good system performance, the safety of the system could become worse and simultaneously the biomass conversion also become worse in the thermodynamic standpoint. Moreover, the BDCLC operating temperature should be over 600 ^{o}C since water condensation is found in the expander at a lower temperature. As such, the operating temperature of the BDCLC unit is determined as 900 ^{o}C in order to obtain a high overall efficiency and simultaneously maintain the biomass-Fe_2O_3 reactions thermodynamically and kinetically well.

6.3.4. Effect of BDCLC pressure

Fig. 6.6a describes the effect of RR operating pressure on the carbon conversion of biomass at a temperature of 900 ^{o}C and an Fe_2O_3/C ratio of 2.02. A higher operating pressure depresses the carbon conversion in the reactor since the volume of produced gas increases so that the reaction equilibrium is changed. One can see that the BDCLC pressure in the range of 1-30 bar should be suitable for the reduction reaction. It is also reported that the low pressure is better for the biomass conversion since the high pressure generally inhibits the carbon gasification [5].

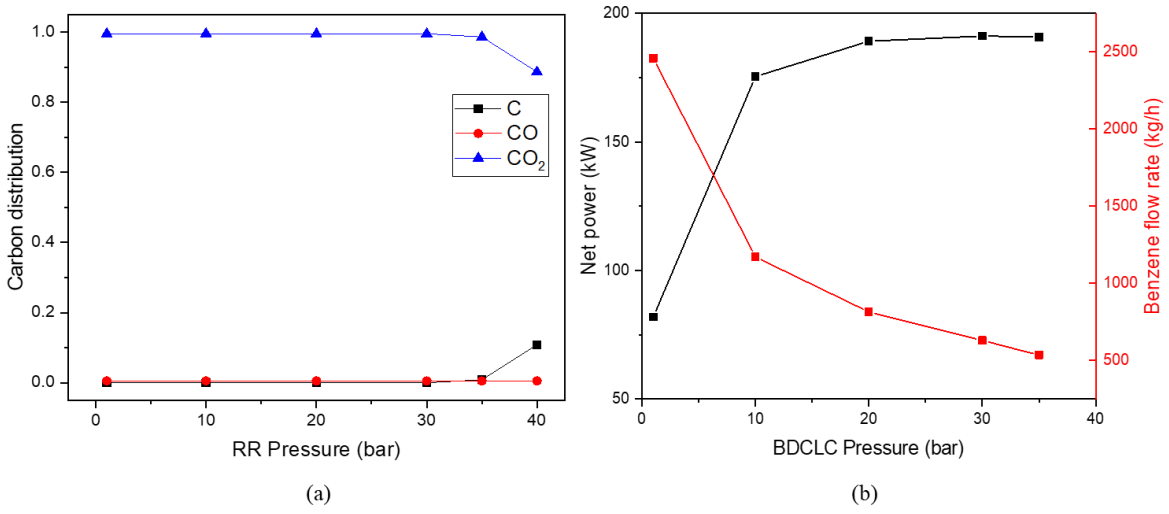

Figure 6.6 The effects of pressure of (a) RR on the carbon conversion and (b) of BDCLC unit on the net power as well as the required benzene flow rate.

Figure 6.6.b shows the effects of BDCLC operating pressure on the overall efficiency and the amount of benzene utilized as the representative of working fluids in the ORC-WHR unit. Herein, pressure is the key component that determines how large power output can be generated by the system since it relies on the pressure expansion to generate power. For 1 bar operation, the power output is totally relied on the ORC-WHR unit since there is no expansion in the BDCLC unit. As the produced gas and exhaust gas directly enter the ORC-WHR unit at their initial temperatures, the amount of benzene utilized is very high to absorb all the heat containing in them. The increase of pressure in the BDCLC unit decreases the temperatures of produced gas and exhaust gas entering the ORC-WHR unit. With the increase in the power output, the amount of benzene circulated in the ORC-WHR unit decreases until 30 bar. At a pressure higher than 30 bar, the difference between temperatures of the produced gas entering evaporator and the saturated benzene leaving it becomes lower than the minimum temperature approach set for the system at the same working pressure of the ORC-WHR unit. Hence, the working pressure of ORC-WHR unit needs to be lowered to adjust the temperature of saturated vapor of benzene leaving evaporator but it will result in worse system efficiency. Besides, 1-30 bar of BDCLC pressure is found to be the proper range for the reduction reaction, and low pressure should be more suitable for the biomass conversion [5].

6.3.5. Overall performance

In the optimum condition of 900 ^{o}C and 30 bar operated in the BDCLC unit, 45 bar of working pressure for benzene as the working fluid in the ORC-WHR unit, and based on other limitations and assumptions in **Table 6.3**, it is found that the overall system can produce 191.2 kWe per 1000 kWth biomass input for the system. Herein, the expansion-compression process in the BDCLC unit contributes 170.2 kWe of net power and the ORC-WHR unit contributes the other 21.0 kWe for the system with a $\eta_{ORC\text{-}WHR}$ of 19.9 % for benzene. It should be noted that the η_{system} of 19.1% is higher than the average electrical efficiency of small-scale biomass-based CHP (17%) reported by Intelligent Energy Europe [29]. **Table 6.4** shows detailed mass and energy balances from each stream described in **Figure 6.1**.

The overall system has an exergy efficiency of 14% including 10.5% and 83% exergy efficiencies of BDCLC and ORC-WHR units, respectively (**Table 6.6**). The exergy efficiency in the system is mainly affected by the significant exergy destruction in the BDCLC unit, which occupies about 97% of total exergy destruction in the system (**Fig. 6.7b**). The exergy destruction in the overall system mainly occurs in the RR and AR (**Fig. 6.7a**) due to the higher temperature operation in both reactors. Nevertheless, the RR and AR still have high exergy efficiencies of 72.5% and 74.2%, respectively and the exergy loss in the BDCLC unit is optimized by selecting the optimum condition of Fe_2O_3/C ratio and working temperature and pressure. The ORC-WHR unit has very low exergy destruction with a high exergy efficiency, indicating that it has a good overall performance as the heat recovery system for the BDCLC process.

Table 6.5 compares the $\eta_{ORC\text{-}WHR}$ of this simulation with other similar work using various working fluids [30-34]. As the optimum working fluid, benzene results in the highest efficiency of 19.9%, which is calculated from 21.0 kWe output from 105.6 kWth total heat absorbed from the produced and exhaust gases. Quoilin *et al.* [35] reported that the electrical efficiency of biomass-based CHP with the ORC-WHR should be limited to about 18%. Comparing to other conventional biomass-fired CHP systems using ORC as the WHR unit with various working fluids (**Table 6.7**), the present system can achieve higher efficiency. Obviously, the present system can achieve higher efficiency. Herein, the application of two evaporators for the produced gas and exhaust gas separately should be the reason for the increase in the $\eta_{ORC\text{-}WHR}$ of this system.

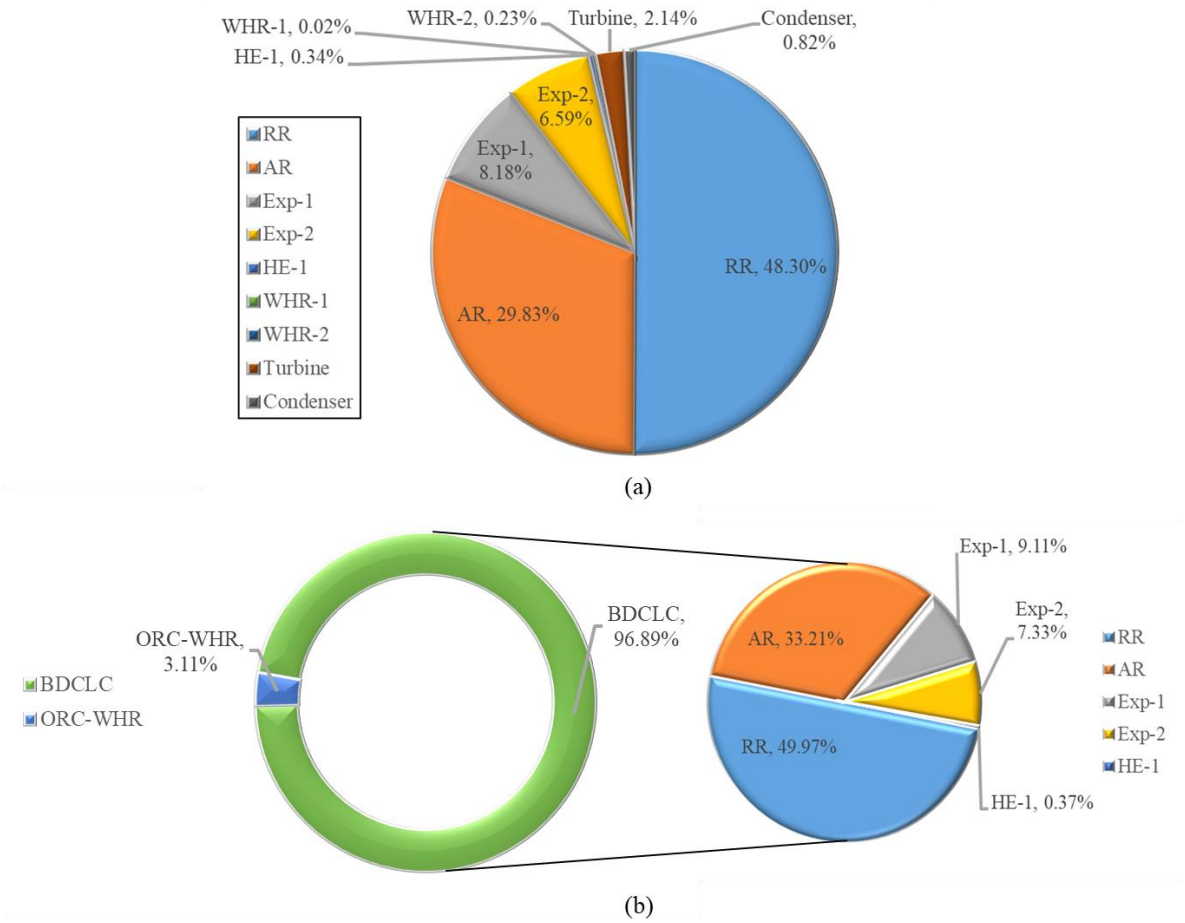

Figure 6.7 Percentages of exergy destruction (a) per equipment in the total system and (b) per unit in the system including the BDCLC unit.

Table 6.5 Detailed streams for this small-scale biomass-based power generation system

Stream	Materials	Flow rate (kg/h)	Temperature (°C)	Pressure (bar)
1	Dried wood feedstock	208.00	25	1
2	Crushed wood	208.00	25	1
3	Fe + FeO	1471.31	900	30

4	Air	884	25	1
5	Compressed air	884	602	30
6	Fe_2O_3 + ash	1676.84	900	30
7	Ash	3.84	900	1
8	Fe_2O_3	1673	900	30
9	Hot produced gas	419.73	900	30
10	Hot exhaust gas	678.49	1462	30
11	Expanded produced gas	419.73	316	1.3
12	Water	10.05	25	1
13	Pumped water	10.05	26	30
14	Steam	10.05	250	30
15	Expanded exhaust gas	678.49	461	1.6
16	Cooled exhaust gas	678.49	423	1.3
17	Exhaust gas	678.49	92	1
18	Produced gas	419.73	92	1
19	Benzene	630.00	80	1
20	Pumped benzene-1	418.00	82	45
21	Pumped benzene-2	212.00	82	45
22	Hot benzene-1	418.00	287	44.7

23	Hot benzene-2	212.00	287	44.7
24	Hot benzene	630.00	287	44.7
25	Expanded benzene	630.00	129	1.3
26	Cooling water	1900.00	25	1
27	Pumped cooling water	1900.00	25	1.5
28	Hot cooling water	1900.00	60	1.2

Table 6.6 Exergy efficiency for each major equipment and unit in the overall system

Equipment/Unit/System	**Exergy efficiency (%)**
RR	72.53
AR	74.19
Exp-1	47.11
Exp-2	71.44
HE-1	91.50
WHR-1	99.76
WHR-2	93.96
Turbine	47.17
Cond	91.48
BDCLC	10.48
ORC-WHR	82.93
System	13.97

Table 6.7 Comparison the ORC efficiency of this system other reported ORC systems

Working fluids	**$\eta_{ORC\text{-}WHR}$ (%)**	**Purposes**	**Ref.**
benzene	19.9	small-scale biomass power generation	*This work*
benzene	12.8	ORC-WHR system	[30]
n-pentane	16.6	micro-scale biomass-fired CHP system	[31]
n-pentane	8.1	small-scale ORC-WHR system	[32]
HFE7000	3.8	micro-scale biomass-fired CHP system	[33]
Cyclo-pentane	6.41	basic biomass micro CHP-ORC	[34]

6.4. Conclusions

The possibility and performance of a small-scale biomass-based power generation system by combining the BDCLC and ORC-WHR processes are studied by using Aspen PlusTM software as well as Aspen HYSYS software. The proposed system shows a higher electrical efficiency than those conventional biomass firing CHPs. The direct feeding of biomass to the CLC process for the CHP utilization opens a door for the effective conversion of biomass to energy. In particular, the implementation of two evaporators in the ORC-WHR unit is found to effectively increase the electrical efficiency of the unit with the isentropic working fluid. However, although the validations of metal oxide in the BDCLC unit and the working fluid stability in the ORC-WHR cycle by the demonstration experiments, and the further detailed assessment on the process design and economic evaluation are still required in the future, this proposed system should be promising for the biomass-based power generation.

References

[1] B. Moghtaderi, Review of the recent chemical looping process developments for novel energy and fuel applications, Energy & Fuels, 26 (2012) 15-40.
[2] Z. Yu, Y. Yang, S. Yang, Q. Zhang, J. Zhao, X. Hao, G. Guan, Iron-based oxygen carriers in chemical looping conversions: A review, Carbon Resources Conversion, 2 (2019) 23-34.
[3] M. Luo, Y. Yi, S. Wang, Z. Wang, M. Du, J. Pan, Q. Wang, Review of hydrogen production using chemical-looping technology, Renewable and Sustainable Energy Reviews, 81 (2018) 3186-3214.
[4] J. Adanez, A. Abad, F. Garcia-Labiano, P. Gayan, L.F.d. Diego, Progress in chemical-looping combustion and reforming technologies, Progress in Energy and Combustion Science, 38 (2012) 215-282.
[5] F. Li, L. Zeng, L.-S. Fan, Biomass direct chemical looping process: Process simulation, Fuel, 89 (2010) 3773–3784.
[6] L. Zeng, F. He, F. Li, L.-S. Fan, Coal-Direct Chemical Looping Gasification for Hydrogen Production: Reactor Modeling and Process Simulation, Energy & Fuels, 26 (2012) 3680-3690.
[7] N. Berguerand, A. Lyngfelt, The use of petroleum coke as fuel in a 10 kWth chemical-looping combustor, International Journal of Greenhouse Control, 2 (2008) 169-179.
[8] N. Berguerand, A. Lyngfelt, Design and operation of a 10 kWth chemical-looping combustor for solid fuels – Testing with South African coal, Fuel, 87 (2008) 2713-2726.
[9] N. Berguerand, A. Lyngfelt, Chemical-looping combustion of petroleum coke using ilmenite in a 10 kwth unit−high-temperature operation, Energy & Fuels, 23 (2009) 5257-5268.
[10] H. Leion, A. Lyngfelt, T. Mattisson, Solid fuels in chemical-looping combustion using a NiO-based oxygen carrier, Chemical Engineering Research and Design, 87 (2009) 1543–1550.

[11] C. Linderholm, E. Jerndal, T. Mattisson, A. Lyngfelt, Investigation of NiO-based mixed oxides in a 300 W chemical-looping combustor, Chemical Engineering Research and Design, 88 (2010) 661-672.
[12] Y.A. Situmorang, Z. Zhao, A. Yoshida, A. Abudula, G. Guan, Potential power generation on a small-scale separated-type biomass gasification system, Energy, 179 (2019) 19-29.
[13] L. Shen, J. Wu, J. Xiao, Q. Song, R. Xiao, Chemical-looping combustion of biomass in a 10 kWth reactor with iron oxide as an oxygen carrier, Energy & Fuels, 23 (2009) 2498-2505.
[14] A. Abad, T. Mattisson, A. Lyngfelt, M. Johansson, The use of iron oxide as oxygen carrier in a chemical-looping reactor, Fuel, 86 (2007) 1021-1035.
[15] H. Ge, W. Guo, L. Shen, T. Song, J. Xiao, Biomass gasification using chemical looping in a 25 kW reactor with natural hematite as oxygen carrier, Chemical Engineering Journal, 286 (2015) 174-183.
[16] N.B. Desai, S. Bandyopadhyay, Process integration of organic Rankine cycle, Energy, 34 (2009) 1674-1686.
[17] D. Wei, X. Lu, Z. Lu, J. Gu, Performance analysis and optimization of organic Rankine cycle (ORC) for waste heat recovery, Energy Conversion and Management, 48 (2007) 1113-1119.
[18] J.M. Smith, H.C.V. Ness, M.M. Abbott, Introduction to Chemical Enginnering Thermodynamics, 6th ed., McGraw Hill2001.
[19] B.-T. Liu, K.-H. Chien, C.-C. Wang, Effect of working fluids on organic Rankine cycle for waste heat recovery, Energy, 29 (2002) 1207-1217.
[20] K. Rahbar, S. Mahmoud, R.K. Al-Dadah, N. Moazami, S.A. Mirhadizadeh, Review of organic Rankine cycle for small-scale applications, Energy Conversion and Management, 134 (2017) 135-155.
[21] U. Drescher, D. Bruggemann, Fluid selection for the Organic Rankine Cycle (ORC) in biomass power and heat plants, Applied Thermal Engineering, 27 (2007) 223-228.

[22] L. Yan, G. Yue, B. He, Exergy analysis of a coal/biomass co-hydrogasification based chemical looping power generation system, Energy, 93 (2015) 1778-1787.
[23] H. Ozcan, I. Dincer, Thermodynamic analysis of a combined chemical looping-based trigeneration system, Energy Conversion and Management, 85 (2014) 477–487.
[24] J. Szargut, Egzergia: poradnik obliczania I stosowania, Wydawnictwo Politechniki Śląskiej2007.
[25] S. Chen, N. Lior, W. Xiang, Coal gasification integration with solid oxide fuel cell and chemical looping combustion for high-efficiency power generation with inherent CO2 capture, Applied Energy, 146 (2015) 298-312.
[26] H. Li, X. Zhang, L. Liu, R. Zeng, G. Zhang, Exergy and environmental assessments of a novel trigeneration system taking biomass and solar energy as co-feeds, Applied Thermal Engineering, 104 (2016) 697-706.
[27] C. Sprouse-III, C. Depcik, Review of organic Rankine cycles for internal combustion engine exhaust waste heat recovery, Applied Thermal Engineering, 51 (2013) 711-722.
[28] T.C. Hung, T.Y. Shai, S.K. Wang, A review of organic Rankine cycles (ORCs) for the recovery of low-grade waste heat, Energy, 22 (1997) 661-667.
[29] IEE, Report on conversion efficiency of biomass, BASIS Bioenergy, 2015,
[30] R.A. Victor, J.-K. Kim, R. Smith, Composition optimisation of working fluids for Organic Rankine Cycles and Kalina cycles, Energy, 55 (2013) 114-126.
[31] H. Liu, Y. Shao, J. Li, A biomass-fired micro-scale CHP system with organic Rankine cycle (ORC) e Thermodynamic modelling studies, Biomass and Bioenergy, 35 (2011) 3985-3394.
[32] S. Quoilin, S. Declaye, B.F. Tchanche, V. Lemort, Thermo-economic optimization of waste heat recovery Organic Rankine Cycles, Applied Thermal Engineering, 31 (2011) 2885-2993.
[33] G. Qiu, Y. Shao, J. Li, H. Liu, S.B. Riffat, Experimental investigation of a biomass-fired ORC-based micro-CHP for domestic applications, Fuel, 96 (2012) 374-382.
[34] Y. Jang, J. Lee, Optimizations of the organic Rankine cycle-based domestic CHP using biomass fuel, Energy Conversion and Management, 160 (2018) 31-47.

[35] S. Quoilin, M.V.D. Broek, S. Declaye, P. Dewallef, V. Lemort, Techno-economic survey of Organic Rankine Cycle (ORC) systems, Renewable and Sustainable Energy Reviews, 22 (2013) 168-186.

CHAPTER 7 : CONCLUSIONS AND FUTURE PERSPECTIVE

7.1. Findings and General Conclusions

As fully described in **Chapter 1**, biomass application on energy perspective is now leading to the development of novel hybrid system that can reduce the unwanted byproducts as less as possible. While, two-stage gasification system tries to solve tar formation in direct biomass gasification process, chemical looping process was proposed to convert biomass into energy with the minimal energy penalty and cleaner waste products. Moreover, problems on long-term sustainability and availability of biomass feedstock for large-scale operation lead to the research and development of small-scale biomass to energy application technologies with the mixing of various types of biomass as the feedstock. Thusly, the studies on the solving of those obstacles in the small-scale biomass conversion systems, especially for power generation and/or hydrogen production, are the main objectives of this dissertation.

As the attempt to find better understanding on the tendency of mixing various kinds of biomass as the feedstock for the two-stage gasification system where the biomass pyrolysis and biochar gasification were conducted separately, the co-pyrolysis of two different biomass followed by the gasification of the co-pyrolysis biochar (co-char) was investigated and described in **Chapter 3**. Particularly, the idea to mix various biomass with less silica species for the two-stage gasification system was found to be able to increase the system efficiency due to synergistic effect of AAEM components during the co-pyrolysis step. However, less reactive co-pyrolysis biochar could be generated from the biomass with high content of silica species such as rice straw and rice husk since the silica species can react with the AAEM species in other biomass to form alkali silicate compounds, which has inhibition effect for the co-char gasification step. Thus, biomass selection for the two-stage gasification system is essential to find compatibility between the different biomass. Application of co-pyrolysis and co-gasification of two or more biomass can solve the problems of feedstock availability in one gasification system.

Further development on the two-stage gasification system in form of a novel hybrid system composed of an auger-type pyrolyzer, a steam tar reformer, an air-steam char fluidized bed gasifier, and a spent char riser-type combustor with circulating heat carrier particles is proposed as a novel small-scale power generation system is presented in **Chapter 4**. The investigation tried to define the system performance based on the biomass pyrolysis rate in the first step of the system based on two extreme pyrolysis ways, i.e., slow and fast pyrolysis. Meanwhile, the conventional way of calculating mass and energy balance using empirical equations was conducted to investigate the system performance. The cold gas efficiency of the system was found to be in the range of 71.7-73.8% from slow to fast pyrolysis. The results showed that the addition of steam tar reforming to the conventional two-stage gasification system should be essential. The fast pyrolysis generated more tar than the slow one, by which the more tar could be converted in the steam reforming section so that the higher system performance was obtained. Sensitivity analysis in this study also concluded that the increase of steam tar reforming conversion had a significant effect on the total system performance.

An alternative strategy by applying chemical looping concept to the previous proposed system was further introduced as a novel hybrid system in the hydrogen production from biomass and described in **Chapter 5**. The CLH process was chosen since it can produce pure H_2 with other gases such as CO and CO_2 separately obtained without using any additional gas treatment and separation processes. The system was designed to be operated auto-thermally by utilizing heat circulation between exothermic and endothermic process within the system. The overall system generated a total of 6.9 kg/h of H_2 and a net power of 58.3 kW simultaneously from a 100 kg/h feeding rate of woody biomass. It is found that combining CLH process with the steam tar reforming can increase the hydrogen production efficiency up to 53% more than that only rely on single CLH process. The proposed system has a high potential to be implemented as the small-scale hydrogen production method in the future.

In the last work as described in **Chapter 6**, a combination of biomass direct chemical looping combustion (BDCLC) with organic Rankine cycle (ORC) as waste heat recovery was

proposed as a novel way for the small-scale combined heat and power (CHP) system. Application of two reactors in the BDCLC unit led to the application of two heat exchangers in ORC unit for the increasing of ORC efficiency from limitation of 18% to 19.9% when the benzene was used as the working fluid. The BDCLC unit can produce 170.2 kWe of power and the ORC-WHR unit contributed the other 21.0 kWe so that the system could produce 191.2 kWe of the total power from a 1000 kWth biomass input. As a result, the system achieved an efficiency of 19.1%, which is higher than the average electrical efficiency of 17% of common small-scale biomass-based CHP system. This proposed system also showed a potential to be implemented as the small-scale biomass power generation in the future.

7.2. Future Perspective and Challenges

Biomass is a potential renewable and sustainable feedstock for energy purposes, especially for power generation and hydrogen production. However, the limitations on its collecting and transporting bring insight on how we can utilize its full potential. Firstly, application of the small-scale biomass to energy system is important, especially in the developing and undeveloped countries and in regional or remote areas. In this respect, the biomass conversion system should be suitable for various types of biomasses and various biomass can be co-utilized. The findings on the work of co-pyrolysis of biomass described in Chapter 4 and some researches about co-gasification show that some biomasses have compatibility with each other. However, availability of biomass in one area to the other is different and the behavior of co-utilization of biomass energy is still not fully understood. There are many gaps to fill in the scope of biomass co-utilization. The decomposition characteristic of some local biomass such as bamboo, palm derivative wastes, i.e. palm kernel shell, palm empty fruit bunch in Southeast Asia; corn cob and wheat straw in America; and municipal solid wastes, e.g., banana peels, eggs shell are still worth to figure out for their utilization in rural areas.

In the other hand, development of new technique or system for converting biomass into energy is necessary for the small-scale operation. For example, to date, almost all commercial small-scale biomass gasification systems use the fixed-bed type gasifiers, e.g., downdraft and

updraft gasifiers, with low gasification efficiency. The novel invention to improve the efficiency of existing system is required. This study opens a way to exhibit a possibility of new proposed small-scale system for generating power as well as hydrogen from biomass, such as a separated-type biomass gasification system for the power generation described in Chapter 4, a hybrid system of biomass pyrolysis, steam tar reforming, and CLH processes for hydrogen production reflected on Chapter 5, and a new CHP system of BDCLC and ORC depicted in Chapter 6. However, those findings only scratch the surface of many opportunities on biomass to energy systems that can be proposed. Fluidized-bed type gasifiers, especially circulating fluidized bed gasifiers such as the dual-bed gasifier with a high efficiency have been widely applied in the large-scale power generation systems. How to miniaturize such systems and let them work efficiently in the small-scale is full of challenge. Furthermore, biomass to energy with carbon capture and storage (BECCS) could be a new attractive insight in scope of developing a new hybrid system. Carbon capture and storage have been an emerging technology to reduce CO_2 emission from energy related fields. Thus, the BECCS offers a unique opportunity for promising system that produces energy with net removal of CO_2. Moreover, utilization of the capture CO_2 to be recycled back into the system that produces it, such as CO_2-gasification and dry reforming processes can reduce the cost of CO_2 storage. However, the BECCS has still limitations on its implementation in terms of technical and economic issues. As to date knowledge, inclusion of CCS to biomass energy conversion system could reduce the energy efficiency to 8-12% yet requires complex set of equipment. Hence, BECCS is only feasible for the large-scale operation. In the research perspective, there are many opportunities to solve these limitations for implementing the BECCS in small-scale processes.

One more important thing, which should be considered in the developing of the new system for biomass to energy, is economic analysis. The economic analysis study should provide the information on whether the developing new system is really feasible to be constructed and will gain profit during the operation. The study and discussion can be conducted separately from performance analysis of the proposed system. In order to conduct economic analysis, a thorough detailed design, equipment sizing, material selection, and collecting database for

equipment cost, operating cost, and materials price are required. It is important to fulfill the feasibility of the system economically since one of the main challenges is still the cost to build a small-scale biomass to energy system. Especially, it is still too high for those developing and undeveloped countries. Accordingly, the researches on the development of lower budget technologies with high efficiency are required.

LIST OF PUBLICATIONS

1. **Yohanes Andre Situmorang**, Zhongkai Zhao, Ping An, Jenny Rizkiana, Tirto Prakoso, Abuliti Abudula, Guoqing Guan. A Small-scale Power Generation System Based on Biomass Direct Chemical Looping Process with Organic Rankine Cycle. *Chemical Engineering and Processing: Process Intensification*, in press.
2. **Yohanes Andre Situmorang**, Zhongkai Zhao, Nichaboon Chaihad, Chao Wang, Aisikaer Anniwaer, Yutaka Kasai, Abuliti Abudula, Guoqing Guan. Steam gasification of co-pyrolysis chars from various types of biomass. *International Journal of Hydrogen Energy*, 46 (2021) 3640-3650.
3. **Yohanes Andre Situmorang**, Zhongkai Zhao, Ping An, Tao Yu, Jenny Rizkiana, Abuliti Abudula, Guoqing Guan. A novel system of biomass-based hydrogen production by combining steam bio-oil reforming and chemical looping process. *Applied Energy*, 268 (2020) 115122.
4. **Yohanes Andre Situmorang**, Zhongkai Zhao, Akihiro Yoshida, Abuliti Abudula, Guoqing Guan. Small-scale biomass gasification systems for power generation (< 200 kW class): A review. *Renewable and Sustainable Energy Reviews*, 117 (2020) 109486.
5. **Yohanes Andre Situmorang**, Zhongkai Zhao, Akihiro Yoshida, Yutaka Kasai, Abuliti Abudula, Guoqing Guan. Potential power generation on a small-scale separated-type biomass gasification system. *Energy*, 179 (2019) 19-29.
6. Nichaboon Chaihad, **Yohanes Andre Situmorang**, Aisikaer Anniwaer, Irwan Kurnia, Surachai Karnjanakon, Yutaka Kasai, Abuliti Abudula, Prasert Reubroycharoen, Guoqing Guan. Preparation of various hierarchical HZSM-5 based catalysts for in-situ fast upgrading of bio-oil. *Renewable Energy*, 169 (2021) 283-292.
7. Zhongkai Zhao, **Yohanes Andre Situmorang**, Ping An, Jingxuan Yang, Xiaogang Hao, Jenny Rizkiana, Abuliti Abudula, Guoqing Guan. A biomass-based small-scale power generation system with energy/exergy recuperation. *Energy Conversion and Management*, 227 (2021) 113623.

8. Aisikaer Anniwaer, Tao Yu, Nichaboon Chaihad, **Yohanes Andre Situmorang**, Chao Wang, Yutaka Kasai, Abuliti Abudula, Guoqing Guan. Steam gasification of marine biomass and its biochars for hydrogen-rich gas production. *Biomass Conversion and Biorefinery* (2020) https://doi.org/10.1007/s13399-020-00868-x.
9. Tao Yu, Abulikemu Abudukeranmu, Aisikaer Anniwaer, **Yohanes Andre Situmorang**, Akihiro Yoshida, Xiaogang Hao, Yutaka Kasai, Abuliti Abudula, Guoqing Guan. Steam gasification of biochars derived from pruned apple branch with various pyrolysis temperatures. *International Journal of Hydrogen Energy*, 45 (36) (2020) 18321-18330.
10. Zhongkai Zhao, **Yohanes Andre Situmorang**, Chihiro Fushimi, Atsushi Tsutsumi, Jingxuan Yang, Xiaogang Hao, Akihiro Yoshida, Abuliti Abudula, Guoqing Guan. Numerical simulation of hydrodynamic behaviors in a gas-solids dense downer reactor. *Advanced Powder Technology*, 31 (7) (2020) 3028-3037.
11. Zhongkai Zhao, **Yohanes A Situmorang**, Ping An, Nichaboon Chaihad, Jing Wang, Xiaogang Hao, Guangwen Xu, Abuliti Abudula, Guoqing Guan. Hydrogen production from catalytic steam reforming of bio-oils: a critical review. *Chemical Engineering & Technology*, 43 (4) (2020) 625-640.
12. Irwan Kurnia, Akihiro Yoshida, **Yohanes Andre Situmorang**, Yutaka Kasai, Abuliti Abudula, Guoqing Guan. Utilization of Dealkaline Lignin as a Source of Sodium-Promoted MoS2/Mo2C Hybrid Catalysts for Hydrogen Production from Formic Acid. *ACS Sustainable Chemistry & Engineering*, 7 (9) (2019) 8670-8677.

List of papers presented in conferences

International Conferences

1. **Yohanes Andre Situmorang**, Zhongkai Zhao, Nichaboon Chaihad, Aisikaer Anniwaer, Akihiro Yoshida, Yutaka Kasai, Abuliti Abudula, Guoqing Guan. Steam Gasification Properties of Bio-Chars Derived from Co-pyrolysis of Rice Straw with Other Biomass. The 7th Asian Conference on Biomass Science, (*Koriyama City Central Community Center, Koriyama, Japan*), December 10, 2019 (Paper ID: OB-1).

2. Zhongkai Zhao, **Yohanes Andre Situmorang**, Ping An, Akihiro Yoshida, Abuliti Abudula, Guoqing Guan. An Exergy-recuperative Biomass-utilized Power Generation System. The 7th Asian Conference on Biomass Science, (*Koriyama City Central Community Center, Koriyama, Japan*), December 10, 2019 (Paper ID: P-10).
3. Aisikaer Anniwaer, **Yohanes Andre Situmorang**, Nichaboon Chaihad, Zhongkai Zhao, Tao Yu, Akihiro Yoshida, Yutaka Kasai, Abuliti Abudula, Guoqing Guan. Co-gasification of rice husk and banana peels for hydrogen-rich gas production. The 7th Asian Conference on Biomass Science, (*Koriyama City Central Community Center, Koriyama, Japan*), December 10, 2019 (Paper ID: P-12).
4. Zhongkai Zhao, **Yohanes Andre Situmorang**, Chihiro Fushimi, Atsushi Tsutsumi, Xiaogang Hao, Akihiro Yoshida, Abuliti Abudula, Guoqing Guan. Numerical simulation of hydrodynamic behaviours in a novel gas-solids moving bed rector under a downer. Fluidization XVI (*Guilin Shangri-La Hotel, Guilin, China*), May 26-31, 2019.
5. **Yohanes Andre Situmorang**, Akihiro Yoshida, Abuliti Abudula,Guoqing Guan. Potential Power Generation on a Small-Scale Biomass Gasification System. The 6th International Symposium on Gasification and its Application (*Wangjiang Hotel, Chengdu, Sichuan Province, China*), October 25-28, 2018.

Domestic Conferences

1. **Yohanes Andre Situmorang**, Zhongkai Zhao, Jenny Rizkiana, Tao Yu, Abuliti Abudula, Guoqing Guan. Co-production of Power and Hydrogen from Biomass by Combining Pyrolysis, Steam Tar Reforming, and Biochar Direct Chemical Looping Process. 第 16 回バイオマス科学会議 (*Online*), January 20-21, 2021. (Paper ID: O-17)
2. **Yohanes Andre Situmorang**, Zhongkai Zhao, Ping An, Jenny Rizkiana, Tirto Prakoso, Abuliti Abudula, Guoqing Guan. Acetone Application for Organic Rankine Cycle in a Small-scale Power Generation System by Biomass Direct Chemical Looping

Combustion. 化学系学協会東北大会 (八戸), September 26-27, 2020. (Paper ID: PD147).

3. **Yohanes Andre Situmorang**, 趙 忠凱, Jenny Rizkiana, 阿布 里提, 官 国清. CO_2-Recycling Biomass Gasification Hydrogen Production System with Water Gas Shift and Membrane CO_2 Captured Method. 化学工学会第 51 回秋季大会 (岩手県), September 24-26, 2020. (Paper ID: PB148).
4. Zhongkai Zhao, **Yohanes Andre Situmorang**, Jenny Rizkiana, Abuliti Abudula, Tao Yu, Guoqing Guan. A small-scale biomass-based combined heat and power generation system with energy/exergy recuperation. 第 16 回バイオマス科学会議 (*Online*), January 20-21, 2021. (Paper ID: O-03).
5. Zhongkai Zhao, **Yohanes Andre Situmorang**, Ping An, Akihiro Yoshida, Abuliti Abudula, Guoqing Guan. An exergy-recuperative system for highly efficient CO2 conversion by combining methane dry reforming and partial oxidation of methane. 第 29 回日本エネルギー学会大会 (富山), August 5-7, 2020. (Paper ID: 2-02).
6. **Situmorang Yohanes Andre**, 趙忠凱, Yu Tao, 吉田 暁弘, 葛西 裕, 阿布 里提, 官 国清. A process design for hydrogen production by combining tar reforming and a chemical looping process for char conversion. 化学工学会第 85 年会 (*Kansai University Senriyama Campus, Osaka*), March 15-17, 2020. (Paper ID: PA157).
7. **Yohanes Andre Situmorang**, 趙忠凱, Nichaboon Chaihad, 吉田暁弘, 葛西裕, 阿布里提, 官国清. Effect Addition of Various Biomass Char on Steam Co-gasification with Rice Straw. 第 15 回バイオマス科学会議 (*Koriyama City Central Community Center, Koriyama*), December 11-13, 2019. (Paper ID: P-09).
8. Aisikaer Anniwaer, **Yohanes Andre Situmorang**, 于涛, 吉田暁弘, 葛西裕, 阿布里提, 官国清. Steam gasification of rice husk in the presence of calcined seashells. 第 15 回バイオマス科学会議 (*Koriyama City Central Community Center, Koriyama*), December 11-13, 2019. (Paper ID: P-10).

9. Zhongkai Zhao, **Yohanes Andre Situmorang**, Ping An, Akihiro Yoshida, Abuliti Abudula, Guoqing Guan. A novel biomass IGFC system with exergy recuperation for high efficiency power generation. 第 56 回石炭科学会議 (ウインクあいち、名古屋), October 28-31, 2019. (Paper ID: 1-2).
10. Irwan Kurnia、**Yohanes Andre Situmorang**、吉田 曉弘、阿布 里提、官 国清、 葛西 裕. Synthesis p-menthane-3,8-diol over sustainable acid carbon catalysts derived from alkaline lignin. 化学工学会第 84 年会 (*Shibaura Institute of Technology, Tokyo*), March 13-15, 2019. (Paper ID: PE350).
11. **Yohanes Andre Situmorang**, Akihiro Yoshida, Abuliti Abudula, Guoqing Guan. Potential Power Generation in a Small-Scale Biomass Gasification System. ４校学術交流会 (*Iwate University, Iwate*), October 30, 2018.
12. **Yohanes Andre Situmorang**, Akihiro Yoshida, Abuliti Abudula, Guoqing Guan. Energy Analysis On A Small-Scale Biomass Gasification System. 第 27 回日本エネルギー学会大会 (日大理工学部駿河台キャンパス, 東京), August 8-9, 2018. (Paper ID: P-3-4).

Honors and Awards

1. Excellent Student Award, Hirosaki University, September 2019

CURRICULUM VITAE

Personal Information

Name : Yohanes Andre Situmorang

Nationality : Indonesian

Educational Background

- **Degree: Ph.D. (Hirosaki University, Japan)**
  Major : Safety System Engineering
  Period : April 2018-March 2021
- **Degree: Master (Institut Teknologi Bandung, Indonesia)**
  Major : Chemical Engineering
  Period : August 2010-October 2012
- **Degree: Bachelor (Institut Teknologi Bandung, Indonesia)**
  Major : Chemical Engineering
  Graduation : August 2006-July 2010

Works Experience

- **Business Development and Biogas Planning Unit at PT. Pasadena Engineering Indonesia** (December 2014-August 2017)
- **Junior Process Engineer at PT. LAPI ITB** (May 2014-April 2015)
- **Junior Process and Safety Engineer at Process Safety and Electrochemical Conversion Laboratory Institut Teknologi Bandung (ITB)** (April 2014-September 2014)
- **Junior Process and Simulation Engineer at Process Simulation Laboratory Institut Teknologi Bandung (ITB)** (August 2012-April 2014)
- **Internship at PT. Chandra Asri Petrochemical Indonesia, Low Linear-Density Polyethylene Plant** (June 2009)

Scholarship	
Doctoral Degree	: Ministry of Education, Culture, Sports, Science and Technology (MEXT) of Japan Scholarship (October 2017-March 2020)
Master Degree	: Voucher Scholaship of Institut Teknologi Bandung (August 2010-July 2011)